MODELING CONTAMINANT TRANSPORT THROUGH POROUS MEDIA USING ASYMPTOTIC DISPERSIVITY

Ph.D. THESIS

by

TEODROSE ATNAFU ABEGAZE

DEPARTMENT OF CIVIL ENGINEERING
INDIAN INSTITUTE OF TECHNOLOGY ROORKEE
ROORKEE-247667 (INDIA)
June, 2016

MODELING CONTAMINANT TRANSPORT THROUGH POROUS MEDIA USING ASYMPTOTIC DISPERSIVITY

A THESIS

Submitted in partial fulfilment of the requirements for the award of the degree

of

DOCTOR OF PHILOSOPHY

in

CIVIL ENGINEERING

by

TEODROSE ATNAFU ABEGAZE

DEPARTMENT OF CIVIL ENGINEERING
INDIAN INSTITUTE OF TECHNOLOGY ROORKEE
ROORKEE-247667 (INDIA)
June, 2016

INDIAN INSTITUTE OF TECHNOLOGY ROORKEE
ROORKEE

CANDIDATE'S DECLARATION

I hereby certify that the work which is being presented in thesis entitled "**MODELING CONTAMINANT TRANSPORT THROUGH POROUS MEDIA USING ASYMPTOTIC DISPERSIVITY**" in partial fulfilment of the requirements for the award of the Degree of Doctor of Philosophy and submitted in the Department of Civil Engineering, Indian Institute of Technology Roorkee, Roorkee is an authentic record of my own work carried out during the period from July, 2012 to June, 2016 under the supervision of Dr P. K. Sharma, Associate Professor, Department of Civil Engineering, Indian Institute of Technology Roorkee, Roorkee, India.

The matter presented in this thesis has not been submitted by me for the award of any other degree of this or any other Institute.

Signature of the Candidate

This is to certify that the above statement made by the candidate is correct to the best of my knowledge.

Signature of Supervisor

The Ph.D. Viva-Voce Examination of **Mr. Teodrose Atnafu Abegaze,** Research Scholar, has been held on.....

Chairman, SRC **Signature of External Examiner**

This is to certify that the student has made all the corrections in the thesis.

Signature of Supervisor **Head of Department**

Date:

ABSTRACT

The quality of subsurface water can be affected by natural processes, nonpoint agricultural and urban runoff, waste-disposal practices and industrial discharges etc. The most challenging task for groundwater hydrologist is to make accurate prediction of arrival times and spatial patterns of toxic levels of a waste substance below the ground. The difficulty in prediction increases with the heterogeneity, and chemical properties of solute and porous medium. Most of the pathogenic bacteria and virus in ground water originate from human and animal sewage from municipal wastewater discharges, septic tanks, sanitary landfills and agricultural processes. The wastewater infiltrates through the vadose zone and, upon reaching the water table, continues to travel for large distances through the subsurface environment. When this water is drawn by wells and consumed without any treatment, it may be hazardous to human health. Hence, it is necessary to study the transport mechanism of reactive chemicals through porous media.

Most of the early studies on contaminant transport through porous media considered the contaminant to be either non-reactive or to have instantaneous reaction with the porous matrix. In such cases, the transport process could be described by advection (including retardation for reactive contaminants), diffusion and dispersion. Advection is governed by the movement of contaminants along with the flowing groundwater at the seepage velocity in porous media. Diffusion is a molecular mass transport process in which contaminants move from area of higher concentration to the area of lower concentration. Dispersion is governed by spatial variability of groundwater velocity in porous media caused by the heterogeneity of hydraulic properties of the porous media. Transport of non-reactive solute through homogeneous and heterogeneous porous media has been investigated experimentally, theoretically, and numerically by a number of researchers. A common approach to study the transport behaviour subjected to the seemingly irregular variation of hydraulic properties in porous media is that based on the stochastic theory. The resulting equations are, however, quite complicated and difficult to solve analytically except for a few simple cases.

There are a number of studies that use mathematical modeling and experimental techniques to study and understand the behaviour of contaminants in a heterogeneous porous medium. It has been widely accepted in the literature that the non-equilibrium conditions significantly affect the solute transport at the field scale. Therefore, the present study focuses on the development of a generalized model, which can incorporate physical and sorption related non-equilibrium in heterogeneous porous media. Physical non-equilibrium (PNE) is accounted by a diffusive mass transfer between the advective and non-advective partitioning within porous medium. Sorption non-equilibrium (SNE) is accounted by using a two-site conceptualization for both advective and nonadvective regions in porous media, where at the first site, the sorption is assumed to be governed by an instantaneous equilibrium adsorption isotherm and at the second site; the sorption is described by a first order rate-limited process.

In this study, semi-analytical solution of multiprocess non-equilibrium (MPNE) transport model with asymptotic distance-dependent dispersion is developed. Semi-analytical solution was developed in Laplace domain which was then inverted numerically to obtain time domain concentration. Semi-analytical solution was developed for constant concentration type input. To describe the features of MPNE transport model, results of breakthrough curves were simulated using constant and asymptotic distance-dependent dispersion models.

An experimental investigation on large heterogeneous soil column is performed for which a 1500 cm long heterogeneous soil column was constructed in the lab using different types of materials. Chloride and Fluoride were used in the experiments which represent conservative and non-conservative solutes, respectively. The developed model is then used to simulate the laboratory experimental data of Chloride and Fluoride, through heterogeneous soil column. It was observed that a better fit to the observed BTC was observed when mass transfer between advective and non-advection region is considered. It was also observed that asymptotic distance-dependent dispersion model gives a good fit to the observed breakthrough curve as compared to constant dispersion model. It is found that physical non-equilibrium significantly affects the breakthrough curves of both non-reactive and reactive solutes through porous media. The mass transfer from advective to non-advective region influence the behaviour of distribution of BTC’s obtained at various distances. Further the, experimental investigation of solute transport through long soil column experiments is studied. Batch sorption study is performed to estimate the linear and nonlinear

sorption coefficients for different types of soil materials. Linear and nonlinear sorption models were used to simulate experimental breakthrough curves through porous media. Analysis and simultion of the observed data of fluoride suggested that nonlinear sorption i.e., Freundlich sorption model simulate better as compared to linear sorption model.

It is also shown that the MIMA model gives the best fit curve of experimental breakthrough curves in long heterogeneous soil column experiment as compared to both MIMC and MIML models. Estimated value of dispersivity is smaller in case of MIMA model as compared to both MIMC and MIML models. Thus MIMA model is efficient to capture the evolution distance-dependent dispersion behavior. Accurate prediction of mass transfer coefficient is also essential and significant for transport of contaminant through porous media. Hence, asymptotic dispersivity including variable mass transfer coefficient can be useful for describing solute transport in long heterogeneous porous media

Finally, the behavior of concenration profiles and spatial moments for reactive transport through triple-permeability porous medium was studied. For this, numerical model has been developed for transport equations using both FDM and FVM methods. A detailed analysis of triple-permeability transport model has been carried out to study its performance for advection and dispersion dominant cases. For an advection dominant flow, FDM model produces oscillation in presence of small and higher values of of mass transfer coefficients. Hence, FVM can be used for both the simulation of solute transport through porous media for any value of Peclet number. The results of mean travel distance and spreading behavior of solutes remain the same in the presence of higher values of mass transfer coefficients.

.

ACKNOWLEDGEMENTS

I wish to express my immense sense of gratitude to my supervisor Dr. P. K. Sharma, Associate Professor, Department of Civil Engineering, Indian Institute of Technology Roorkee, Roorkee for his invaluable time, guidance and constant encouragement throughout the tenure of this work.

I would like to thank all the faculty and staff of Department of Civil Engineering, Indian Institute of Technology Roorkee, for their support during the course of this study. I would also like to thank the members of student research committee for their efforts in evaluating the work.

Finally, I would like to thank all those who have directly and indirectly helped me through this work and made this work possible. Above all, I am thankful to Almighty for his divine blessings and giving me the required courage and strength during the difficult times.

(Teodrose Atnafu)

TABLE OF CONTENT

LIST OF FIGURES

LIST OF TABLES

LIST OF NOTATIONS

a_1	Coefficient for exponential distance-dependent dispersivity, (L)
b_1	Coefficient for exponential distance-dependent dispersivity, (L^{-1})
α	Dispersivity, (L)
$\alpha(x)$	Distance dependent dispersivity, (L)
C_i	Initial injected solute concentration, (ML^{-3})
C_n	Solute concentration in solution phase for nonadvective region, (ML^{-3})
C_0	Initial injected concentration of solute, (ML^{-3})
D_0	Free water diffusion coefficient, (L^2T^{-1})
D_{L}	Hydrodynamic dispersion coefficient, (L^2T^{-1})
D_{m}	Diffusion coefficient in porous medium, (L^2T^{-1})
$D(x)$	distance dependent hydrodynamic dispersion coefficient (L^2T^{-1})
f	Mass fraction of sorbent constituting the advective region, (M^0)
F_a	Mass fraction of sorbent for which sorption is essentially instantaneous in the advective region
F_n	Mass fraction of sorbent for which sorption is essentially instantaneous in the non advective region
k	Constant for linear distance dependent dispersivity, (L^0)
k_{a2}, k_{n2}	Reverse sorption rate coefficient for advective region and non-advective regions respectively, (T^{-1})
K_a	Equilibrium sorption coefficient for the advective region, ($M^{-1}L^3$)
K_n	Equilibrium sorption coefficient for the nonadvective region, ($M^{-1}L^3$)
P	Laplace transform variable
q	Flow rate, (LT^{-1})
Q_e	Sorbed concentration (ML^{-3})
S_{a2}	Rate-limited sorbed-phase concentration in advective region, (M^0)
S_i	Initial sorbed phase solute concentration, (M^0)
S_{n2}	rate-limited sorbed-phase concentration in nonadvective region, (M^0)
t	Time, (T)
t_0	Pulse duration, (T)
θ_n	Volumetric water content of the non-advective region (L^0),

θ	Total volumetric water content (L^0)
v_a	pore velocity in advective region, (L/T)
ω	Coefficient of mass transfer between the advective and non-advective regions, (T^{-1})
x	Travel distance, (L)
$\bar{x}$	Mean travel distance, (L)
μ_a, μ_n	The first-order transformation coefficient for the solution phase in advective and non-advective regions, (T^{-1})
μ_{al}, μ_{nl}	The transformation coefficients for the instantaneous sorbed-phase of advective and non-advective regions, (T^{-1})
μ_{a2}, μ_{n2}	The transformation coefficients for rate-limited sorbed-phase domains of advective and non-advective regions, (T^{-1})
ρ	Bulk density of the porous medium, (ML^{-3})
CDEC	Conventional dispersion equation with constant dispersivity
CDEL	Conventional Dispersion equation with linear distance-dependent dispersivity
MIM	Mobile immobile model
MIMC	Mobile immobile model with constant dispersion
MIML	Mobile immobile model with linear distance dependent dispersion
MIMA	Mobile immobile model with Asymptotic distance dependent dispersion
MPNE	Multiprocess non-equilibrium transport model
MPNEC	Multiprocess non-equilibrium transport model with constant dispersion
MPNEA	Multiprocess non-equilibrium transport model with Asymptotic distance dependent dispersion
NSE	Nash-Sutcliff model efficiency coefficient
RMSE	Root mean squared error
R^2	Coefficient of determination

Chapter 1

INTRODUCTION

1.1 General

Groundwater is an important natural resource that is extensively used for various industrial, agricultural and domestic purposes. In a large part of the country, ground water is the only source of water for human consumption. Ground water can become contaminated from point source pollution that comes from a single source, such as wastewater treatment plants. Fertilizers and pesticides, surface run-off, septic wastes, and household wastes are also the various sources of non-point source pollution. Sometimes, leaching of wastes from landfills or discharge of industrial wastes to the soil without treatment also affects ground water (Fetter 1999). Different chemicals like chloride, arsenic, fluoride, etc. are dissolved in the water. Polluted ground water is difficult to purify. Different types of contaminant have different transport properties and depend on the size of grain of porous medium. Contaminated groundwater can have serious health effects. Therefore, it becomes critical to prevent groundwater contamination due to natural processes as well as human activities.

In contamination due to natural processes, the leaching of natural chemical deposits increases the concentrations of chloride, nitrate, iron and other organic and inorganic chemicals. On the other hand, agricultural activities and waste disposal on the land surface change the chemical composition of the ground water. The wastewater infiltrates through the vadose zone and, upon reaching the water table, continues to travel for large distances through the subsurface environment. When this water is drawn by wells and consumed without any treatment, it may be hazardous to human health. Hence, it is necessary to study the transport mechanism of reactive chemicals through porous media.

Solute transport in soil and groundwater systems is affected by various factors such as physical, chemical, and microbiological processes. Various mathematical models have been developed

by researchers to evaluate the transport of linearly interacting solutes in porous media (Ogata and Banks, 1961; Remson et al., 1971; Bear, 1972, 1979; Selim and Mansell, 1976; Goltz and Roberts, 1986; Selim et al., 1999; Abulaban and Nieber, 2000; Fitts, 2002; Berkowitz et al., 2008, Gao et al., 2009, 2012). The transport of chemical is affected by different processes and porous media properties including convective transport with flowing water, molecular diffusion, hydrodynamic dispersion, equilibrium or non-equilibrium exchange with the solid phase if reactive solutes are involved, and decay processes.

1.2 Motivation of present study

It is generally seen that the Advective dispersion transport equation was widely used to model solute transport through homogeneous porous media (Ogata and Banks 1961; Ogata 1970, Freeze and Cherry, 1979). Both analytical and numerical methods have been used to get the solution of transport equation by various investigators (Chiou et al., 1979; Eldho and Rao, 1997; Mohrlok et al., 1997; Delay et al., 1998; Elzein and Booker, 1999; Shashidhar et al., 2007; Bethe and Mohrlok, 2008; Mohrlok et al., 2010; Meenal and Eldho, 2012; Singh et al., 2010, 2012, 2013; Sharma et al. 2014). Most of the models were initially based on the classical one dimensional Advection-dispersion equation as studied by Lapidus and Amundson (1952), Van Genutcheten et al. (1974) and Van Genutcheten and Alves (1982). For a pulse input, this approach predicts symmetrical, bell-shaped breakthrough curves. Departures from this ideal behavior have been observed at scales of investigation ranging from column experiments to field-scale tests. Conservative solute transport in porous media is typically modeled using the generalized advection and dispersion equation (ADE) (Bear, 1972). The solution of ADE's in most groundwater transport applications requires numerical methods, excepting the limited cases where analytical solutions exist (van Genuchten and Alves, 1982 and Jarvis et al., 1991). Analytical solutions have an important role to play because they offer fundamental insight into governing physical processes, provide useful tools for validating numerical solutions, and are sometimes more computationally efficient. Most previously published analytical solutions to advective-dispersive transport problems are predicated on the assumption of a homogeneous porous medium (van Genuchten and Alves, 1982). In reality, subsurface porous media is seldom homogeneous and significant spatial variability of transport properties can be expected

(Gelhar, 1993; Dagan, 1982 and Dagan, 1984; Yates, 1992; Deng et al. 1993; Zhou and Selim, 2003;Chaudhuri and Sekhar 2007).

However, in case of heterogeneous porous medium,Advective dispersion transport equation fails to describe the solute transport by ADE because of the long tailing effect in that all the available water is not equally involved in solute transport. This results in dividing the available water into two components, which leads to the development of more complex models such as mobile-immobile model (MIM). The MIM model (van Genuchten and Wierenga, 1976) conceptualized the porous medium into mobile and stagnant immobile domains and takes into account the exchange between mobile and stagnant domains. There have been number of studies which gave better performance of mobile-immobile model than ADE for both homogeneous and heterogeneous media (Bond and Wierenga, 1990; Toride et al., 2003; Gao et al., 2009, 2010, 2012). Conceptually, the transport of solute through mobile-immobile zone is analogous to that of fractured porous medium (Tang et al., 1981.; Van Genuchten and Wierenga, 1976; Kumar and Sekhar, 2005; Kumar et al., 2006; Sekhar et al., 2006). An advance form of mobile-immobile is also studied by further dividing immobile liquid phase in slow and fast moving liquid (Kartha and Srivastava, 2008a, 2008b, 2012).

Reactive transport through porous media is affected by various factors such as equilibrium sorption, first order mass transfer coefficients, reverse sorption coefficients. After such extensive analysis of various forms of ADE and MIM were done. Later they considered one dimensional and multidimensional models for increasing complicated process and soil properties. This was done by extending the models to include different types of sorption sites, and different expressions characterizing physical and chemical non-equilibrium, and alternative geometries of immobile (stagnant) liquid phases in the medium (de Smedt and Wierenga 1984; Valocchi,1985 and 1988; Brusseau et al.,1989; Srivastava and Brusseau, 1996).

Hence, Brusseaue et al. (1989) had developed multi-process non-equilibrium (MPNE) model that includes both physical and chemical non-equilibrium for reactive solute movement through porous medium. The physical non-equilibrium transport is caused due to preferential and stagnant flows. The chemical non-equilibrium is caused due to the simultaneous presence of instantaneous and rate limted sorption of the solute in the solid and liquid forms. Most of the

studies were focused on the formulation of appropriate mass balance equations governing solute transport through porous media. The transport of sorbing solutes is modeled with mobile-immobile model, in which the porous media is represented as an interconnected continuum, and sorption is represented as an equilibrium process which is instantaneous and reversible with a linear isotherm.

As general the use of ADE has been frequently questioned by many investigators in recent years, as it cannot adequately account for anomalous transport in heterogeneous porous media, and alternative models have been proposed. The mobile-immobile model (MIM) presented by van Genuchten and Wierenga (1976) is a practical and physically based approach to describe anomalous solute transport behavior. Also, the presence of dead end pores in the medium influence the transport process. The liquid filled dead end pores were called immobile water and transfer of mass occurs between the mobile and immobile liquid zones. A model that accounts for multiple sources of non-equilibrium would be required to accurately represent these systems. Such model was developed by Brusseau et al. (1989).

It was found that there are other factors which affect the transport of reactive solute through porous medium. It is also known that distance-dependent dispersion has long been a focus of experimental and theoretical research in solute transport through porous media. The essence of distance-dependent dispersion is that the dispersion coefficients obtained from the analysis of the breakthrough curves by the Advective–dispersion equation (ADE) are not constant but increases with travel distance. The tracer test was used to measure dispersivity along with travel distance; the large value of the dispersivity was computed by Molz et al. (1983). This type of phenomenon occurred in the field-scale transport and in laboratory-scale transport (Pickens and Grisak, 198b; Gelhar et al., 1992; Gelhar, 1993; Vanderborght and Vereecken, 2007). The magnitude of dispersivities acquired from laboratory observation are usually in the order of a few to tens millimeters, while those from the field can be several orders of higher magnitude as reported by many authors (Pickens and Grisak, 1981a; Dagan 1982; Vanderborght and Vereecken, 2007; Gao et al. 2010, 2012). A general consensus at present is that the distance-dependent dispersion is used to represent the heterogeneous nature of porous media at different scales (Huang et al., 2006). Hence, ADE with a constant dispersion model cannot satisfactorily describe the solute transport at various scales in subsurface groundwater

systems (Pickens and Grisak, 1981b; Gao et al., 2009, 2010 and 2012). Huang et al. (1996) had developed analytical solution for one dimensional transport with linear asymptotic scale-dependent dispersion using the MIM model. They assumed that the dispersivity increases linearly with distance until some travel distance after which the dispersivity reached an asymptotic value.

From above discussion, it is clear that analytical solution of multiprocess non-equilibrium (MPNE) transport equations is not developed using asymptotic distance-dependent dispersion model. Hence, in the present study, an attempt has been made to derive semi-analytical solution of MPNE transport equations by using Laplace transform technique and the power series method with asymptotic dispersion model for constant concentration boundary condition (de Hoog et al., 1982; Moench, 1991). It is expected that the MPNE model with asymptotic distance- dependent dispersion can much better describe the behaviour of reactive contaminant transport through heterogeneous porous media. There are very few studies available in literature which uses long soil column (smaller than 12m) experimental data to study the behaviour of non-reactive solute in heterogeneous porous medium. Thus, there is a need to investigate the behaviour of reactive transport through long heterogeneous soil column. On the basis of literature review, following objectives were decided for this study:-

1.3 Objectives

The objectives of the present study are following:

1. To develop analytical solution of multiprocess non-equilibrium (MPNE) transport equations using asymptotic dispersivity.
2. To analyze the behavior of breakthrough curves in presence of both constant and asymptotic dispersion models
3. To conduct the soil column experiments for solute transport in 1500 cm long soil column experiments in the lab
4. To simulate the experimental breakthrough curves using asymptotic and constant dispersion models and to estimate transport parameters.
5. To conduct batch sorption experiments to estimate linear and nonlinear sorption isotherm of fluoride in soil media and these isotherms are used to simulate fluoride

transport through porous media.

6. To develop numerical model with finite difference and finit volume method and study its performance for advection and dispersion dominant cases.
7. To simulate breakthrough curves using variable mass transfer coefficient in presence of asymptotic distance dependent dispersion model.

1.4 Organisation of thesis

The thesis is organised in following chapters, the contents of which are briefly described.

Chapter 1 presents the introduction, motivation of present study and research objectives.

Chapter 2 presents the comprehensive review of literature pertinent to the field of solute transport through porous medium; recent development and gap found in the studies are identified.

Chapter 3 presents the conceptualisation of MPNE model and analytical solution of MPNE model with asymptotic distance-dependent dispersivity. Both physical and sorption related non-equilibrium are incorporated in the solution developed with asymptotic dispersivity which makes it more effective for the field application. Presented analytical solution is verified with existing analytical solution. Analytical solution was then used to simulate experimental breakthrough curves of non-reactive and reactive solute transport in 1500 cm long soil column experiments.

Chapter 4 presents the estimation of sorption isotherm of fluoride in different types of soil media via batch sorption and these isotherms are used to simulate fluoride transport through porous media. Freundlich and Langmuir isotherms are tested in case of fine sand and natural soil. Subsequently, implicit finite difference numerical technique is used to solve one-dimensional advection-dispersion transport equation. Transport of fluoride through a porous bed has been simulated with linear and nonlinear sorption models. Results show that fluoride breakthrough curves simulated by using the Freundlich nonlinear sorption model reveal good agreement with experimental observed data through soil column. Further, it is also seen that the

Freundlich nonlinear isotherm model gives best fit of concentration profiles in case of both fine sand and natural soil, as compared to Langmuir sorption model.

Chapter 5 presents the behavior of breakthrough curves in mixed heterogeneous soil column experiments. Advective dispersive transport equations are used for solute transport through mobile-immobile porous medium. In first part of the study, constant dispersion, linear and asymptotic distance-dependent dispersion functions are used to describe the scale effect and to simulate the experimental breakthrough curves observed in long soil column experiment. Also, a comparative study has been done among distance-dependent and constant-dispersion models, while simulating the experimental data of solute transport through soil column with constant mass transfer coefficient. In second part of the study, variable mass transfer coefficient as function of pore velocity and travel distance is considered and an empirical relation is derived from observed data from experiments.

Chapter 6 deals with finite volume method (FVM) and implicit finite difference method (FDM) used to solve transport equations for reactive solute transport through triple-permeability porous media. Performance of both FDM and FVM have been evaluated in presence of high value of Peclet number (Pe) for reactive transport through triple-permeability porous media. It is shown that, in case of advection dominant transport (i.e. at high value of Pe), numerical oscillation has been obtained by FDM, while oscillation-free result is seen by FVM in the presence of both small and higher values of mass transfer coefficients. In addition to this, behavior of spatial moments are investigated in the presence of various transport paramteres.

Chapter 7 summarises the work done and specifies the main conclusions based on experimental and numerical investigations of reactive solute transport through heterogeneous porous media, and provides suggestions for future studies.

Chapter 2

REVIEW OF LITRATURE

2.1 General

A comprehensive review of the available literature was undertaken to ascertain the current status of research in the field of reactive transport through saturated porous media with constant and distance-dependent dispersivity. It is also known that the groundwater quality is susceptible to natural and man-made contaminant sources. The reason for the degradation of the quality of groundwater includes municipal waste, waste from chemical industry, fertilizer used in the irrigation field etc. Therefore for the prevention and minimisation of pollution in groundwater, it becomes essential to understand the transport processes associated with contaminant through porous media. Follwoing transport mechanisms such as advection, dipersion, diffusion, sorption are occurred during reactive transport through porous media.

2.2 Advection transport

The advection transport is the movement of a chemical substance as it is carried along with bulk fluid movement or the movement of solute caused by groundwater flow. Advection is the most significant mass transport process. It results from large-scale gradients in fluid energy, although the resulting rates of mass transport are much less than those found for surface water transport. Advection is the primary process by which solute moves in the groundwater system (Bear, 1979). It is the fastest form of chemical transport in porous media and its concentration decrease in the direction of fluid movement.It can be expressed as

$$\frac{\partial C}{\partial t} = -V\frac{\partial C}{\partial x} \tag{2.1}$$

2.3 Dispersion transport

Dispersion is an effect of the departure of an individual particle from the average groundwater velocity, results from simultaneous action of both a purely mechanical and physiochemical phenomenon. Mechanical dispersion is basically the mean deviation in the velocity vector in both longitudinal and transverse directions caused due to the change in direction of velocity vector at every point of the fluid flowing through a porous media. The change in the direction of the velocity vector at any point depends upon the heterogeneity of porous media.Hence Variations in hydraulic conductivity due to lithological heterogeneities are the main sources of velocity variations. The hydrodynamic dispersion coefficient (D) is combination of mechanical dispersion (D_m) and bulk diffusion (D_0)..The advective flow velocity (v) and mean grain diameter (dm) have been shown to be the main controls on longitudinal dispersion parallel to the flow direction. it can be expressed as:

$$\frac{\partial C}{\partial t} = D\frac{\partial^2 C}{\partial x^2} \tag{2.2}$$

2.4 Diffusion transport

The domain of diffusion is the scattering of particles by random or turbulent motion at microscopic scale. Diffusion and dispersion takes place in two different types of domain. Diffusion is a component of dispersion. As flow takes place, the solute spreads in all directions at molecular scale for the reason that of concentration gradient and random motion on account of diffusion. The solute particles move from region of higher concentration to the areas of lower concentration due to diffusive transport, which also occurs in the absence of velocity of flow. This transport mechanism is associated with the molecular motions instead of bulk fluid movement (Bear, 1979).

2.5 Sorption transport

Sorption is the process by which chemicals are either entrained into soil or leaches out from the soil particles. Physical adsorption depends on Vander Waals forces of attraction between

molecules and resembles condensation of liquids. In chemical adsorption, the solute particle is held to the surface by chemical forces specific to the chemicals involved, and formation of the bond may require activation energy. The most common sorption transport mechanisms are Linear, Nonlinear, Freundlich, Langmuir, and Irreversible Reactions.

Specific sorption represents a chemical interaction between sorbet and sorbent, and occurs at specific sites on the surface of the sorbet. In chemisorptions, the chemical bonds between sorbet and sorbent usually is covalent. A molecule undergoing chemisorptions may lose its identity as atoms are rearranged to form new compounds fulfilling the unsatisfied valences of the surface atoms. Nonspecific sorption is the process in which solutes are attracted to the surface of the soil particles, generally from London-Vander walls or electrostatic bonds.

2.6 Review of literatures

In the following section, an attempt has been made to describe various analytical/numerical studies related to the solute transport through porous media for constant and distance-dependent dispersion models.

Valocchi (1985) had made an attempt to assess the criteria to find out the validity of local equilibrium assumptions for one-dimensional steady state homogeneous flow condition. A method is described to determine solute breakthrough curve for time moments. It is observed that validity of linear equilibrium assumption depends upon several macroscopic and microscopic parameters. Macroscopic parameter includes seepage velocity, hydrodynamic dispersion, time variation of mass input and microscopic parameters includes mass transfer coefficient, aggregate size distribution and distribution coefficient. Time moment methodology is used because analytical solution for coupled differential equation cannot be applied to non-equilibrium readily. It is also noted that the linear equilibrium assumption (LEA) criteria developed in this study is strongly dependent on hypothesized kinetic model.

Duijn and van der Zee (1986) had studied the transport of solute in two different regions which are separated by very sharp interface in the flow direction. Physical and chemical properties of both the regions are different but remain same throughout the experiments. First expression for approximate concentration is derived at interface boundary and then analytical solution is

derived for the solute transport in both the regions. Numerical and analytical solutions are compared and it was found that for larger values of retardation factor of lesser permeable region, a good agreement is achieved. A finite boundary in case of numerical simulation and an infinite boundary length in analytical solution were found to be the main differences for the out come of the solution. Analytical solution was found to be useful when the thickness of both regions is considered to be of same dimension. It was found that system resembling the flow domain is comparable for numerical and analytical solution.

Goltz and Roberts (1986) had developed three dimensional solutions for solute transport in an infinite medium considering porous medium in distributed discrete mobile-immobile zones to observe the tailing effect of breakthrough curve. Authors presented three dimensional solutions for advective-diffusive transport equation with infinite boundary condition. Analytical solution for point source was derived for infinite medium incorporating first order reaction and diffusion rate limitations. The solution was found to be similar for semi finite and infinite mediums at larger values of Peclet number.

Brusseau et al. (1989) had described the solute transport through porous media under the influence of multiprocess non-equilibrium. They considered two types of non-equilibrium for reactive transport through porous media. One is physical or transport related non-equilibrium which is present in the system because of the combination of mobile immobile regions and due to diffusive mass transfer from mobile or advective flow regions to immobile or non-advective flow region, second is the chemical or sorption related non-equilibrium is caused by the rate limited interactions between solute and the specific sites of sorbent. Authors had stated that employing bicontinuum model gives the combined effect of lumped kinetic terms causing the non-equilibrium while employing the MPNE is useful for detailed analysis. In the proposed model mobile and immobile regions are coupled by diffusive mass transfer within the intra aggregate pores. Then further the rate limited and instantaneous regions are coupled through instantaneous and rate limited coefficients. According to the above conceptualisation a mathematical model has been developed incorporating all types of non-equilibrium in the system. Model accounts explicitly for the multiprocess non-equilibrium, and the performance as compared to the bicontinuum model is found obviously superior if the parameters estimated for input are available. This model is aimed for the process level investigation. Model required

number of parameters, without that evaluation of model is dubious.

Valocchi (1989) had studied the spatial moments to analyse the depth average solute pulse in stratified porous media. Transport equation incorporated arbitrary variation in porous water velocity, dispersivity, and adsorption with first order reversible kinetic law. This paper presents more general solution to the problem discussed by the author in previous paper (Valocchi, 1988). It is found that dispersion term can be divided in three major components, hydrodynamic dispersion; vertical variation in velocity generates Taylor dispersion and dispersion due to kinetic sorption reactions. It is also found that deviation from local equilibrium behaviour depends on interexchange reaction and spatial variation of retardation factor and pore water velocity. The spreading is also affected by nature of correlation in pore water and retardation factor and slow sorption kinetics. At field scale the results obtained provide a good insight to physical and chemical parameters varying spatially.

Bond and Wierenga (1990) had made an attempt to investigate the effect of immobile water in unsaturated fine sand under steady and unsteady flow regimes. The results of experiments were simulated with two numerical models with immobile water and without immobile water. It was found that in case of steady state flow numerical solution of equation containing immobile water terms gives better representations of experimental data. The RMS value was significantly reduced by applying the numerical solution including the immobile water term. In case of unsteady flow experiments, immobile water terms was found to be lesser influencing the observed and simulated BTC's . The reason of this was explained in terms of wetting patterns, which was found to be different in both cases.

Brusseau (1991) had evaluated the capability of multiprocess non-equilibrium (MPNE) model to predict the transport of solute through stratified porous medium under the influence of multiprocess non-equilibrium. Starr et al.(1985) used data from the experiments which were performed by Sudicky et al. (1985) using chloride as non-reactive solute and strontium as reactive solute. It is found that MPNE model provides a valid representation of sorption dynamics for the stratified porous medium under the influence of multiple sources of non-equilibrium.

Goltz and Oxley (1991) had developed analytical model for organic contaminant specifically considering clean up well sites problem. Rate limited desorption was considered to be major reason for influencing contaminant load discharge. The analytical solution presented in Laplace domain solved for radial advection, dispersion and rate limited sorption. It was observed that analytical solution can be applied to estimate concentration filtered through well and concentration remaining in aquifer. Brusseau (1992) evaluated one-dimensional multifactor non-ideality model to represent the transport of sorbing solute under nonideal flow conditions. Results obtained from several field experiments have been simulated applying the numerical model. It is observed that single factor non-ideality model will give a lumped value for discrete parameters and this value cannot give proper information about discrete processes causing non-ideality in the transport. Proposed model accounts separately for multifactor participations in non-ideality. Field scale data are very well represented by the model, considering that all input parameters are obtained separately. Two domain approaches is found to be successfully applicable to represent the heterogeneity of hydraulic conductivity on solute transport. The only limitation of model is found to be its lacking of multi-dimensional solution. A more complex model can be used for representing the transport by enhancing dimension dependency.

Brusseau et al. (1992) presented a numerical model which explicitly accounts for conceptual MPNE model combining transformation reactions. This is an advance version of MPNE model represented by Brusseau et al. (1989), incorporating biotic/abiotic transformation reactions. The combination of transport related, sorption related processes with first order transformation reaction considered for more realistic representation. In this work potential impact of transformation reaction on solute transport is studied. Model was found to predict accurately the experimental data through a soil column packed with aggregated soil. MPNE transport model was founded very useful for the system affected by non-ideal transport and complex transformation reactions.

Tang and Aral (1992) had tested closed form solution for the transport through layered aquifer system. Verification of the analytical solution was done with standard examples available in the literature. The range of prediction of present solution is then tested for other aquifer-aquitard combinations. The present solution incorporates non-uniform, time dependent first type boundary conditions at influent and effluent end of domain. Advection, diffusion and first order

reaction terms are considered in both aquitard and main aquifer. Main aquifers are assumed to be two dimension finite systems and aquitard are one dimension infinite system. Laplace transformation is used for solving partial differential equation and separation of variable technique is used to assemble the solution. Vertical diffusion and advection in adjacent layer of aquitard is given. It was found that in most stratified aquifer is influenced with vertical advection in between the layers and cannot be ignored.

Brusseau (1994) reviewed the basic concepts related to contaminant transport, which is given by the results obtained from well-controlled field experiments designed to investigate the transport of reactive contaminants in the subsurface flow. Burr et al. (1994) had analysed the transport of reactive and non-reactive contaminant through heterogeneous and anisotropic geological formation by using multi-realization numerical model. Field scale displacement and dispersion behaviour of reactive and non-reactive solute was observed carefully and other non-ideality is lumped together in single factor of realization. The data of Bordon aquifer test was analysed and compared with several other solution given by different authors. It was found that a temporal increase in retardation factor was due to several local non-idealities and effect of intraparticle diffusion is negligible. In Bordon aquifer scenario nonlinear equilibrium sorption and sorption desorption processes are not significant. It is found that stochastic theories applied by Dagan (1982) provides upper limits of concentration standard deviation with decreases limits of concentration standard deviation with decreases eventually with travel distance. The uncertainty in concentration profile is compared for reactive and nonreactive solute after an equivalent travel distance. It was because local scale solute velocity enhances dispersion, which in turn decreases the uncertainty because plume smearing increases.

Xu and Brusseau (1996) had developed semi analytical solution for solute transport in porous media with spatially variable reaction processes, reverse sorption, reversible mass transfer and reversible transformations (radioactive decay, hydrolysis reaction and biodegradation). Laplace transformation technique is used to obtain the analytical solution in Laplace domain. It is found that constant obtained for spatial variation of transformation reaction decreases the rate of mass loss and affects the solute transport in the porous system. Brusseau et al. (1997) used a flow interruption, which can be used to discriminate between various sets of processes, such as rate-limited vs non-linear sorption and physical non-equilibrium vs heterogeneity.

Robinson et al. (1998) developed steady state and transient state analytical solution for solute transport in a finite system of parallel fractures with fracture skins using dual porosity model. For transient solution, Laplace transforms were inverted numerically and they presented a series solution. The steady state solution derived was closed form analytical solutions for solute transport in finite system of fracture porous media. Author also analysed the effect of fracture skins and reported an increase in distances of transport with thicker skins of lower porosity and lower diffusivity.

Zhan (1998) had investigated the transport of contaminant under different landfill conditions in a stratified formation. Considering leakage scenarios of continues waste leakage, temporal waste leakage, continues deep well injection wastes and temporal deep well injection wastes. Transport in a strongly heterogeneous aquifer is solved analytically without any perturbation approach and solution obtained for average and variable concentration. Author also considered field heterogeneity as the reason of dispersion and local dispersivity and hence diffusion can be neglected in field.

Elzein and Booker (1999) had investigated transport of solute through stratified porous media under the influence of multiprocess non-equilibrium condition. Numerical solution generally restricted to single layer and includes a single source of non-equilibrium. In this work author tried to implement boundary element method in Laplace domain to solve the advection-dispersion equation under the influence of multiple sources causing non-equilibrium and rate limited mass transfer. Infinite and semi-infinite domains are modelled accurately by using Green's function and using Laplace transformation eases out the need of time stepping and associated numerical complexity. The proposed boundary element solution is validated by predicting analytical solution developed in available literature. Presented solution is very well capable of dealing with heterogeneous porous media and anisotropic transport, parameter partitioning porous medium with lesser computational requirements. By deploying this method single layer and multilayer soil breakthrough curve has been predicted with good agreement. This method is also used for studying the migration of solute in sand aquifer bounded by silt layer at a nearby infiltration boundary of a lake. Inclusion of scale dependent dispersion function can improve the solution for more realistic and field scale problem.

Abulaban and Nieber (2000) studied the transport of sorbing solute from a heterogeneous porous medium. The sorption isotherm was considered to be linear and Freundlich behaviour of pulse of sorbing solute observed. Heterogeneity of porous medium was introduced both physically and chemically for observing the skewness of solute plume. Results of homogeneous and heterogeneous field test are compared and it is seen that plume was more scattered in former case. The retardation of solute plume also causes a slower solute moment through porous medium. The effect of nonlinear sorption was found more in field heterogeneity which is also supported by the studies performed by Jury and Utermann (1992). In large heterogeneous medium a shorter pulse input is found to be scattered in starting of simulation. This broken up of plume initiates oscillatory behaviour of spatial moments derived in homogeneous medium. The oscillatory behaviour causes the skewness of solute plume.

Neville et al. (2000) had developed analytical solution for one-dimensional advection-dispersion equation under the influence of multiprocess non-equilibrium model based on theory developed by Brusseau et al. (1992). The solution is derived in Laplace domain and de Hoog et al. (1982) algorithm is used for inverting Laplace solution. The solution is extended for different boundary conditions and found to be satisfactorily applicable on controlled lab experimental data. The solution is also used for estimation of parameters at field scale. By using Laplace techniques, solution is remained free from spatial discretization and time stepping which can be obtained easily.

Al-Tabbaa et al. (2000) Had performed laboratory experiments for migration of nonreactive solute (NaCl) through short length of stratified porous media. Authors had atempt to investigate the effect of different direction of stratification on the dispersion coefficient. Parallel perpendicular and inclined directions of layers to the flow direction have been arranged. Author also tried to evaluate the effect of scale of heterogeneity on dispersion coefficient. Dispersion coefficients from three different methods have been calculated and it was found that dispersion coefficient increases with the volume under same porosity.

Toride et al. (2003) had examined the variation of dispersion as a function of water content in homogeneous dune sand by applying mobile-immobile model. An experimental setup was

prepared of dune sand soil column. A comparison of dispersivity at various water contents has been tried to evaluate the functional relationship interlinking the parameters. It was found that at lower water content, pore water velocity is lower but resistance to solute transfer between mobile-immobile phase's increases, which in turn causes the transverse diffusion to be higher. Peclet number was found lower at lower water content. In the solution it was found that lower water content, lower velocity and thinner water films between pore spaces resulted in maximum dispersivity. Bhallamudi et al. (2003) described a sub-time stepping approach for fluid dynamics problems in which a implicit formulations is used to obtain transient solutions. This method is suitable for extensive simulations where portions of a domain are temporally over-discretized by conventional implicit time-stepping approaches.

Chastanet and Wood (2008) had attempt to apply volume averaging method on solute transport through highly heterogeneous porous media. In the proposed solution decoupling of macro and micro solution system are done by neglecting concentration variation. Spherical inclusion geometry is considered and convective terms are neglected to determine the analytical expression. Convective terms in low conductivity region can be important but in higher conductivity region convective terms are neglected for simplicity. Proposed model can be applied to any bimodal geometry except uncoupled transient model and need to be analysed in that case. Bethge and Mohrlok (2008) studied the risk of groundwater contamination by flood water seepage from retention areas and calculated contaminant infiltration.

Avila and Brieter (2009) had developed a mathematical model for solving advection-dispersion equation for mobile-immobile region including two site non-ideality and first order transformation reaction introducing multiple solutes. Simultaneously, two solutes were injected and both follows nonlinear sorption isotherm. FORTRAN numerical solution is developed and tested for adequacy and capability with experimental data obtained from soil column experiments. Materials used in soil column were silica gel and soil from a specified landfill. It was found that advantages of taking general bicontinuum model is that effect of dual porosity and non-equilibrium can be solved simultaneously or one be switched off for simpler solution. Sorption is best observed in silica gel as compared to soil sample because of heterogeneity. Proposed mathematical model was found performing satisfactorily with experimental data. But for more extensive computations, the competitive sorption term should be given more attention.

In proposed model if competitive sorption is ignored, false prediction may observe and error in estimation of isotherm parameters may be noticed. Brindha and Elango (2011) studied in detail about fluoride in groundwater, which has a major problem to human society in the world. The main source of fluoride in groundwater is the rocks which are rich in fluoride. The other sources for fluoride are infiltration of agricultural runoff containing chemical fertilisers, improper disposal of liquid waste from industries, alumina smelting, cement production and ceramic and brick firing.

Leij et al. (2012) had developed a new dual advection dispersion equation (DADE) model for solving solute transport through layered porous medium. It was assumed that flow rates were nonzero in distinct pore domains and solute transport was linear. The basic equation used for developing the model is combination of advection dispersion equation for transport in uniform porous medium and mobile-immobile model for mass transfer in between mobile and immobile regions. In continuation to the transport model presented by Leij and Bradford (2009), an analytical solution for DADE is derived using Laplace transformation technique while assuming the uniform dispersivity in both the regions. Explicit nonzero solutions for solute concentration are derived which the function of time and position of both domains is including time moments of BTC's. Presented analytical solution is used for describing the transport of solute pulse through a dual-velocity medium including different combinations of Darcy's flux, water content and rate parameters. Solution was found to show double peaks in volume and flux averaged concentrations varying spatially and temporally respectively. The reason for double peak was found to be travel time difference in the separate processes of advection and first order mass transfer. Advection was found to be dominating in mobile domain and first order mass transfer in between mobile and immobile domains. Presented solution was found to illustrate in depth scenario of bimodal behaviour of BTC's obtained for Japanese Andisol soil having distinct intra and inter aggregate porosity.

Pickens et al. (1981a) demonstrated the method for the in situ determination of adsorptive and dispersive properties of sandy aquifer using radial injection dual tracer test. Reactive (85Sr) and non-reactive (131I) tracers were introduced together. Using multilevel point sampling device at various radial distances and depths, spreading and adsorption of both were compared. The effect of physical and chemical non-equilibrium is incorporated in "effective dispersivity" term

rather than using a separate kinetic term. Values of effective dispersivity for reactive solute were found 2-5 times to that of non-reactive solute. Inclusion of non-equilibrium effects in effective dispersivities found to be very effective analysing reactive solute transport in the field.

Pickens et al. (1981b) had carried out study on scale and time dependency of dispersion coefficient and stated that the scale which is used to define the flow domain and obtain groundwater samples can result in a scale dependency of the mechanical dispersion coefficient or dispersivity. Author conducted several tests in the laboratory and in the field and derived an expression relating longitudinal dispersivity to the statistical properties of a stratified medium and the mean travel distance of the solute. It is found that the concentration profile within an aquifer or breakthrough curve at sampling position depends on monitoring system and it can result in some apparent spreading and subsequently larger dispersivity. It is also found that wide distribution of permeability at field causes the increased longitudinal dispersion. The spreading and reversal of spreading in the direction of flow results from the law of mass conservation and can also be caused by porosity and moisture content variations within the stratified medium.

Molz et al. (1983) investigated the scale dependency of dispersivity in field expression. Authors introduced a new formulation and used recent field experimental data for representing scale-dependent dispersion coefficient (Pickens and Grisak 1981b). By the analysis of observed data of several well tracer tests, it was found that hydraulic conductivity and local transverse hydrodynamic dispersion influences dispersion term. The scale dependent dispersivity alone cannot adequately represent the processes causing spreading due to dispersion. The effect of field scale, accurate value of hydraulic conductivity and scale of heterogeneity are given more emphasis in accounting arbitrary dispersion coefficient. By giving more attention to these parameters, good agreement is found with experimental data. The present study is limited to perfectly stratified porous media. It was found that macrodispersivity contains a convective term that dominates hydrodynamic dispersion and for a finite value of local transverse dispersivity this convective term attains an asymptotic value. The present solution was found to be erroneous when applied near to source for the case of scale dependent dispersive coefficient.

Mackay et al. (1986) had conducted a large-scale field experiment on natural gradient transport

of solute in groundwater. By introducing two inorganic, five halogenated organic tracers and over 5000 sampling points to collect over 19,900 samples, fate of tracers elucidated in a 3-D porous medium. A spatial and temporally detailed data set in high contrast is collected for 7 different types of solutes. By observing the collected samples it was found that tracer trajectory and velocity followed the same path, which could be predicted by conventional techniques and hypothesis.

Roberts et al. (1986) had studied the long-term behaviour of organic solutes under natural gradient conditions by mean of moment estimates. It was found that mass was conserved for two of the solute (carbon tetrachloride and tetra-dichlorobenzene) and rest of the solute converted their masses in different compounds. A markedly increment in the value of retardation factor was found as much as by 150% from its initial value for all tracers due to heterogeneity and deviation from local equilibrium. It was also found that the behaviour of organic plume through heterogeneous porous medium can be very well described by the model considering porous medium as a quasi-homogeneous continuum.

Barry and Sposito (1989) had developed a closed form solution of the transport equation with time dependent dispersion coefficient in a semi-infinite spatial domain. Solution incorporated arbitrary initial and boundary conditions. A stable numerical scheme utilizing a trapezoidal quadrature rule has been used, and for small time step solution is found to be stable. It was found that this solution is a reliable result for solute transport problem through a wide variety of heterogeneous porous material.

Yates (1990) had developed analytical solution for the transport of dissolved substances through heterogeneous porous medium. Dispersion was assumed to be distance dependent in the solution. Constant concentration and constant flux type boundary condition has been imposed and solution obtained using inverse of Laplace transformation of advection-dispersion transport equation. The solution was very useful in verifying the numerical accuracy of comprehensive finite element solutions, and for investigation some aspects of scale dependency of dispersion coefficient.

Dykhuizen (1991) had developed asymptotic solutions for solute transport in dual porosity

model. A general equation is derived from porosity models and solution is obtained by analysing moments of particular solution. It is found that dual velocity model is generally governed by same set of equations. Temporal behaviour of various moments of solution equation is used to investigate effective velocity and dispersion coefficient. It is also observed that the asymptotic solution is found to valid for a very large time and for a particular greater distance. Early time behaviour can be predicted by more velocity model region while neglecting the slower velocity model region. The importance of dual porosity model complexity is important in the intermediate time interval only.

Sternberg and Greenkorn (1994) had performed several experiments in linear, homogeneous and non-uniform porous medium using spherical glass bed in Lucite columns. The experiments were similar to Taylor (1953) except different combinations of columns were joined in series in order to create a series of layered heterogeneous porous media. The effect of porosity, permeability, velocity, length and column position are tried to investigate the dispersion values obtained from homogeneous porous medium, whether can predict the dispersion in heterogeneous medium or not. It is found that averaging the dispersivity in serial system for predicting the accurate value of dispersivity is not enough for heterogeneous medium. General linear model of variables showed that for layered homogeneous-heterogeneous porous material advective velocity, permeability, kinematic viscosity, length and layer order play significant role is prediction of dispersion values. Prediction of dispersion based on average of dispersion coefficient, Peclet number and Reynolds number of homogeneous porous medium were found inappropriate. By this experiment it is clear that extrapolation of dispersion from one media to similar other one on the basis of permeability is not possible.

Aral and Liao (1996) had developed analytical solution for time dependent dispersion coefficient of two-dimensional advection-dispersion equations for infinite aquifer domain. Constant, linear, asymptotic and exponential function of dispersivity is considered for pulse and continues contaminant point source boundary conditions. In this solution dispersivity is assumed to be the function of travel time from its source under steady and uniform flow field conditions. It is found that analytically point pulse initial distribution and instantaneous pulse injection tend towards similar solutions. It was also observed that dispersivity can be analysed in two parts firstly at small time scale where it continues to grow with position and time

secondly at larger time when it attains a maximum value and becomes constant. This behaviour of dispersivity is found to influence longitudinal and transverse dispersivity at small times. It is also noticed that for observing a non-expansion and constant behaviour of dispersivity, a very large time scale will be needed. That is why the dispersivity is considered pre-asymptotic because practically it is impossible for dispersivity to achieve infinite time step. It is found that increase in dispersion is significant in longitudinal direction as compared to transverse direction during pre-asymptotic time period. It is observed from analytical solution that time dependent nature of dispersion equation do not influence solute transport pattern significantly. Presented solution is found useful in case of 2-D domains with scale dependent dispersion function. Analytical solution is very useful in evaluating field problem under influence of scale dependent dispersion.

Gerke and van Genuchten (1996) had analysed dual porosity model of first order by introducing geometry dependent coefficient β in transport equation. This term represents macroscopically size and shape of particles of soil and rock matrix. First order model is used for calculating the values of β by a direct matching with the solution of the diffusion model under standard boundary condition. It is seen that dual porosity model generally required geometrical information of soil or rock matrix and the geometry information of interface area through which solute will be exchanged. Naturally porous media consists of combination of matrix blocks of different size and shape which leads to very complex interfacial geometries. An expression is derived to appropriately describe the geometrical structure of dual porosity medium. Preferential flow in dual porosity system of various matrix geometries is simulated using a first order type water transfer term. Comparison of simulation with two dimensional reference model showed that proposed approach has limitation due to simplifying highly nonlinear transfer processes in an approximate first order rate model. Mass transfer coefficient is found sensitive to the geometry matrix pore system. Proposed approach provides a good approximation of more realistic two dimensional representations of mass transfer processes. This approach provides the capability to measure the porous material properties in dual porosity model. This model is not limited to homogeneous matrix formation; it can be explored for other combinations as well.

Hunt (1998) had obtained solution for advection-dispersion equation with distance dependent

dispersion coefficient for unsteady flow under instantaneous source and for steady flow condition for constant contaminant source boundary condition. The solution was presented ranging from one-dimensional to three-dimensional and compared with corresponding standard solution of constant dispersivity. The comparison of both the solutions showed that constant dispersivity calculated by considering maximum flow length over estimates the dispersion of smaller travel distance and underestimates at the point of maximum dispersion. It is also found that with constant dispersion function the point of maximum concentration reaches slightly earlier as compared to scale dependent dispersivity for instantaneous source input. Concentrations are found exactly zero at upstream in case of scale dependent dispersivity whereas a finite concentration appeared at the same point when considered constant dispersivity. The comparison clearly showed the advantages of scale dependent dispersivity over constant dispersivity and for any flow length scale dependent dispersivity provides better solution.

Matrix diffusion is an important transport process in subsurface soil media of low hydraulic conductivity to predict transport of contaminant. Boving and Grathwohl (2001) studied the diffusive transport in different geological media such as limestone and sandstone rocks. Pung and Hunt (2001) developed a one-dimensional analytical solution of transport equation with a dispersion coefficient linearly increasing with distance. Hunt (2002) had suggested single perturbation approximation approach for the solute transport through porous media including scale dependent dispersivity. Author presented comparison of exact and approximate solution for a pit of source located in uniform flow region. The advection-dispersion equation is solved in two dimensions for dispersion. Dispersivity is assumed to be linearly increasing with an increase in distance from the pit to downstream. Comparison of exact solution with approximate perturbation solution shows that former solution has acceptable accuracy for field problem.

Srivastava et al. (2002) had investigated the effect of rate-limited sorption, first order mass transfer and first order transformation on one-dimensional solute transport through heterogeneous porous medium. Analytical solution is derived using an exponentially distance dependent dispersivity function for spatial moment of solute in solution phase. Spatial moments are calculated for solute present in the advective region only. A comparative study is also

performed for observed temporal moments that whether simple ADR model or MPNE model are suitable and more appropriate. It is found that heterogeneous porous medium can be satisfactorily represented by increasing macrodispersivity value. It is also observed that heterogeneity and nonideality both contributes equally to second moments and third moment is largely contributed by heterogeneity of the medium.

Chen et al. (2003) had presented mathematical model to describe transport of contaminant in cylindrical coordinate system with scale dependent dispersion coefficient. Dispersion is assumed to be increasing linearly with distance from input source. Scale dependent advection-dispersion equation is solved in a radially convergent flow field using Laplace transform power series technique with variable coefficient. The accuracy of proposed analytical solution has been verified by employing Laplace transform finite difference solution of transport equation. A comparison has been done of two solution obtained using constant dispersivity and scale dependent dispersion coefficient. The comparison of breakthrough curves showed that rising limbs and spreading tail were found similar but intermediate portion showed small differences. Proposed solution is used for simulating field tracer test and found following the linear function of dispersivity. It is also observed that constant dispersion assumption underestimates the dispersivity values whereas scale dependent dispersivity estimates the near about accurate value. It is suggested that dispersivity/distance ratio derived from constant dispersion for a radially convergent tracer test should be multiplied by 4 for a close approximation in scale dependent dispersion.

Furman et al. (2003) had proposed Laplace-transform analytic element method (LT-AEM) for the solution of transient flow problems in porous media. Analytic element method (AEM) is used to solve the resultant time-independent modified Helmholtz equation, and the solution is inverted numerically back into the time domain. It is especially well suited for problems in which a solution is required in limited number of points in space time, and for problems involving materials with sharply contrasting hydraulic properties. The solution is general, retaining the mathematical elegance (in the Laplace domain) and computational efficiency of the AEM. They illustrated the method by solving the problem of transient flow to a well through a uniform confined aquifer with a circular inclusion of contrasting hydraulic conductivity and speicific storage.Rao et al. (2004) studied an approach for planning

groundwater development to control seawater intrusion by using barrier extraction wells in coastal aquifer.

Huang et al. (2006) had analysed laboratory experimental data of conservative solute transport obtained in earlier experiments.. Parameter estimations for Fractional advection dispersion equation (FADE) is developed using semi analytical solution of FADE to the measured data of different transport scales. Semi analytical solution is used for estimation of input parameters for FADE for steady state flow conditions and step input of solute. Analysis of data set obtained from a 12.5 m long homogeneous and heterogeneous soil column showed scale dependency of dispersion coefficient. Dispersion is found to be increasing with distance in both homogeneous and heterogeneous soil column but spreading was more in heterogeneous soil comparatively. It is found that for homogeneous soil an exponential relation between dispersion coefficient and distance and for heterogeneous soil power function showed best results. Three kinds of FADE models were used for depicting the transport in homogeneous and heterogeneous soil medium. In homogeneous soil all three model found in good agreement with scale dependent dispersion but for heterogeneous soil agreement was less satisfactory.

Chen et al. (2008a) used analytical power series solution for transport equation considering hyperbolic asymptotic distance-dependent dispersivity. Chen et al. (2008b) had presented analytical technique to solve two-dimensional advection-dispersion equation with dispersivity as a linear function of distance. Analytical solution for two-dimensional advection-dispersion equation. Power series method is used to obtain the solution in addition to Laplace transformation and finite Fourier cosine transform. Longitudinal and transverse dispersivity both considered being linearly dependent function of distance. Power series method is found to be effective for solving advection-dispersion equation with distance dependent dispersivity function in two dimensions, incorporating changes in transport coefficient.

Gao et al. (2010) had presented mobile immobile model for depicting the processes included in solute transport through heterogeneous porous medium. The proposed model includes scale dependent dispersion coefficient. Linear and exponential dependencies of dispersivity are considered in the proposed model. First order degradation and linear adsorption are also included in model. The transport equation is solved in Laplace domain by applying de Hoog

techniques for Laplace inversion. An arithmetic mean of distance dependent dispersivity is calculated and it was found that at medium heterogeneity MIM produced comparable results as with scale dependent dispersivity function. In case of strongly heterogeneous porous medium discrepancies are found due to accumulated effect of scale dependency of dispersivity. It was found that constant and linear dependent dispersivity used in MIM model gives lesser satisfactory results as compared to exponential dependent dispersivity. Experimental results of 1250cm heterogeneous soil column experiments are represented accurately by including exponential distance dependent dispersivity in MIM model.

Gao et al. (2012) had combined the mobile–immobile model (MIM) with an asymptotic dispersivity function of travel distance to embrace the concept of scale-dependent dispersion during solute transport in finite heterogeneous porous media. The proposed MIM with an asymptotic scale-dependent dispersivity (MIMA) was analytically solved by the Laplace transform technique and the extended power series technique. The semi-analytical solution of MIMA compared with the Laplace transformed finite-difference numerical solution, and they are agreed well with each other. The applicability of MIMA was tested with simulation of experimental solute concentration data through 1250cm long heterogeneous soil column. Simulation results were indicated that MIMC could not adequately describe solute transport in the large heterogeneous soil column and it overestimated solute transport dispersion at foregoing distances away from 1200 cm. In contrast to MIMC, the simulation results of MIMA were in satisfactory agreement with the measured ones as MIMA considered the asymptotic characteristic of increased dispersion in porous media. These results indicate that MIMA was efficient to capture the evolution of scale-dependent dispersion behavior, and it was useful for describing solute transport in heterogeneous porous media.

Sharma and Srivastava (2012) had investigated the effect of heterogeneity on spatial concentration profile by employing advection dispersion equation incorporating terms for physical and chemical non-equilibrium. Numerical solution for spatial moments of the advection dispersion equation adding exponential dispersivity function is presented. Implicit finite difference methodology is used for obtaining numerical solution of the ADE for reactive solute. Linear distance-dependent and exponential time dependent dispersion coefficients are considered for observing the comparison on breakthrough curves. It is found in the

concentration profile that time dependent dispersivity simulates a lower peak as compared to distance dependent dispersivity. It was also observed that present numerical solution is much simpler than stochastic analytical method and more efficient than solution given by Monte Carlo method. It was also noted that obtained solution is much simpler and reproduces the results at same level accuracy as by rigorous complex computational model. The only limitation observed in the model is in the estimation of uncertainty analysis of field data including single realization. Leij et al. (2012) presented a dual-advection dispersion equation to describe one-dimensional solute transport in dual-permeability medium with different flow rates and linear solute transfer between two domains. They derived an analytical solution using Laplace transform method with time and modal decomposition based on matrix diagonalization, and assuming the same dispersivity for both domains. Meenal and Eldho (2013) used a Mesh free point collocation method (PCM) with radial basis function (RBF) to study flow and contaminant transport simulation and decontamination in porous media. They studied the effects of decontamination strategies such as flushing and pumping effects with a total dissolved solids contaminated aquifer. Morales et al (2014) conducted experiments to study the behavior of pathogen through porous media and their results showed that the early arrival of breakthrough curve of bacteria and virus indicated the presence of preferential flow.
Boving (2014) studied the contamination of groundwater with hydrocarbons methyl ter-butyl ether, which occurs from leaking of gas stations. Kuranchie et al (2015) conducted experiment to study electrical resistivity of iron ore of mine tailing. Further, Sciortino et al. (2015) developed both numerical and analytical solutions of transport equation for solute in dual-permeability media considering the two domains having different velocities and dispersivities. Sharma et al. (2016) conducted mobile-immobile soil column experiments to investigate the behavior of concentration profile for both conservative and non-conservative tracer.

2.7 Summary

Several studies are done on emphasising the nonideal transport behaviour of solute through porous medium. It is also found that solute transport through heterogeneous porous medium is mainly influenced by physical and chemical non-equilibrium. Inclusion of physical and chemical non-equilibrium in the contaminant transport model developed for porous medium, explores the opportunity for the process level investigation. Further the scale dependent

behaviour of dispersivity attracted lots of research; different scale dependent functions of dispersivity (linear, exponential and asymptotic) have been included in several studies.

From above discussion, it is clear that analytical solution of multiprocess non-equilibrium (MPNE) transport equations is not developed using asymptotic dispersion model. There is a need of study, to develop an analytical solution of non-equilibrium transport model with asymptotic dependent dispersion coefficient. The inclusion of scale dependent dispersivity in MPNE model is expected to enhance the prediction of solute transport at lab and field scale. It is also found that not much of literature is available on the experimental investigation of reactive solute transport through porous medium with large travel distance. Therefore a study of reactive solute transport through porous medium is needed, using MPNE with scale dependent dispersivity function.

Chapter 3

DEVELOPMENT OF SEMI-ANALYTICAL SOLUTION AND APPLICATION

3.1 General

In this chapter, an attempt has been made to describe the conceptual model of multiprocess non-equilibrium transport model, which was given by Brusseau et al. (1992). However, many experimental, theoretical and numerical studies have been performed to understand the physical process of solutes transport in porous media. A number of approaches towards the solution of flow and transport equations have been proposed. Analytical solutions have been developed to obtain the concentration of solutes in aqueous phase for some simple cases. A brief description of the conceptual model and the governing equations are used in the present study. Afterwards, analytical solution of multi process non-equilibrium transport equations with asymptotic dispersion function is developed. The developed model is used to simulate observed breakthrough curves for both non-reactive and reactive solutes through long soil column experiments.

3.2 Conceptual model of non-equilibrium transport

Early studies on the transport process in porous media modelled only the advection and diffusion/dispersion processes. Also, the porous medium was typically idealized as homogeneous. For these models, the governing equations were simple enough to be solved analytically. As more and more knowledge of the heterogeneity of porous media and the reactivity of the solutes was gained, the conceptual model and the governing equations tended towards more complexity. Obviously, it is almost impossible to exactly represent the transport process by a conceptual model. However, it is now well established that a realistic conceptualization of the transport process for typically encountered pollutants in the porous media must account for multiple reactions including sorption and transformation. In this study

we have used a state of the art of the conceptual model, which accounts for multiple sources of non-equilibrium and transformation. Two types of processes leading to non-equilibrium during transport of a reactive solute have been suggested. First is the transport-related non-equilibrium (also known as physical non-equilibrium) and second is the sorption-related non-equilibrium (chemical non-equilibrium). Physical non-equilibrium is generally attributed to the presence of regions within the porous medium in which there is minimum advective flow and has been observed in aggregated soils and in a heterogeneous porous media. This affects the transport of both non-sorbing and sorbing solutes. Chemical non-equilibrium, on the other hand, is typically caused by intrasorbent diffusion and by rate-limited interactions between the solute and specific sorption sites of the sorbent. Non-equilibrium resulting from intrasorbent diffusion involves the diffusive mass transfer of sorbent within the sorbent matrix. Both physical non-equilibrium and intrasorbent diffusion involve a diffusive mass transfer mechanism. However, these are considered to be different because physical non-equilibrium is a pore diffusive process and intrasorbent diffusion is similar to a solid diffusion process. In contrast to transport-related non-equilibrium, sorption-related non-equilibrium influences only sorbing-solutes.

Most early studies conceptually model non-equilibrium by using a bicontinuum approach, in which the porous medium is divided into two domains. During applications of bicontinuum models, it is assumed that a single process is responsible for the non-equilibrium. Brusseau et al. (1989) developed a conceptual model based on multiple processes of non-equilibrium (MPNE) to simulate solute transport in porous media where both transport-related and sorption-related non-equilibrium processes occur. This model was further extended (Brusseau et al. 1992) to include transformation reactions, which were described as a first order process. Since this model is central to the work performed in this thesis, a detailed description of the model is given in this section.

The conceptual model for multiprocess non-equilibrium with transformation (MPNET) divides the porous media into two solution phases and four sorption domains as shown in Figure 3.1. The two solution phases are characterized by widely different flow velocities and are termed advective (or mobile) and non-advective (or immobile) regions. Each region comprises two sorption domains, one where instantaneous sorption occurs (domains 1 and 3) and the other where sorption is rate-limited (domains 2 and 4). The model is formulated by linking 1 and 2 in

parallel to the advective region and domains 3 and 4 in parallel to the non-advective region.

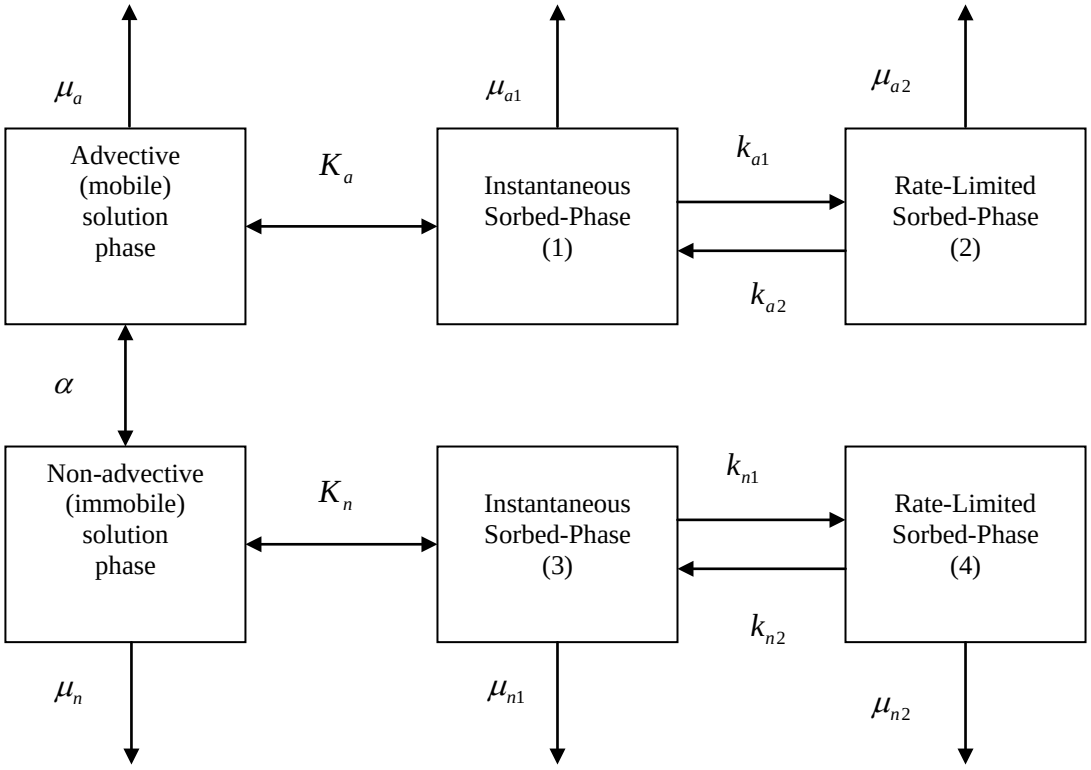

Figure 3.1 The conceptual model for the multiprocess non-equilibrium with transformation model of reactive transport through porous medium.

The instantaneous transfer of solute occurs between the interaggregate (advective) region and the surface of the organic matter situated on external surfaces of the aggregates (sorption domain 1). Diffusive mass transfer within the matrix of the organic matter couples sorption domain 1 and 2. The advective and non-advective (intraaggregate) regions are coupled with diffusive mass transfer within the intraaggregate pores. Transfer between the non-advective region and sorption domain 3 is instantaneous as it was between the advective region and domain 1. The coupling between sorption domains 3 and 4 is similar to that between domains 1 and 2. Transformation is assumed to take place in all the domains and regions.

3.3 Governing Equations

Based on this conceptual model, Brusseau et al. (1992) developed general transport equations that account for both the physical and chemical non-equilibrium for reactive solute transport through porous media. The advective-dispersive-reactive transport equation for transport of solute through the advective region of a porous media can be written as:

$$(\theta_a + f\,\rho F_a K_a)\frac{\partial C_a}{\partial t} + f\,\rho\frac{\partial S_{a2}}{\partial t} = \frac{\partial}{\partial x}\left[\theta_a D(x)\frac{\partial C_a}{\partial x}\right] - q\frac{\partial C_a}{\partial x} - w(C_a - C_n) - (\mu_a\theta_a + \mu_{a1} f\,\rho F_a K_a)C_a - \mu_{a2} f\rho S_{a2} \quad (3.1)$$

The mass balance for the non-advective region can be described by the following equation:

$$(\theta_n + (1-f)\rho F_n K_n)\frac{\partial C_n}{\partial t} + (1-f)\rho\frac{\partial S_{n2}}{\partial t} = w(C_a - C_n) - (\mu_n\theta_n + \mu_{n1}(1-f)\rho F_n K_n)C_n - \mu_{n2}(1-f)\rho S_{n2} \quad (3.2)$$

where, x is the spatial coordinate (L), θ_a is the fractional volumetric water content of the advective region (L^3/L^3), θ_n is the fractional volumetric water content of the non-advective region (L^3/L^3), f is the mass fraction of sorbent constituting the advective region, ρ is the bulk density of the porous medium (ML^{-3}), F_a and F_n are the mass fraction of sorbent for which sorption is essentially instantaneous, K_a and K_n are the equilibrium sorption coefficient for advective and non-advective region (L^3M^{-1}), C_a is the concentration of solute in the solution phase for advective region (ML^{-3}), C_n is the concentration of solute in solution phase for non-advective region (ML^{-3}), t is the time (T), S_{a2} and S_{n2} are the rate-limited sorbed-phase concentration in advective and non-advective regions, respectively (MM^{-1}), q is the specific discharge (LT^{-1}), w is the first-order coefficient for mass transfer between the advective and non-advective regions (T^{-1}), μ_a and μ_n are the first-order transformation coefficient for the solution phase in advective and non-advective regions, μ_{a1} and μ_{n1} are the transformation coefficients (T^{-1}) for the instantaneous sorbed-phase of advective and non-advective regions, respectively, and μ_{a2} and μ_{n2} are the transformation coefficients for rate-limited sorbed-phase

domains of advective and non-advective regions, respectively (T^{-1}). Dynamics of sorption and transformation for the rate-limited domains are described by:

$$\frac{\partial S_{a2}}{\partial t} = k_{a2}\left[(1-F_a)K_aC_a - S_{a2}\right] - \mu_{a2}S_{a2} \tag{3.3}$$

$$\frac{\partial S_{n2}}{\partial t} = k_{n2}\left[(1-F_n)K_nC_n - S_{n2}\right] - \mu_{n2}S_{n2} \tag{3.4}$$

where k_{a2} and k_{n2} are the first-order reverse sorption rate coefficients (T^{-1}) for the advective and non-advective regions, respectively.

It is generally accepted that the solute transport can be well described by the advection dispersion equation for laboratory column packed with homogeneous soils (Bear 1972). However, in heterogeneous soils the measured breakthrough curves usually show early arrival and long tailing due to the inherent heterogeneity of natural soils at various scales (Berkowitz et al., 2006). Such phenomena can be found during solute transport in repacked soil column. It is also recognized that the estimated dispersivity is not constant but varies with spatial scales (Gelhar et al., 1992). Even if the field is macroscopically homogeneous, the dispersion coefficient is not a constant from the beginning, but only after the tracer plume has been transported over a large enough domains, containing several correlation lengths (Dentz et al 2011). Therefore, it is difficult for advection dispersion equation with a single set of parameters to predict breakthrough curves at different distances. Hence, asymptotic dispersivity function of travel distance is used to embrace the concept of scale-dependent dispersion during solute transport in heterogeneous media.

The hydrodynamic dispersion coefficient $D(x)$ is a function of distance in the porous media (L^2T^{-1}). It is commonly expressed as follows without consideration of molecular diffusion (Bear, 1972):

$$D(x) = \alpha(x)V_a \tag{3.5}$$

where, $\alpha(x)$ is the dispersivity (L) and $V_a = q/\theta_a$ is the pore water velocity in advective region. It is observed that the dispersivity generally increases with transport distance in the subsurface groundwater systems. However, an asymptotic dispersivity is considered to account for the heterogeneity of the porous media. For this case, the dispersivity is assumed to initially increase with travel distance and approach an asymptotic value eventually.

Asymptotic distance dependent dispersion coefficient is given by (Picken and Grisak 1981b):

$$D(x) = a\left(1 - \frac{b}{x+b}\right)V_a \tag{3.6}$$

where *a* is an asymptotic dispersivity value (*L*) and *b* is a characteristic distance (L) which determine the travel distance for the dispersivity to reach half of the asymptotic value. Figure 3.2 shows the spatial variation of the asymptotic dispersion function equal to the ratio between distance dependent dispersion coefficient and asymptotic dispersivity for different values of *b*. The values of b depend on the extent of the pre-asymptotic zone. For a smaller value of *b* the dispersivity will approach the asymptotic value faster. The value *b* equal to zero indicates the constant dispersion.

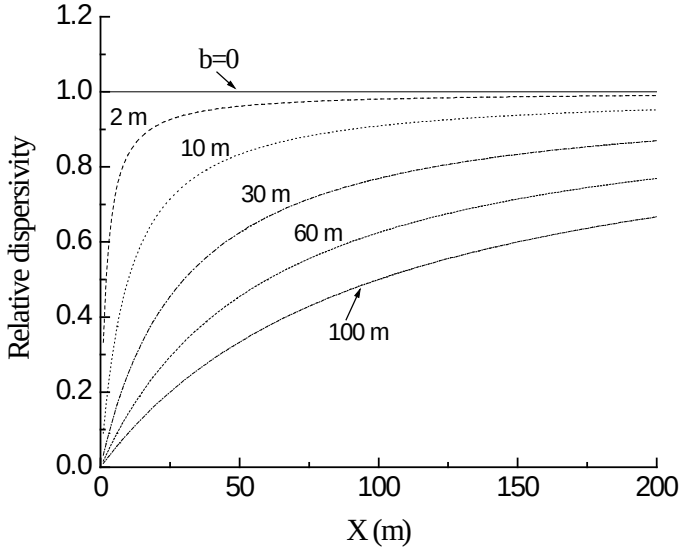

Figure 3.2 Variation of relative dispersivity with different values of characteristic distance (b).

3.4 Initial and Boundary conditions

The initial solute concentrations are assumed to be uniform with C_i for the entire domain. It assumed that the initial rate limited sorbed phase concentrations S_i (at time t= 0) are same in both the mobile and immobile regions of the porous medium. The zero gradient boundary condition is imposed at the exit, which can satisfy the mass balance requirement and ensure the continuity in concentration at x=L. The initial and the exit boundary conditions can be written as:

$$C_a(x,0) = C_n(x,0) = C_i \qquad 0 \le x \le L \tag{3.7a}$$

$$\frac{\partial C_a(L,t)}{\partial x} = 0 \qquad 0 \le t \le \infty \tag{3.7b}$$

Constant concentration condition at inlet can be written as:

$$C_a(0,t) = C_0 \qquad 0 \le t \le \infty \tag{3.7c}$$

where C_0 is the constant source concentration (ML^{-3}). The value of dispersion coefficient, $D(x)$ is equal to zero at x=0.

3.5 Semi-analytical solution

There are several modeling techniques ranging from simple analytical, semi-analytical solutions and too complex numerical codes which were developed in recent years. The procedure of derivation of the semi-analytical model is described below.

Taking Laplace transform of Equation (3.3) with respect to time, t

$$P\overline{S_{a2}} - S_i = k_{a2}\left[(1-F_a)K_a\overline{C_a} - \overline{S_{a2}}\right] - \mu_{a2}\overline{S_{a2}} \tag{3.8}$$

After simplifying,

$$\overline{S_{a2}} = \frac{\left[k_{a2}(1-F_a)K_a\right]\overline{C_a} + S_i}{P + k_{a2} + \mu_{a2}} \tag{3.9}$$

Similarly, Laplace transform of Equation (3.4) can be written in simplified form as:

$$\overline{S_{n2}} = \frac{[k_{n2}(1-F_n)K_n]\overline{C_n} + S_i}{P + k_{n2} + \mu_{n2}} \tag{3.10}$$

Laplace transform of Equation (3.2) can be written as:

$$R_n P\overline{C_n} - R_n C_i + (1-f)\rho P\overline{S_{n2}} - (1-f)\rho S_i = w(\overline{C_a} - \overline{C_n}) - [\mu_n\theta_n + \mu_{n1}(1-f)\rho F_n K_n]\overline{C_n} - \mu_{n2}(1-f)\rho\overline{S_{n2}} \tag{3.11}$$

Substituting the value of $\overline{S_{n2}}$ from Equation (3.10) into Equation (3.11) and after simplifying following expression can be obtained as:

$$\overline{C_n} = \frac{w(P + k_{n2} + \mu_{n2})\overline{C_a} + R_n(P + k_{n2} + \mu_{n2})C_i + (1-f)\rho k_{n2} S_i}{R_n P^2 + A_1 P + A_2} \tag{3.12}$$

where coefficients are:

$$A_1 = R_n(k_{n2} + \mu_{n2}) + w + \mu_n\theta_n + \mu_{nl}(1-f)\rho F_n K_n + (1-f)(1-F_n)\rho K_n k_{n2} \tag{3.13a}$$

$$A_2 = (w + \mu_n\theta_n + \mu_{nl}(1-f)\rho F_n K_n)((k_{n2} + \mu_{n2}) + (1-f)(1-F_n)\rho K_n k_{n2} \tag{3.13b}$$

$$R_a = \theta_a + f\,\rho\,F_a\,K_a \tag{3.13c}$$

$$R_n = \theta_n + (1-f)\,\rho\,F_n\,K_n \tag{3.13d}$$

Taking Laplace-transform of Equation (3.1) and after simplifying:

$$\theta_a D(x)\frac{d^2\overline{C_a}}{dx^2} + \left(\theta_a\frac{\partial D(x)}{\partial x} - q\right)\frac{d\overline{C_a}}{dx} - \overline{C_a}\left(w + \mu_a\theta_a + \mu_{al}f\rho F_a K_a + R_a P\right) + w\overline{C_n} - \overline{S_{a2}}\left(\mu_{a2}f\rho + f\rho P\right) + R_a C_i + f\rho S_i = 0 \tag{3.14}$$

And after substituting the value of $\overline{C_n}$ from Equation (3.12) and $\overline{S_{a2}}$ from Equation (3.9) into above Equation (3.14) and simplified form can be written as:

$$D(x)\frac{d^2\overline{C_a}}{dx^2}+\left(\theta_a\frac{\partial D(x)}{\partial x}-q\right)\frac{d\overline{C_a}}{dx}-A_3\overline{C_a}+A_4=0 \tag{3.15}$$

where

$$A_3=w+\mu_a\theta_a+\mu_{al}f\rho F_aK_a+R_aP-\frac{w^2\left(P+k_{n2}+\mu_{n2}\right)}{R_nP^2+A_1P+A_2}+\frac{f\rho\left(\mu_{a2}+P\right)k_{a2}K_a\left(1-F_a\right)}{\left(P+k_{a2}+\mu_{a2}\right)} \tag{3.16a}$$

$$A_4=C_i\left[R_a+\frac{wR_n\left(P+k_{n2}+\mu_{n2}\right)}{R_nP^2+A_1P+A_2}\right]+S_i\left[\frac{w(1-f)\rho k_{n2}}{R_nP^2+A_1P+A_2}-\frac{f\rho\left(\mu_{a2}+P\right)}{\left(P+k_{a2}+\mu_{a2}\right)}+f\rho\right] \tag{3.16b}$$

Substituting the value of $D(x)=a\left(1-\frac{b}{x+b}\right)V_a$ into Equation (3.15) and yields the following final simplified equation:

$$\frac{(ax)V_a}{(x+b)}\frac{d^2\overline{C_a}}{dx^2}-V_a\left[1-\frac{(ab)}{(x+b)^2}\right]\frac{d\overline{C_a}}{dx}-\frac{A_3}{\theta_a}\left[\overline{C_a}-\frac{A_4}{A_3}\right]=0 \tag{3.17}$$

Defining, $Y=\overline{C_a}-\frac{A_4}{A_3}$, Equation 3.17 can be changed to the following equation:

$$\frac{(ax)V_a}{(x+b)}\frac{d^2Y}{dx^2}-V_a\left[1-\frac{(a\,b)}{(x+b)^2}\right]\frac{dY}{dx}-\psi Y=0 \tag{3.18}$$

where, $\psi=A_3/\theta_a$

The solution of Equation (3.18) can be described by power series method with undetermined coefficients as (Kreyszig, 1999; Chen et al., 2008a)

$$Y(x,p)=x^r\sum_{m=0}^{\infty}a_mx^m=\sum_{m=0}^{\infty}a_mx^{m+r} \tag{3.19}$$

where the exponent r is a constant and it can be determined using an indicial equation. Substituting Equation (3.19) together with its term-wise differentiation into Equation (3.18) and following equation can be obtained:

$$\left(\frac{ax}{x+b}\right)V_a\sum_{m=0}^{\infty}(m+r)(m+r-1)a_m x^{m+r-2}-\left[V_a-\frac{ab}{(x+b)^2}\right]\sum_{m=0}^{\infty}(m+r)a_m x^{m+r-1}-\psi\sum_{m=0}^{\infty}a_m x^{m+r}=0 \tag{3.20}$$

Rearranging the terms of Equation (3.20) can be related as:-

$$\begin{aligned}\sum_{m=0}^{\infty}\left[ab(m+r)(m+r-1)+(ab-b^2)(m+r)\right]a_m x^{m+r-1}\\ +\sum_{m=1}^{\infty}\left[a(m+r-1)(m+r-2)-2b(m+r-1)-\frac{\psi}{V_a}b^2\right]a_{m-1}x^{m+r-1}\\ -\sum_{m=2}^{\infty}\left[(m+r-2)+2\frac{\psi}{V_a}b\right]a_{m-2}x^{m+r-1}-\frac{\psi}{V_a}\sum_{m=3}^{\infty}a_{m-3}x^{m+r-1}=0\end{aligned} \tag{3.21}$$

Equation (3.21) works for any given value of x. The sum of coefficient of power x^{m+r-1} on the left hand side of Equation (3.21) should be zero (Chen et al., 2008a). For m=0, it gives following equation:

$$\left[abr(r-1)+(ab-b^2)r\right]a_0=0 \tag{3.22}$$

As a_0 cannot be equal to zero, the indicial equation of Equation (3.22) can be written as:

$$ar^2-br=0 \tag{3.23}$$

The two roots of equation (3.23) are r=0 and r=b/a, respectively. Using equation (3.21) and for m=1,2,3,..... following equations can be obtained:

$$a_1=\left[\frac{-ar(r-1)+2br+\frac{\psi}{V_a}b^2}{ab(r+1)r+(ab-b^2)(r+1)}\right]a_0 \tag{3.24a}$$

$$a_2 = \frac{-\left[a(r+1)r - 2b(r+1) - \frac{\psi}{V_a}b^2\right]a_1 + (r + 2\frac{\psi}{V_a}b)a_0}{ab(r+2)(r+1) + (ab - b^2)(r+2)} \tag{3.24b}$$

$$a_m = \frac{-\left[a(m+r-1)(m+r-2) - 2b(m+r-1) - \frac{\psi}{V_a}b^2\right]a_{m-1} + \left[(m+r-2) + 2\frac{\psi}{V_a}b\right]a_{m-2} + \frac{\psi}{V_a}a_{m-3}}{ab(m+r)(m+r-1) + (ab - b^2)(m+r)} \tag{3.24c}$$

(Equation (3.24c) can be used to obtain the value of m=3,4,5,.....).

Introducing the coefficients of equation (3.24a-c) into Equation (3.19) with different roots, i.e., $r = 0$ and $r = b/a$, following two linearly independent solutions $Y_1(x, p)$ and $Y_2(x, p)$ can be obtained of Equation (3.18) (Chen et al., 2008). Therefore, the general solution of Equation (3.18) can be expressed in terms of $Y_1(x, p)$ and $Y_2(x, p)$.

$$Y(x, p) = B_1 Y_1(x, p) + B_2 Y_2(x, p) \tag{3.25}$$

where,

$$Y_1(x, p) = \sum_{m=0}^{\infty} a_m x^m \tag{3.26}$$

$$Y_2(x, p) = \sum_{m=0}^{\infty} a_m x^{m+b/a} \tag{3.27}$$

where B_1 and B_2 are two coefficients which can be determined using two prescribed boundary conditions. The value of B_1 and B_2 can be obtained in terms of the inlet and exit boundary conditions. The solution of MPNE in the Laplace domain can be expressed as:

$$\overline{C_a} = B_1 Y_1(x, p) + \mathrm{B}_2 \mathrm{Y}_2(\mathrm{x},\mathrm{p}) + \frac{\mathrm{A}_4}{A_3} \tag{3.28}$$

The value of B_1 and B_2 can be obtained in terms of inlet and exit boundary condition using $Y_1(x = 0, P) = a_0 = 1$ and $Y_2(x = 0, P) = 0$. The following expressions can be written as:

$$B_1 = \frac{C_0 - C_i}{P} \tag{3.29a}$$

$$B_2 = \left(\frac{C_i - C_0}{P}\right)\frac{\frac{dY_1(L,P)}{dx}}{\frac{dY_2(L,P)}{dx}} \tag{3.29b}$$

In this study, the value of the coefficient a_0 is considered as 1. After derived solutions in terms of Laplace domain, numerical Laplace inversion method is used to obtain in real time domain. In this paper, the numerical inversion of Laplace transform is done by de Hoog algorithm (de Hoog et al., 1982). The de Hoog's algorithm has been widely applied on numerous flow and transport problems and has been found to perform satisfactory on both advection and dispersion dominated cases (Moench, 1991; Park and Zhan, 2003; and Furman and Neuman, 2003; Gao et al., 2010). The de Hoog's algorithm of the inverse Laplace transform approximates in the form of a Fourier series.

$$C(x,t) = \frac{1}{\mathrm{T}}\exp(aT)\,Re\left(\frac{\bar{C}(x,a)}{2} + \sum_{k-1}^{2M}\bar{C}\left(x, a + \frac{ik\pi}{T}\right)\right) \tag{3.30}$$

where T is the period of approximating the Fourier series and the value is taken as $T = 0.80\mathrm{t}$ (Neviile et al., 2000), a is related to the the singularities in the transformed solution which is estimated as:

$$a = \alpha - \frac{\ln(E_r)}{2T} \tag{3.31}$$

The value of $\alpha = 0,\ E_r = 0.001\ and\ M = 7$ is taken as suggested by de Hoog et al. (1982).

3.6 Validation of the semi-analytical solution

The analytical solution for multiprocess non-equilibrium (MPNE) transport equation is not available in the literature for asymptotic dispersivity. Hence, present semi-analytical solution of MPNE model is validated for simplified case of mobile immobile (MIM) model with asymptotic dispersivity of Gao et al. (2012). In the comparison cases, adsorption of the solute is not considered and the initial concentration in the medium is taken equal to zero. The length of finite system is taken as 10 m. The flow rate (q) is 0.4 m/day. The water content of the medium system is taken to be θ=0.4 and water content in the mobile region equal to θ_a=0.3 and in immobile region is θ_n=0.1. The value of mass transfer coefficient (w) is 0.01 per day. The

comparison tests are conducted under various combinations of *a* and *b* values which are key parameters. Figure 3.3 shows the comparison of concentration profile obtained at 10 m from present semi-analytical solution and with different values of *a* (*a*=2m, 4 m, 6 m and 10 m) and a fixed value of *b*=10 m.

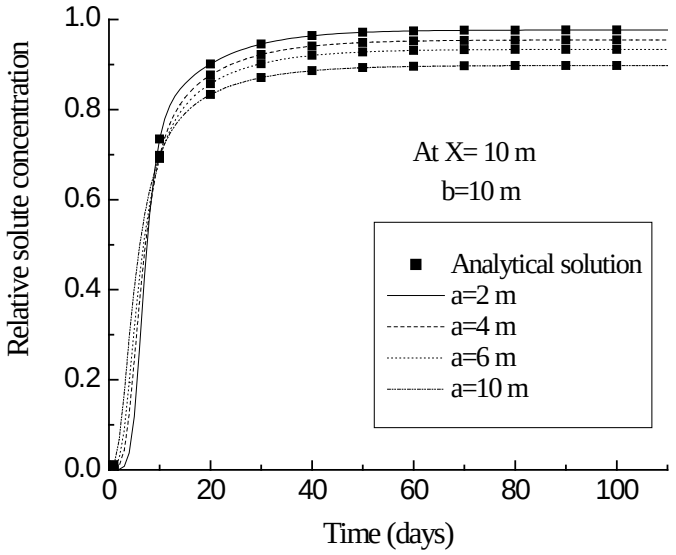

Figure 3.3 Comparison of the concentration profile at 10 m obtained from semi-analytical solution with different values of 'a' for a fixed value of 'b' equal to 10m.

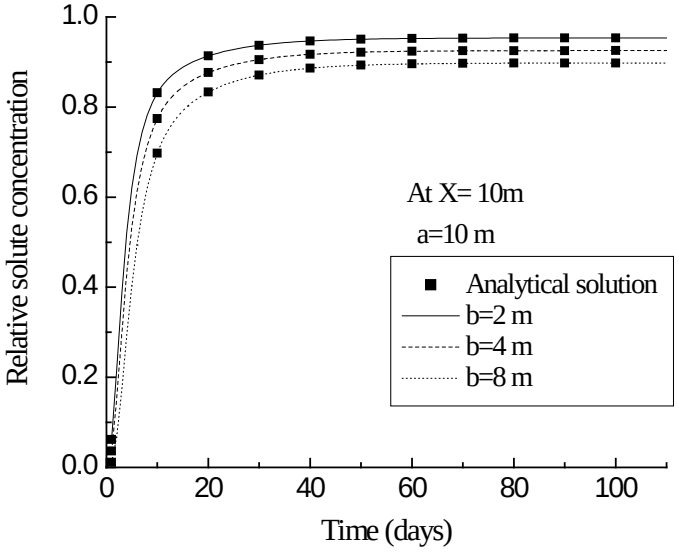

Figure 3.4 Comparison of the concentration profile at 10 m obtained from semi-analytical solution with different values of 'b' for a fixed value of 'a' equal to 10m.

Similar, comparison results are shown in Figure 3.4 with different values of *b* (*b* = 2 m, 4 m, 8 m) and a fixed value of *a* = 10 m. Comparison results between present solution as compared with the analytical solution gives very good match.

3.7 Application of model

3.7.1 Solute transport Experiments in long soil column

For applicability of developed model, laboratory experiments were conducted on a 1500 cm long horizontally placed heterogeneous soil column. Figure 3.5 represents the line diagram of soil column experiments in the lab and also actual photograph of experimental model is shown in Figure 3.6.

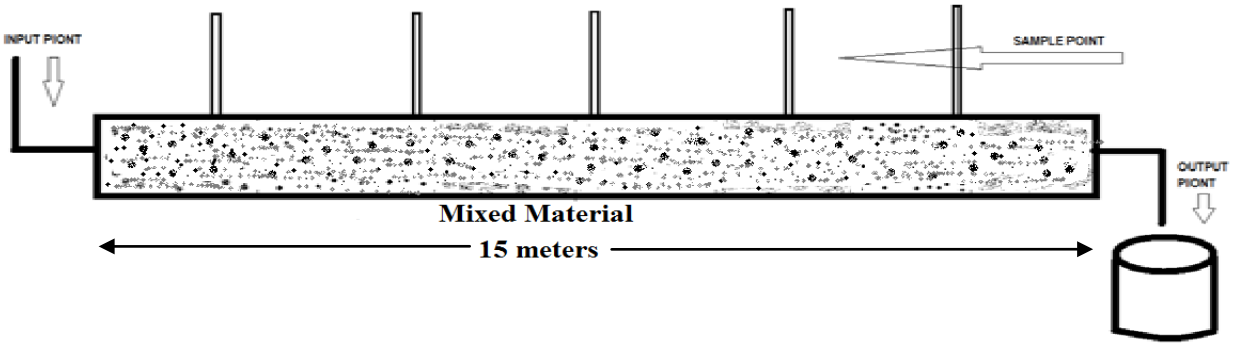

Figure 3.5 Line diagram of experimental set-up filled with mixed soils in long horizontal column.

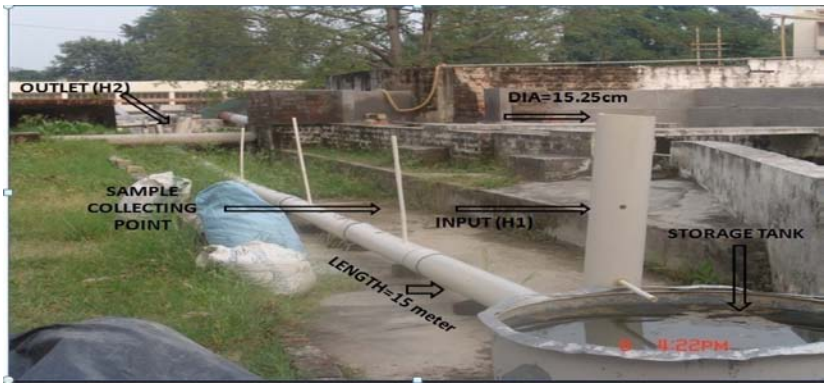

Figure 3.6 Photograph of experimental set-up for long horizontal column.

Sodium chloride and sodium fluoride were used as non-reactive and reactive tracers in the experiments. A horizontally placed column made-up of acrylic pipe with size of 6 mm thickness, having 15 cm diameter and 1500 cm long was considered. The soil column was packed with soil mixtures of natural soil, gravel, fine sand and coarse sand in equal proportion by weight. The mean particle size (D_{50}) of natural soil is 0.33 mm, gravel is 6 mm, fine sand is 0.75 mm and coarse sand is 1.1 mm. Figure 3.7 represents the grain size distribution curve for mixed soil media used in the experiment. The mixed soil had a median size, D_{50}=0.9 mm, D_{60}=1.1 mm, D_{30}= 0.33 mm, D_{10}=0.11 mm. The dry bulk density of mixed soil was found to be equal to 1.72 g/cm^3.

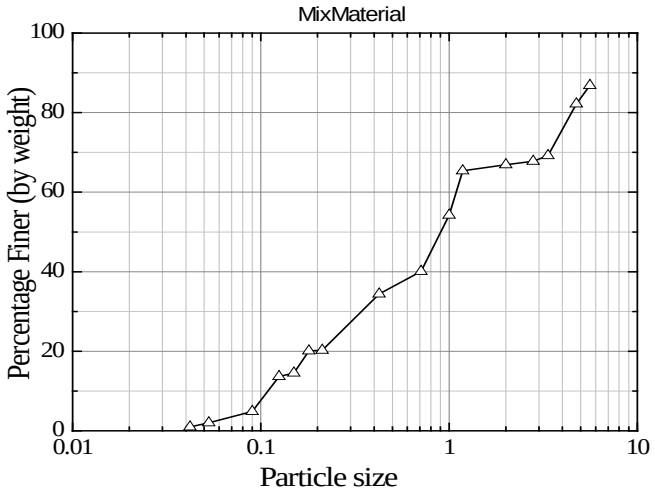

Figure 3.7 Grain size distribution curve of mix soil media.

Prior to filing, the soil material was cleaned, washed and dried to ensure that the material free from organic matters. The soil column was packed with mixture of materials in layer by layer to get the uniform density throughout the column length. During packing, piezometers were installed laterally at 100 cm intervals in the center along the length of column. The horizontally placed soil column was fully saturated slowly with tap water for three to four days, and the steady-state water flow condition was established by using peristaltic pump. The soil column was saturated slowly from inlet of the soil column with deaired tap water during start of the solute transport experiment. Thus, entrapped air in the soil column was removed. A peristaltic pump is used to obtain a steady saturated flow in the soil column. Sodium chloride (NaCl) solution with initial solute concentration of C_0=60 mg/L was injected into the soil column

through peristaltic pump. Similarly fluoride with an initial solute concentration of 5 mg/L in solution phase was injected at inlet of soil column through peristaltic pump.

A continuous concentration type input is maintained at the inlet of the column and solute concentration in solution phase was measured for different time interval at a distance of 300 cm, 600 cm, 900 cm, 1200 cm and 1500 cm along the soil column and also pulse type boundary condition also done for Chloride at the above different distance in the analysis of Mobile Immobile model (MIM) of chapter 5 of this thesis. The samples at this interval were taken with sampling bottles after sampling and labeling the sample were tested for the reactive and non reactive solute of fluoride and chloride, respectively. Fluoride was tested with SPADNS method using the HACH DR 5000 spectrophotometer (APHA 1995) where as Chloride was done using Silver nitrate titration method as follows:

i) Chloride

The amount of chloride (conservative solute) present in water can be easily by titrating the given water sample with siliver nitrate solution.

The silver nitrate reacts with chloride ion according to 1 mole of AGNO3 reacts with 1 mole of chloride. The titrant concentration is generally 0.02M.Silver chloride is precipitated quantitatively, before red silver chromate is formed.

The end of titration is indicated by formation of red silver chromate from excess silver nitrate the result is expressed in mg/L of chloride (with a molecular weight of 35.45 g/mol. The procedure is as follows;-

1. Sodium chloride of 99.5% purity was used.
2. 1 gm of sodium chloride was dissolved in 1 lit of water which introduces 0.60PPM Conc.
3. Potassium chromate was used as indicator.
4. For preparation of the titrant, 2.395 gm silver nitrate was dissolved.
5. 50ml volume of samples was taken in conical flask, then after 1 ml of potassium chromate indicator was mixed.
6. Then the samples were titrated till the yellow colour turned in to brick red.
7. The initial and the final reading was noted down and the concentration was calculated by the following formula:

Mg Cl-/L= (A-B) xN x 35.450 x 1000/ (ml sample) (3.35)

Where:

A= ml titration of sample

B = ml titration for blank, and

N= Normality of silver nitrate

Mg NaCl=(mg Cl-/L) x 1.65 (3.36)

where, concentration units are in mg/l

ii) Fluoride

For the testing of the samples HACH DR5000 Spectrometer is used the methods for computing the concentration of the samples is as follows:

1. Each of the 10ml sample was mixed with 2ml of SPADNS dye and provided 1 minute of reaction time.
2. Then small Vials were filled with mixture and the absorbance of the sample is observed at 570 nm using the instrument.
3. This absorbance was then converted into the concentration using standard concentration absorbance profile plotted for the range of 10 ppm.
4. Before testing in spectrometer, all the samples were filtered with 0.45µm cellulose acetate syringe filter for avoiding any interference caused by turbidity or colloid particles.

The estimated value of total volumetric water content, i.e., $\theta = (\theta_a + \theta_n)$ of the soil media within the column was measured as 0.38, and the observed flow rate (q) at the outlet of the soil column was 0.326 cm/min. The computed value of bulk density (ρ) of the soil media was found to be equal to 1.74 g/cm^3.

3.7.2 Parameter estimation and simulation of experimental data of chloride

The MPNE model is identical to MIM model for non-reactive transport through porous media. The breakthrough curves of Chloride were observed at 300 cm, 600 cm, 1200cm and 1500cm down gradient in the flow direction. These data of experimental breakthrough curves are simulated using mobile-immobile model with constant dispersivity (MIMC) and mobile-immobile model with asymptotic dispersivity (MIMA). There are three parameters in MIMC model, i.e., (θ_a, w and D) and four parameters (θ_a, w, a and b) in MIMA. However, MIMC and MIMA models have similar mobile water fraction and mass transfer coefficient values. The

main difference between them was that MIMC has a constant dispersion coefficient in the mobile region, whereas the dispersivity in MIMA has an asymptotic distance–dependent function with parameters of a and b. Thus, in the simulation process, the Levenberg-Marquardt nonlinear least square optimization approach was firstly used to fit the breakthrough curve at 1500 cm with MIMC to determine the values of θ_a, w and D. The fixed value of θ_a and w, the other two parameters (a and b) in MIMA are determined by fitting it with breakthrough curve at 1500 cm.

Firstly, the experimental breakthrough curve of chloride obtained at 1500cm was fitted using MIMC model with constant dispersion model. Estimated value of dispersivity was found to be equal to 108.56 cm, the value of mass transfer coefficient, w=2.31E-05 min^{-1} and the value of water content in the mobile region was θ_a =0.34. Other measured parameters were kept same as measured. Now the experimental BTC was simulated with constant and asymptotic distance-dependent dispersion models. The model parameters are estimated with optimization algorithm and their values were a =82.73 cm, b =148.21 cm for asymptotic distance-dependent model. The estimated model parameters for constant and asymptotic distance-dependent dispersion models are listed in Table 3.1.

Table 3.1 Model parameters used for simulation of Chloride BTC.

Parameters	MIM model
q (cm/min)	0.326
θ_a	0.34
θ_n	0.04
w (min^{-1})	2.31E-05
Dispersivity (cm)	108.56
Asymptotic distance dependent coefficient,	a=82.73 cm b=148.21 cm

Figure 3.8a shows the fitted BTC at 1500 cm distance with constant (MIMC) and asymptotic distance dependent (MIMA) dispersion models. It can be seen that constant dispersion model tends to overestimate the BTC at small transport time. Also, the estimated value of coefficient of correlation r^2=0.9754 and RMSE=0.0814 for MIMC model, and value r^2=0.9965 and root mean square error, RMSE=0.02631 are obtained for the MIMA model. This value indicates that

the value of coefficient of correlation is higher for MIMA model as compared to MIMC model. Thus, indicating the unsuitability of MIMC to simulate the BTC as compared to MIMA model. These estimated model parameters for constant and asymptotic distance dependent are kept fixed and the experimental BTC at 300 cm, 600 cm and 1200cm are simulated using these parameters. The simulated experimental breakthrough curves at 300 cm, 600 cm and 1200 cm are shown in Figures 3.8b, 3.8c, 3.8d. The estimated value of coefficient of correlation and RMSE is shown in Table 3.2 for MIMC and MIMA dispersion models. It can be seen from Figures 3.8(b-d) that a higher arrival time is observed with constant dispersion model as compared to MIMA model. A much better fit was obtained with asymptotic distance dependent model as compared to constant dispersion model.

Table 3.2 Goodness of fit values for Chloride BTC simulation using MIMC and MIMA models

Distance	MIMC		MIMA	
(cm)	r^2	RMSE	r^2	RMSE
1500	0.9754	0.0814	0.9965	0.0263
1200	0.9881	0.0569	0.9988	0.0176
600	0.9651	0.0832	0.9947	0.0259
300	0.9895	0.0389	0.9897	0.0472

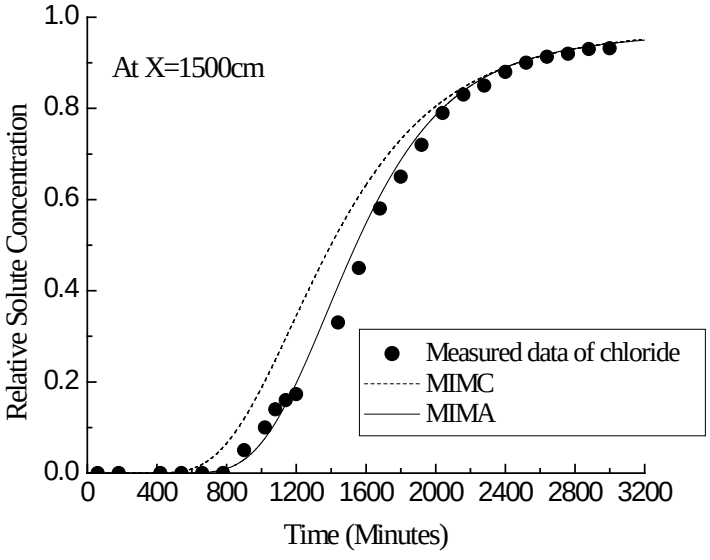

Figure 3.8a Simulation of observed experimental data of chloride at 1500 cm down gradient distance using MIMC and MIMA dispersion models.

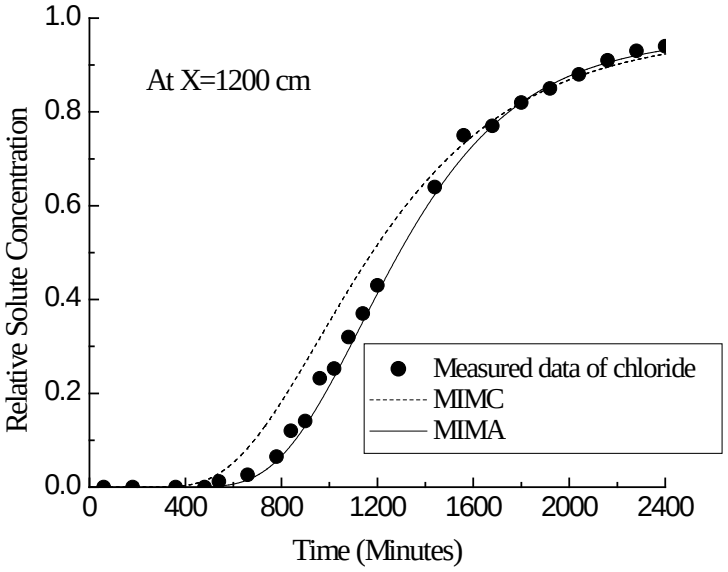

Figure 3.8b Simulation of observed experimental data of chloride at 1200 cm down gradient distance using MIMC and MIMA dispersion models.

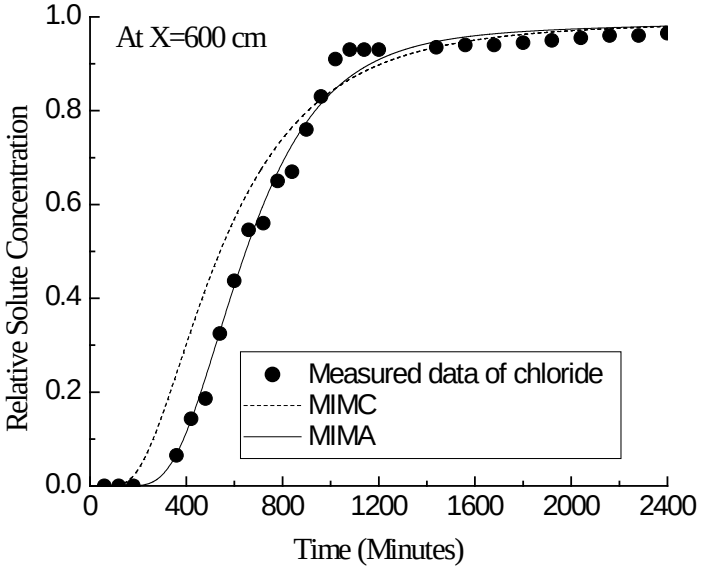

Figure 3.8c Simulation of observed experimental data of chloride at 600 cm down gradient distance using MIMC and MIMA dispersion models.

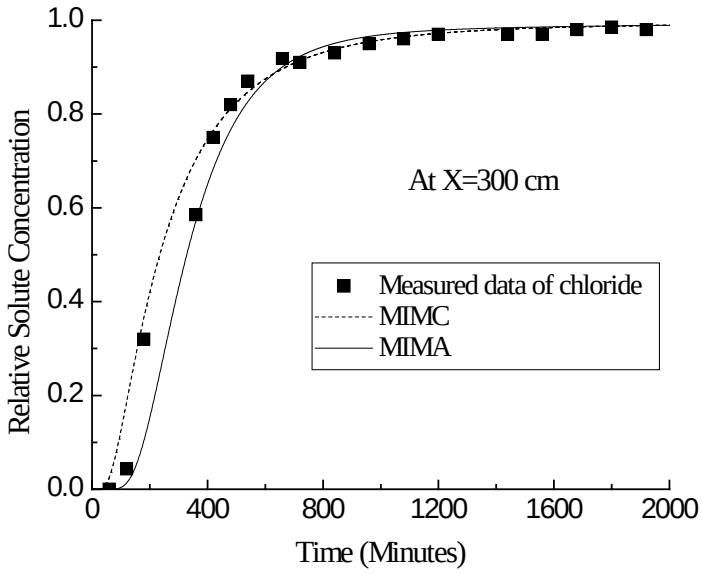

Figure 3.8d Simulation of observed experimental data of chloride at 300 cm down gradient distance using MIMC and MIMA dispersion models.

3.7.3 Simulation of experimental breakthrough curves of fluoride data

In order to simulate fluoride experimental observed breakthrough data, multiprocess non-equilibrium (MPNE) transport model is used. For the constant and asymptotic distance-dependent dispersion models, the values of dispersion coefficient and advective region volumetric water content were taken same as estimated from chloride data simulation. However, the value of mass transfer coefficient (w) of fluoride is obtained by correcting the value of w=2.31E-05 min^{-1} from chloride by multiplying it with ratio of free water diffusion coefficient of fluoride and chloride. Thus the value of mass transfer coefficient for fluoride was obtained as equal to 1.66E-05 per min. Value of f was taken as ratio of advective and non-advective porosity, i.e, f = 0.89. In order to estimate the transport parameters in case of reactive case, it is assumed that $F_a = F_n$, $K_a = K_n$ and $k_{a2} = k_{n2}$. The fluoride data at 1500 cm was first simulated using constant dispersion model. Transport parameters, i.e., F_a, K_a, k_{a2} were estimated using Levenberg Marquardt nonlinear least square optimization algorithm.

The estimated value of transport parameters are obtained as $F_a = F_n = 0.758$; $K_a = K_n = 0.021$ ml/g; and $k_{a2} = k_{n2} = 0.02$ min^{-1}. Using the above estimated parameters, Fluoride data were simulated at 1500 cm using multiprocess non-equilibrium constant dispersion (MPNEC) and asymptotic distance-dependent dispersion (MPNEA) models. Thus all the parameters of Fluoride data were independently simulated. The BTC curves for constant and asymptotic distance dependent models are shown in Figure 3.9a.

It can be seen here that both models estimate BTC very well however, for asymptotic distance dependent models all the parameters were independently estimated. Using the estimated parameters for constant and asymptotic distance dependent dispersion models, BTC were simulated at 1200 cm 600 cm and 300 cm as shown in Figures 3.9b, 3.9c and 3.9d, respectively. Goodness of fit values for Fluoride simulation using constant and asymptotic distance dependent model is shown in Table 3.3. The computed value of RMSE is smaller in case of MPNEA dispersion model as compared to MPNEC dispersion model. It can be seen that at 1500 cm and 1200 cm MPNEC model tends to overestimate the observed BTC. From the simulated results of measured concentration profile, it can be seen that the asymptotic distance dependent dispersion model fits the experimental data much better as compared to constant dispersion model.

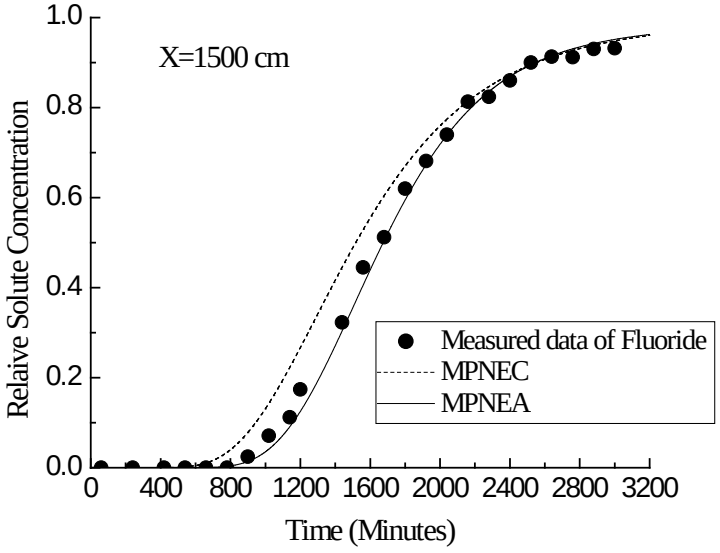

Figure 3.9a Simulation of observed experimental data of fluoride at 1500 cm using MPNEC and MPNEA dispersion models.

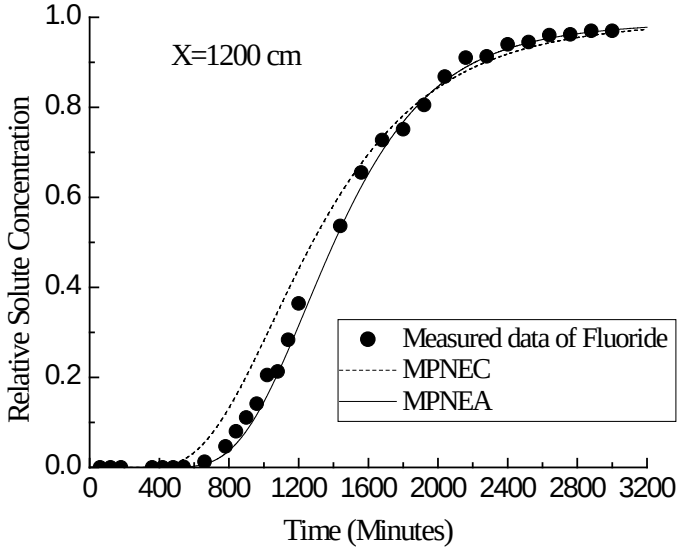

Figure 3.9b Simulation of observed experimental data of fluoride at 1200 cm using MPNEC and MPNEA models.

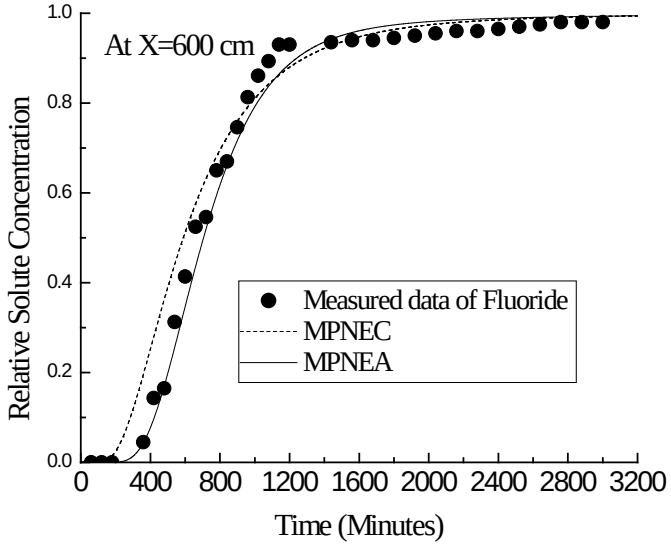

Figure 3.9c Simulation of observed experimental data of fluoride at 600 cm using MPNEC and MPNEA models.

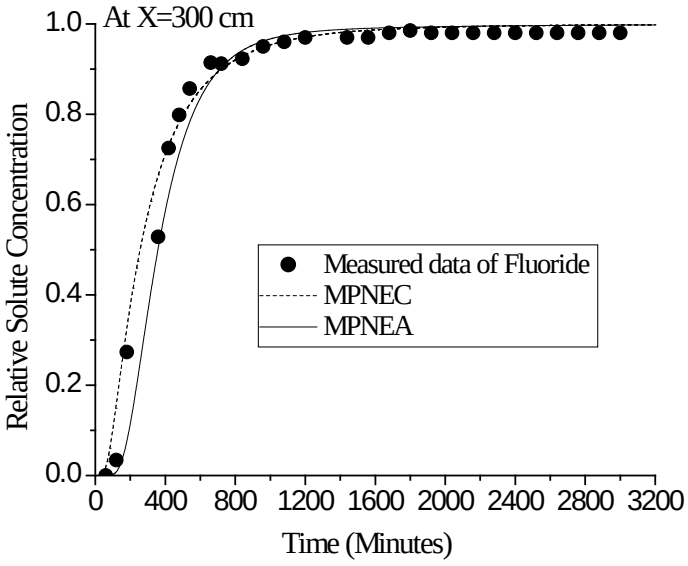

Figure 3.9d Simulation of observed experimental data of fluoride at 300 cm using MPNEC and MPNEA models.

Table 3.3: Goodness of fit values for Fluoride data simulation using MPNEC and MPNEA

Distance	MPNEC		MPNEA	
(cm)	r^2	RMSE	r^2	RMSE
1500	0.9897	0.0544	0.9982	0.0187
1200	0.9892	0.0522	0.9988	0.0168
600	0.9776	0.0654	0.9911	0.0369
300	0.9862	0.0397	0.9804	0.0507

3.8 Summary

In this chapter, semi-analytical solution of multiprocess non-equilibrium transport model with an asymptotic distance-dependent dispersion (MPNEA) is developed for constant concentration type boundary condition. Analytical solution is derived in Laplace domain which has then inverted numerically by using de Hoog's algorithm. To describe the features of multiprocess

non-equilibrium transport model, results of experimental breakthrough curves are compared between constant and asymptotic distance dependent dispersion models. The present semi-analytical solution of MPNEA model was used to describe solute transport in 1500 cm long heterogeneous soil column. Transport parameters estimated at 1500 cm was used to simulate breakthrough curves at fore going distances. Results show that a better fit to the experimental BTC is observed when mass transfer between advective and non-advection region was considered. It was also observed that asymptotic distance-dependent dispersion model gave a good fit to the observed BTC as compared to constant dispersion model. The simulation results demonstrated that multiprocess non-equilibrium with constant dispersion model could not adequately describe solute transport in large heterogeneous soil column and it overestimated solute transport dispersion at fore going distances away from 1500 cm long soil column. Finally, in this study the developed MPNEA model has been tested by solute transport in a laboratory long column experiment.

Chapter 4

SIMULATION OF EXPERIMENTAL DATA USING NONLINEAR SORPTION MODEL

4.1 General

In this chapter, Freundlich and Langmuir isotherms are tested in case of fine sand and natural soil. Subsequently, implicit finite difference numerical technique is used to solve one-dimensional advection-dispersion transport equation considering non-linear sorptions. Transport of fluoride through a porous bed has been simulated with linear and non-linear sorption models.

4.2 Governing Equation

For a homogeneous, isotropic, and fully saturated porous medium and with no dispersion in the transverse direction to the flow direction, one dimensional advective dispersive reactive transport equation including equilibrium sorption can be written as (Lapidus Amundson, 1952):

$$\frac{\partial C}{\partial t}+\frac{\rho}{n}\frac{\partial Q}{\partial t}=D\frac{\partial^2 C}{\partial x^2}-v\frac{\partial C}{\partial x} \qquad (4.1)$$

where, C is the concentration of solute in the solution phase (M/L^3); Q is the amount of mass sorbed per unit weight of soil solids (M/M); ρ is the bulk density of soil media (M/L^3), n is the porosity of the soil media; D is the hydrodynamic dispersion coefficient (L^2/T), which includes two components of the molecular and mechanical dispersion; v is pore water velocity along flow path (L/T); t is time (T); and x is distance along the flow path (L). In this study, an attempt is made to study the sorption characteristics of fluoride through both fine sand and natural soil. Subsequently, the use of these parameters has been investigated in simulating transport of fluoride through long soil column.

4.3 Material used and Soil Column experiment

The natural soil used in this experiment has been obtained from 20 to 50 cm below the ground surface from IIT Roorkee campus. Both fine sand and natural soil are used for column experiment, respectively. Chloride and Fluoride are used as non-reactive and reactive tracers, respectively. It is also seen that the value of permeability is equal to 10^{-3} cm /min in case of fine sand and the value of permeability is equal to 10^{-4} cm /min in case of natural soil. It indicates that the fine sand is having higher permeability as compared to natural soil. The different tests were also performed in the laboratory to determine the particle size analysis, moisture content and bulk density of soil media as shown in Table 4.1.

Table 4.1 Properties of fine sand and natural soil

S. No.	Soil media	Particle size distribution (mm)			Moisture content (%)	Bulk density (ρ) (g/cm^3)	Porosity (n) (%)
		D_{10}	C_C	C_U			
1.	Fine sand	0.15	1.014	1.67	17.36	1.86	36
2.	Natural soil	0.085	0.795	2.94	16.95	1.84	38

4.4 Batch test

Batch equilibrium tests were performed to determine sorption of reactive solute to solids in the soil. A number of solutions of the chemical were tested at varying concentrations. The solutions are then mixed with soil solids until the equilibrium degree of adsorption, if any, occurs. The concentrations of the chemical in the solutions are then measured and any decrease in mass of the chemicals in the solutions was assumed to be due to adsorption onto the soil solids, and sorbed concentrations can be calculated. A relationship is then established between the equilibrium aqueous concentration of the chemical and the sorbed concentration of the chemical.

4.5 Soil column Experiment

The experimental set-up consists of a column, made-up of acrylic pipe of 600 cm long and it is placed horizontal. The acrylic pipe was of 6 mm thickness, internal dimension of 15 cm diameter and cross sectional area of 176.71 cm^2. A schematic sketch of experimental set-up of long soil column has been shown in Figure 4.1. Oven-dry soil was carefully packed in small increments into column (acrylic pipe) avoiding any soil particle size segregation and kept constant density through out the column length.

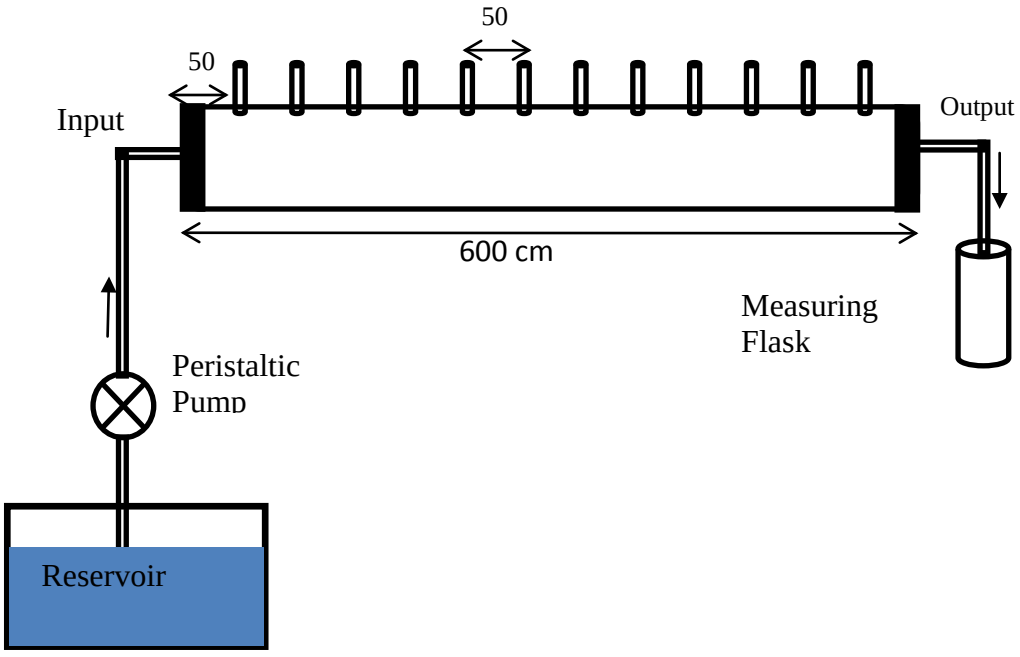

Figure 4.1 Schematic diagram of one dimensional soil column experiment.

Peristaltic pump was used to provide constant flow rate through soil column in order to maintain the same pore water velocity. A porous plate was provided at the inlet in order to achieve a uniform entry of water into the soil column. Before the experiment, soil column was saturated with water for time duration of three days. The concentration of solute at different outlet of soil column was measured at various intervals of time. Conservative solute such as chloride has been passed in to the soil column in order to determine the dispersion coefficient.

The Spadns method (Eaton et al. 1995) has been described to estimate fluoride concentration from collected sample at different outlets along the length of soil column. The prepared

solution was introduced into the soil column at a constant flux through peristaltic pump. The effluent solutions were collected in fractions at different time of interval according to the suitability of the sample, so that minimum 300ml effluent can be obtained for proper execution of titration. At the end of soil column experiment, the soil was carefully extruded and the volume of water contained in soil was gravimetrically determined. The effluent solute concentrations were expressed as relative concentrations $\left(C/C_0\right)$, where C and C_0 are solute concentration in an effluent fraction and input solution, respectively.

4.6 Sorption isotherms

The relationship between the amount of adsorbate on the adsorbent surface and the concentration in solution at given temperature is generally known as adsorption isotherm. Freundlich proposed an empirical formula which describes the adsorption isotherm (Freundlich, 1906). Afterwards, Langmuir proposed a hypothesis for monolayer molecular adsorption (Langmuir, 1916). Also, it is seen that the many solute transport models are based on both linear and nonlinear sorption models. Therefore, sorption isotherm equation for the case of linear, Freundlich and Langmuir are described below:

4.6.1 Linear sorption

In case of linear equilibrium isotherm, it is assumed that the sorbed phase concentration is directly proportional to solution phase solute concentration. Based on this assumption, the linear isotherm can be represented as:

$$\mathrm{Q} = K_\mathrm{d}\, C \tag{4.2}$$

Using Equation (4.2)

$$\frac{\partial \mathrm{Q}}{\partial t} = K_\mathrm{d}\frac{\partial C}{\partial t} \tag{4.3}$$

Substituting Equation (4.3) into the Equation (4.1) and simplifying, following equation can be obtained:

$$\left(1+\frac{\rho K_d}{n}\right)\frac{\partial C}{\partial t}=D\frac{\partial^2 C}{\partial x^2}-v\frac{\partial C}{\partial x} \quad (4.4)$$

Or in general form:

$$R\frac{\partial C}{\partial t}=D\frac{\partial^2 C}{\partial x^2}-v\frac{\partial C}{\partial x} \quad (4.5)$$

where $R=\left(1+\frac{\rho K_d}{n}\right)$ is known as the retardation factor and it retards the transport of adsorbed species relative to the advection front; K_d represents the distribution coefficient (L/M).

4.6.2 Nonlinear sorption

It is seen that many natural systems represent non-linear sorption behavior which can be described by the Freundlich or Langmuir isotherm models. However, on the basis of adsorption process on a heterogeneous surface, Freundlich equation can be written as (Freundlich, 1906; Nandi et al. 2009):

$$Q = K_e C^b \quad (4.6)$$

Where K_e represents the Freundlich sorption coefficient (M/M)/(M/L)^b and b is Freundlich exponent. In case of linear sorption b=1 and K_e is equal to K_d (the linear distribution coefficient).

Langmuir equation can be written as (Langmuir, 1916; Weng et al 2008):

$$Q=\frac{Q_S K_a C}{1+K_a C} \quad (4.7)$$

where Q_s represents the maximum sorption capacity (M/M) and K_a represents an absorption constant related to binding energy (L^3/M).

Again it is assumed that local conditions of equilibrium exist between sorbed and solution phase solute concentration. Equation (4.6) is differentiated with respect to time and substituted in Equation (4.1) and after simplifying lead to:

$$\left(1+\frac{\rho K_{\mathrm{e}} \mathrm{b} C^{(\mathrm{b}-1)}}{n}\right)\frac{\partial C}{\partial t}=D\frac{\partial^2 C}{\partial x^2}-v\frac{\partial C}{\partial x} \tag{4.8}$$

Now, retardation factor for Freundlich nonlinear sorption isotherm can be written as:

$$R=\left(1+\frac{\rho K_{\mathrm{e}} \mathrm{b} C^{(\mathrm{b}-1)}}{n}\right) \tag{4.9}$$

For the Langmuir isotherm model, we used same approach to Equation (4.7) and obtained following transport equation:

$$\left(1+\frac{\rho Q_{\mathrm{S}} K_{\mathrm{a}}}{n(1+K_{\mathrm{a}}C)^2}\right)\frac{\partial C}{\partial t}=D\frac{\partial^2 C}{\partial x^2}-v\frac{\partial C}{\partial x} \tag{4.10}$$

And retardation factor for Langmuir isotherm can be written from Equation (10) as:

$$R=\left(1+\frac{\rho Q_{\mathrm{S}} K_{\mathrm{a}}}{n(1+K_{\mathrm{a}}C)^2}\right) \tag{4.11}$$

4.7 Numerical model development and validation

An implicit finite-difference numerical technique was used to solve the governing equations for linear sorption, Freundlich and Langmuir nonlinear isotherm models. Implicit finite difference formulation of Equation (4.5) can be written as:

$$R\frac{C_{\mathrm{i}}^{\mathrm{l}+1}-C_{\mathrm{i}}^{\mathrm{l}}}{\Delta t}+v\frac{C_{\mathrm{i}+1}^{\mathrm{l}+1}-C_{\mathrm{i}-1}^{\mathrm{l}+1}}{2\Delta x}-D\frac{C_{\mathrm{i}+1}^{\mathrm{l}+1}-2C_{\mathrm{i}}^{\mathrm{l}+1}+C_{\mathrm{i}-1}^{\mathrm{l}+1}}{\Delta x^2}=0 \tag{4.12a}$$

In case of linear sorption, the term of retardation factor (R) can be replaced by $\left(1+\frac{\rho K_{\mathrm{d}}}{n}\right)$. For the case of Freundlich nonlinear isotherm, the term of retardation factor can be replaced by Equation (4.9) and its finite difference formulation can be written as:

$$R=\left(1+\frac{\rho K_{\mathrm{e}} \mathrm{b}\left(C_{\mathrm{i}}^{\mathrm{l}+1}\right)^{(\mathrm{b}-1)}}{n}\right) \tag{4.12b}$$

And for the case of Langmuir isotherm model, the finite difference formulation of Equation (4.11) can be represented as:

$$R = \left(1 + \frac{\rho Q_S K_a}{n\left(1 + K_a C_i^{l+1}\right)^2}\right) \tag{4.12c}$$

where i represents the grid number; l represents the known time; $l+1$ represents the unknown time level; Δx represents the grid size along the length of domain; and Δt represents the computational time step. Following initial and boundary conditions have been used:

$$C(x,0) = 0 \tag{4.13a}$$

$$C(0,t) = C_0 \tag{4.13b}$$

$$\left.\frac{\partial C(x,t)}{\partial x}\right|_{x=L} = 0 \tag{4.13c}$$

where, C_0 represents the injected solute concentration at the inlet.

Thomas algorithm is used to solve the set of linear simultaneous equations. Picard's iteration method is used to solve nonlinear sorption model. For verification of the numerical model, spatial relative concentration profiles have been simulated for a constant concentration boundary condition and are compared with analytical solutions given by Ogata and Banks (1961) for linear sorption model. The results obtained for both analytical and numerical breakthrough curves are well matched and are shown in Figure 4.2. The numerical model is verified with analytical solution given by Serrano (2001) for both cases of Freundlich and Langmuir nonlinear sorption models, as shown in Figures 4.3a and 4.3b. Input parameters such as Freundlich sorption coefficient, K_e=0.001 (mg/g)/(mg/L)^b ;Freundlich exponent, b=0.6; porosity, n=0.1; dispersion coefficient, D=10 m^2/month, pore water velocity, v=1 m/month and initial solute concentration, C_0=100 mg/L are used in simulation, as shown in Figure 4.3a. However, in case of Figure 4.3b, following input parameters, such as, maximum sorption capacity, Q_s=1.0 *mg/g*; absorption capacity, K_a=0.01 and 0.0003 L/mg; dispersion coefficient, D=1m^2/month, and initial solute concentration, C_0=10000 mg/L are used. In this simulation, both Peclet number ($P_e = \frac{v\Delta x}{D}$) and Courant number ($C_r = \frac{v\Delta t}{\Delta x}$) are kept less than one to reduce the numerical error. The following grid size i.e., $\Delta x = 0.1$ m and $\Delta t = 0.025$ day are used.

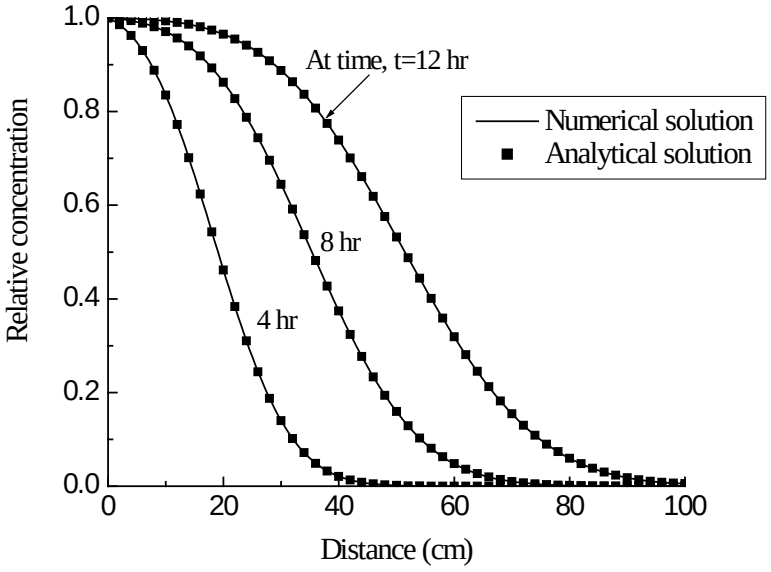

Figure 4.2 Simulated spatial concentration profile with both analytical (Ogata and Banks 1961) and present numerical model (pore velocity, v= 4 cm/hr. dispersion coefficient, D = 12 cm^2/hr and retardation factor, R=1).

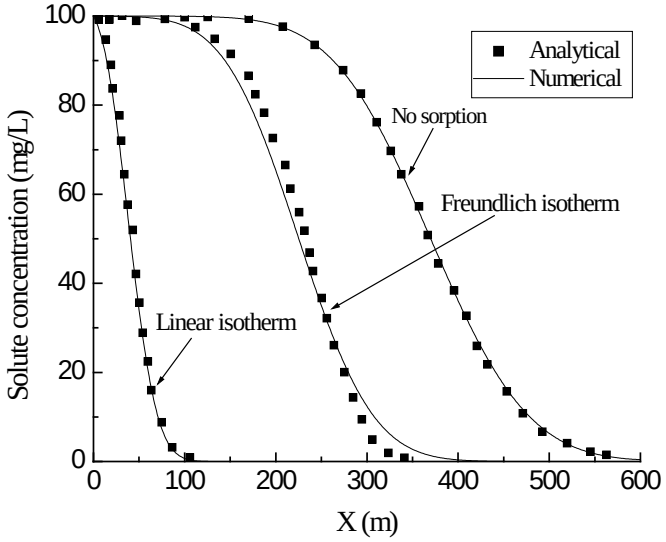

Figure 4.3a Simulated spatial concentration profiles with both analytical (Serrano 2001) and present numerical model for linear and non-linear Freundlich isotherm.

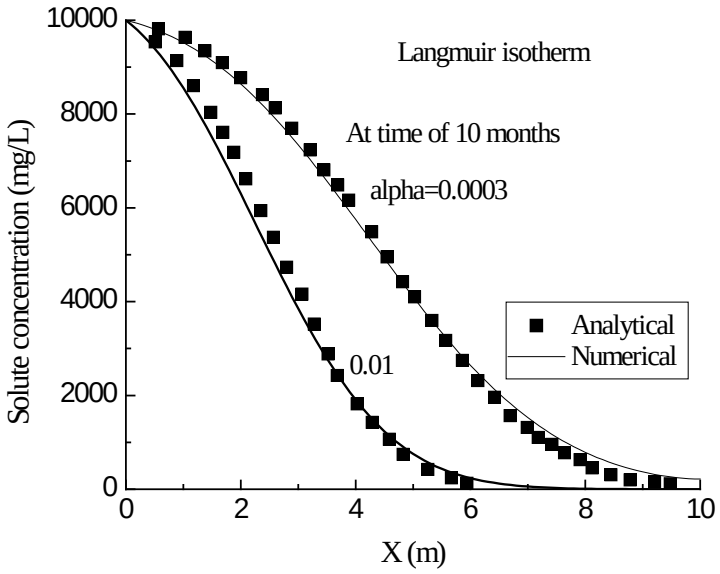

Figure 4.3b Simulated spatial concentration profiles with both analytical (Serrano 2001) and numerical model for Langmuir isotherm model.

4.8 Results and Discussion

4.8.1 Batch adsorption Studies

Batch kinetics and sorption studies were conducted to understand the role of adsorption on the transport of fluoride in subsurface soils at room temperature. Both batch kinetics and sorption isotherm experiments were conducted in 50 ml glass tubes (Figure 4.4) at room temperature. The amount of fluoride adsorbed by soil was calculated from the difference between the initial concentration and final concentration after the specified period of shaking using the following equation (Gupta et al., 2009):

$$Q_{\mathrm{F}} = \left(C_0 - C_{\mathrm{e}}\right) * \frac{V}{M} \tag{4.14}$$

where Q_F is the fluoride sorption (mg/g) for the specified period, C_0 and C_e are the initial and equilibrium solute concentrations in the solution (mg/L), respectively. V and M are the volume of aqueous solution and mass of sorbent, respectively.

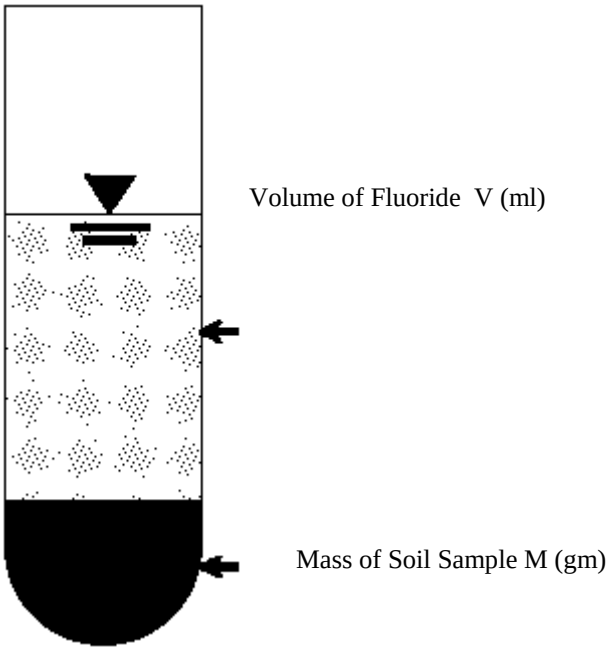

Figure 4.4 Glass tube filled with fluoride and soil sample.

The kinetics of fluoride retention was studied for a standard sodium fluoride (NaF) solution of concentration of 20 mg/L. A glass tube containing 10 gm of soil in 200 ml fluoride solution was mixed for 12 hours. During the experiment, 5 ml aliquots were sampled from the glass tube at different time of intervals, and it is filtered and then analysed for fluoride concentration.

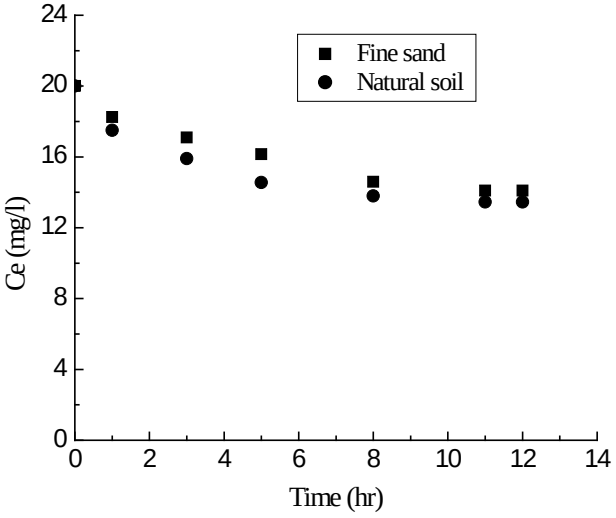

Figure 4.5 Kinetic of adsorption of fluoride by fine sand and natural soil, respectively.

It can be seen from Figure 4.5 that adsorption attained an equilibrium state at approximately at time of 11hrs for both fine sand and natural soil. All batch experiments were carried out at initial fluoride concentrations of 5, 8, 10, 20, 25 and 40 mg/L, blank samples with no added NaF were also included in the experiments to verify whether natural background fluoride was desorbing from the soil. The sample tubes containing 10g of soil in 100ml of fluoride solution were shaken by shaking machine for time of 24 hours at regular interval and then samples were filtered using a 0.45 µm cellulose acetate syringe filter and analysed for fluoride concentration.

In this study, the coefficient of correlation i.e., R^2 has been used to test the fitting of equilibrium isotherms for given set of experimental data of fluoride (Chapra and Canale, 2000):

$$R^2 = 1 - \frac{\sum_{i=1}^{N} (Q_e - Q_c)^2}{\sum_{i=1}^{N} \left(Q_e - \overline{Q_e}\right)^2} \tag{4.15}$$

where, Q_c is the equilibrium capacity obtained from the isotherm model, Q_e is the equilibrium capacity obtained from experiment, and $\overline{Q_e}$ is the average of Q_e obtained from experiment.

Langmuir isotherm can be linearized in four different ways, as shown in Table 4.2 and the parameters were calculated for all the forms (Parimal et al. 2010). It is seen that due to the transformations into different linear forms, the error structures were changed in different forms; hence, the results obtained would be different for all of them. Table 4.3 represents the Freundlich and Langmuir coefficients and the corresponding correlation coefficient for three cases of fine sand and natural soil at equilibrium. Freundlich isotherm plots have been shown in Figure 4.6 for fine sand and natural soil respectively. Similarly, Langmuir-1, 2, 3 and 4 types of plots have been shown in Figures 4.7-4.10 for both fine sand and for natural soil, respectively.

Table 4.2: Isotherm models and their linear forms

Isotherm		Linear form	Plot
Freundlich	$Q_e = K_e C_e^{\,b}$	$\log(Q_e) = \log(K_e) + b\log(C_e)$	$\log(Q_e)$ *vs* $\log(C_e)$
Langmuir-1	$Q_e = \frac{Q_s K_a C_e}{1 + K_a C_e}$	$\frac{C_e}{Q_e} = \frac{C_e}{Q_s} + \frac{1}{K_a Q_s}$	$\frac{C_e}{Q_e}$ *vs* C_e
Langmuir-2		$\frac{1}{Q_e} = \left(\frac{1}{K_a Q_s}\right)\frac{1}{C_e} + \frac{1}{Q_s}$	$\frac{1}{Q_e}$ *vs* $\frac{1}{C_e}$
Langmuir-3		$Q_e = Q_s - \left(\frac{1}{K_a}\right)\frac{Q_e}{C_e}$	Q_e *vs* $\frac{Q_e}{C_e}$
Langmuir-4		$\frac{Q_e}{C_e} = K_a Q_s - K_a Q_e$	$\frac{Q_e}{C_e}$ *vs* Q_e

Table 4.3: Freundlich and Langmuir isotherm parameters obtained using linear method for fine sand and natural soil

Isotherms	Parameters	Fine Sand	Natural Soil
Fruendlich	K_e ((mg/g)/(mg/L)^b)	0.0171	0.0051
	b	0.3736	0.4264
	R^2	0.8306	0.8673
Langmuir-1	Q_s (mg/g)	0.06014	0.0255
	K_a (L/mg)	0.246	0.1338
	R^2	0.9063	0.9272
Langmuir-2	Q_s (mg/g)	0.0629	0.0252
	K_a (L/mg)	0.218	0.135
	R^2	0.908	0.8963
Langmuir-3	Q_s (mg/g)	0.06	0.0248
	K_a (l/mg)	0.2696	0.1483
	R^2	0.6545	0.616
Langmuir-4	Q_s (mg/g)	0.069	0.0306
	K_a (L/mg)	0.1765	0.0913
	R^2	0.6545	0.616

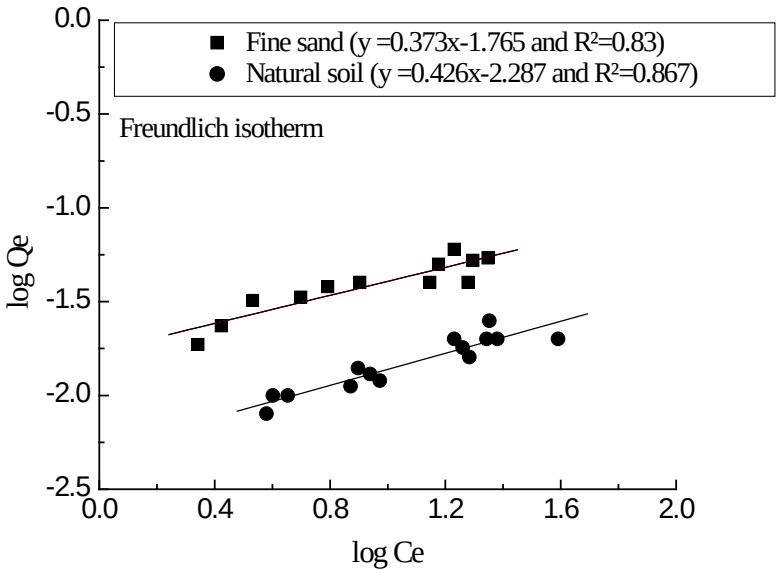

Figure 4.6 Freundlich adsorption of fluoride by fine sand and natural soil respectively.

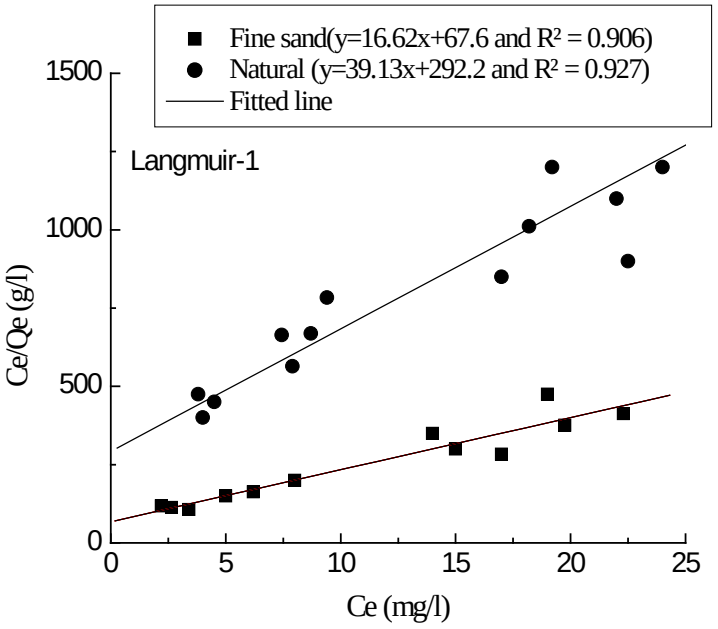

Figure 4.7 Langmuir-1 adsorption of fluoride by fine sand and natural soil respectively.

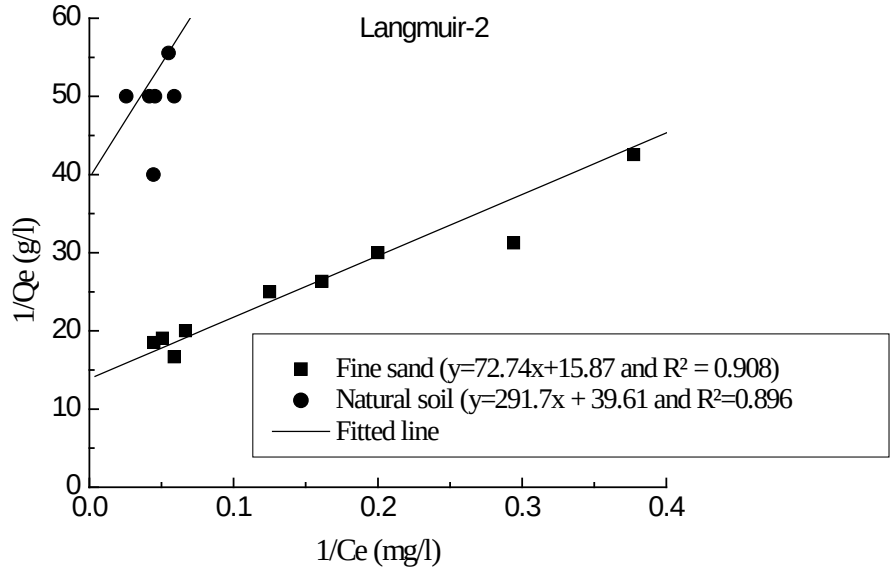

Figure 4.8 Langmuir-2 adsorption of fluoride by fine sand and natural soil, respectively.

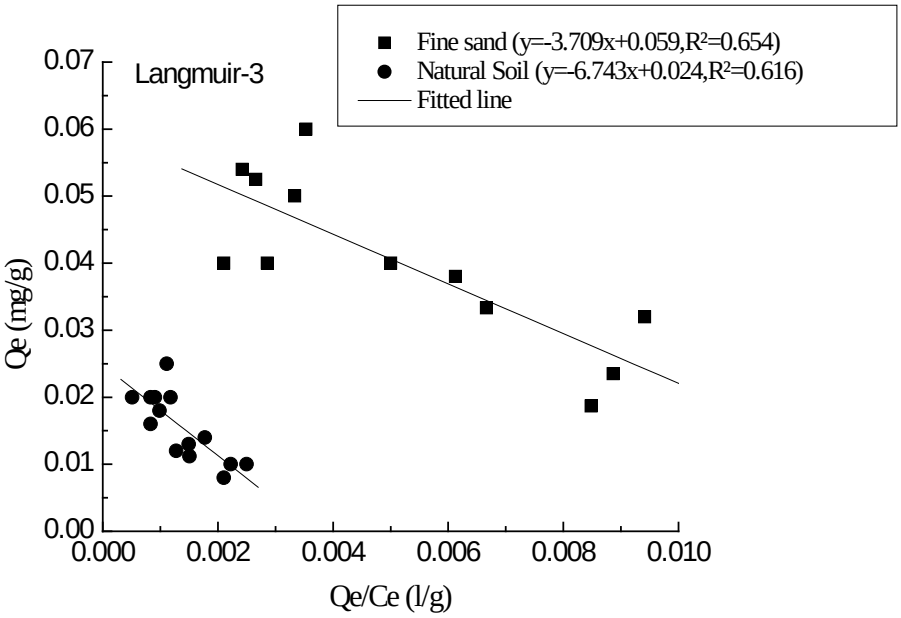

Figure 4.9 Langmuir-3 isotherm for fluoride adsorption by fine sand and natural soil.

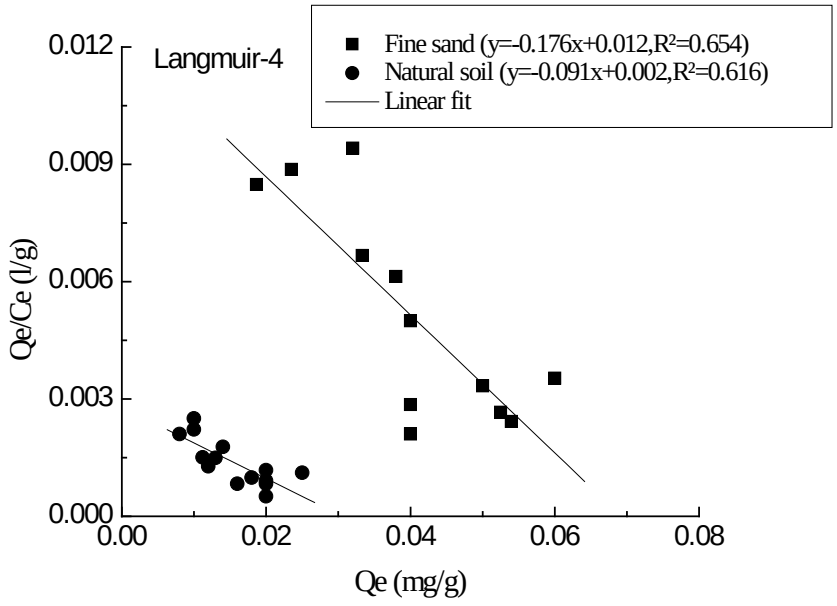

Figure 4.10 Langmuir-4 isothetrm for fluoride adsorption by fine sand and natural soil.

The various linear plots of *log* C_e versus *log* Q_e were plotted for both cases of fine sand and natural soil, and the various sorption parameters were estimated for analyzing the applicability of the Freundlich nonlinear sorption isotherm. The parameter Q_e represents equilibrium capacity. The parameter, Q_s represents the saturated monolayer sorption capacity, and K_a represents the sorption equilibrium constant, and the values of Langmuir constants were calculated for all the forms of linear Langmuir isotherms and have been listed in Table 4.3. It is observed that in case of fine sand, the best fit is given by Langmuir -2 linear isotherms in comparison to other Langmuir linear isotherms (i.e. Langmuir-1, 3 and 4). However, in case of natural soil, Langmuir-1 linear isotherm gives the best fit.

In case of fine sand, the value of correlation coefficient (R^2=0.8306 and 0.908) were calculated for Freundlich linear isotherm and Langmuir-2 linear isotherms, respectively. The above results show that the Langmuir-2 linear isotherms can be used more precisely as compared to Freundlich linear isotherm. For the analysis of natural soil, the value of correlation coefficient (R^2=0.8673 and 0.9272) were calculated for both Freundlich linear isotherm and Langmuir-1 linear isotherms, respectively. The above results show that the Langmuir-1 linear isotherms can be used more precisely as compared to Freundlich linear isotherm. It is seen that both values of coefficient of determination, R^2 are approximately equal; hence both Freundlich and Langmuir-2 linear isotherm can be used.

4.8.2 Simulation of breakthrough curves for Chloride data

In view of the objectives of the study, experiments were performed in order to investigate the concentration profiles through one-dimensional soil column using solute tracers such as chloride and fluoride. First, conservative chloride as a tracer was passed through soil column to get the breakthrough curves through both fine sand and natural soils, respectively. The pore water velocity through the soil column is estimated from discharge of Peristaltic pump. The other parameter i.e., dispersion coefficient is estimated through simulation of breakthrough curve of chloride. These transport parameters are used to simulate the breakthrough curves for reactive fluoride. Figures 4.11 and 4.12 represent observed and numerically simulated temporal relative concentration profiles for chloride tracer in natural soil and fine sand, respectively. It is observed that the magnitude of solute concentration is almost zero during small transport time. It means that solute tracer moves along with water pore velocity in the soil filled column. The observed and numerical results show approximately a good match. The following parameters, i.e., pore water velocity, v=2.24 cm/min and dispersion coefficient, D=12 cm^2/min for natural soil and v =2.8 cm/min and D=8.5 cm^2/min in case of fine sand have been estimated through simulation.

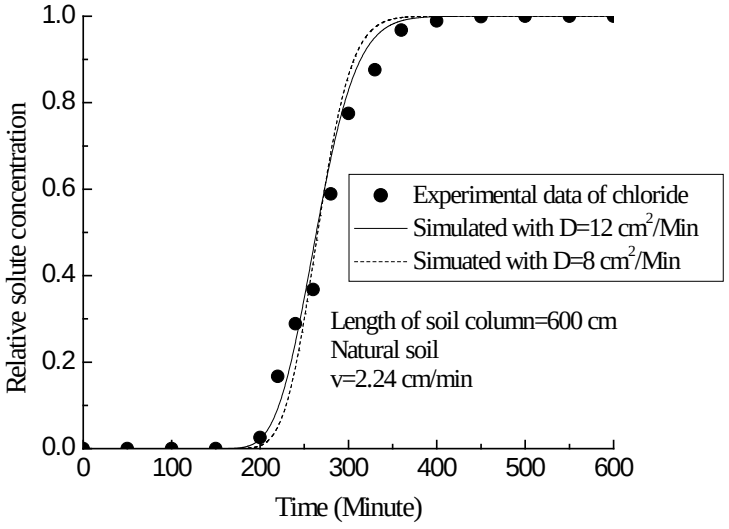

Figure 4.11 Simulation of experimental data of chloride through natural soil column.

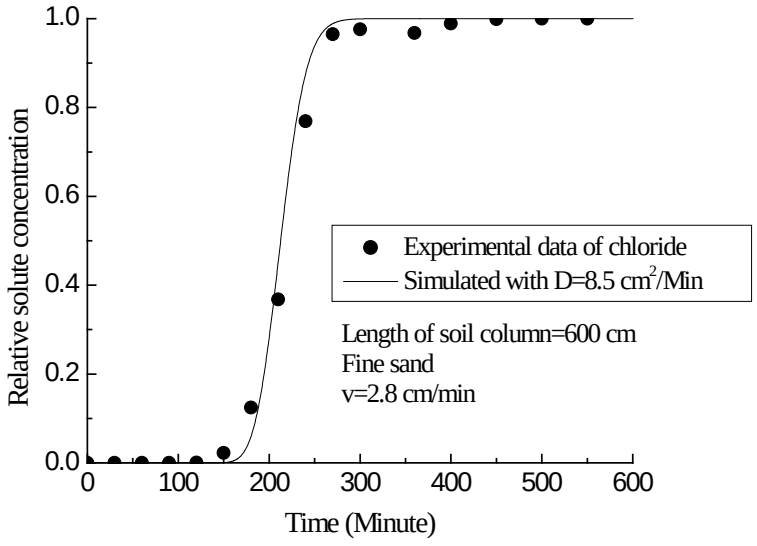

Figure 4.12 Simulation of experimental data of chloride through fine sand column.

4.8.3 Simulation of break through curves for Fluoride data

In this section, transport parameters i.e. pore water velocity and dispersion coefficient are used to simulate the breakthrough curves of experimental data of fluoride through both natural soil and fine sand, respectively. It is also well known that fluoride is reactive in nature. Once it occurs in contact of soil media, it is adsorbed on the soil surface. While conducting experiment through soil column, the pore velocity i.e., v=2.24 cm /min in case of natural soil and v=2.8 cm/min in case of fine sand are found. The behavior of temporal and spatial concentration profiles for fluoride is observed through soil column of length of 600 cm.

Figures 4.13 and 4.14 represent the temporal relative concentration profiles of fluoride in case of both natural soil and fine sand, respectively. The parameters used for numerical simulation of fluoride through natural soil are dispersion coefficient, D=12 cm^2/min and pore water velocity, v =2.24 cm/min. However, in case of fine sand the values of transport parameters i.e., D=8.5 cm^2/min and v =2.8 cm/min are used. The soil column was solute free initially, so the relative concentration in both soil media starts from zero value and increases rapidly and thereafter being constant during large transport time. The three values of retardation factor i.e., R= 1, 1.24 and 1.5 are used to simulate the observed temporal concentration profiles in case of

natural soil, as shown in Figure 4.13. It is seen that observed and numerical results show relatively a good match with value of retardation factor of 1.24. While the value of retardation factor *R*=1.2 gives best fit curve in case of fine sand as shown in Figure 4.14.

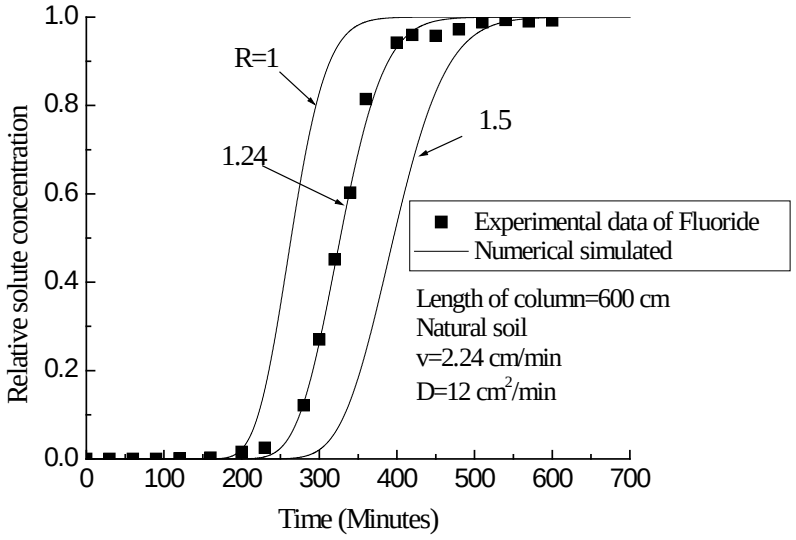

Figure 4.13 Simulation of experimental data of fluoride through natural soil column.

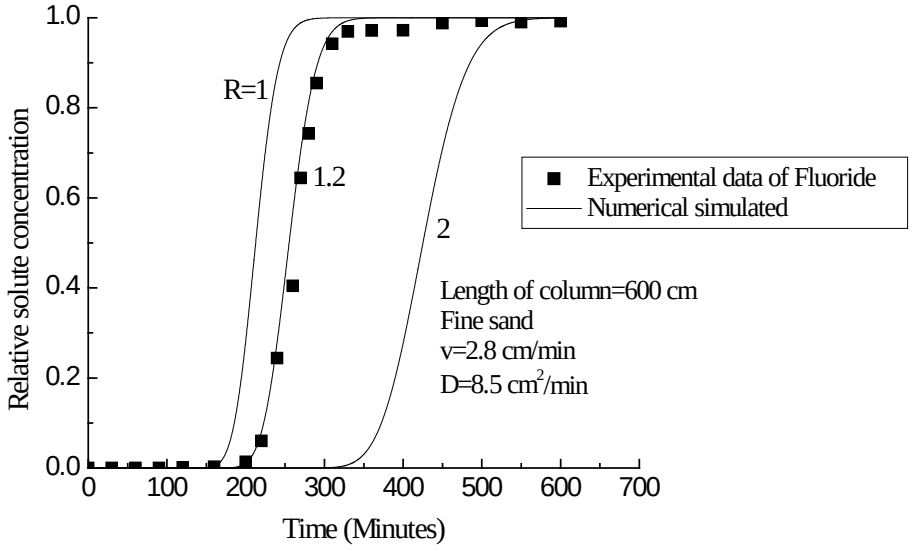

Figure 4.14 Simulation of experimental data of fluoride through fine sand column.

Further, spatial concentration profiles have been predicted at time of 200 minutes along the length of flow direction in case of both fine sand and natural soil, respectively. The observed spatial concentration profiles for fluoride have been shown in Figures 4.15 and 16. The

parameters used for numerical simulation are dispersion coefficient, D=8.5 cm^2/min and pore velocity, v =2.2 cm/min for fine sand and D=12 cm^2/min and v =1.8 cm/min in case of natural soil. Afterwards, linear sorption, Freundlich and Langmuir nonlinear isotherm models are used to simulate experimental data of fluoride through soil column. In case of linear adsorption isotherm, the value of distribution coefficients for both natural soil and fine sand were computed by using least square method.

The value of distribution coefficient equal to 0.000856 l/g for natural soil and 0.00297 l/g for fine sand were found. The value of porosity and density of both soils as shown in Table 4.1 were used to compute the value of retardation factor in case linear sorption. The computed value of retardation factor, R=5.14 in case of natural soil and R=16.69 in case of fine sand were found. Sorption parameters for Langmuir-2 are used in case of fine sand and sorption parameters of Langmuir-1 are used in case of natural soil. The estimated sorption parameters for Freundlich and Langmuir sorption isotherm have been shown in Table 4.3. The observed and numerical results show an excellent match in case of Freundlich isotherm model in comparison to Langmuir sorption isotherm model. It indicates that the Freundlich nonlinear sorption model revealed good agreement with the experimental observed data of fluoride.

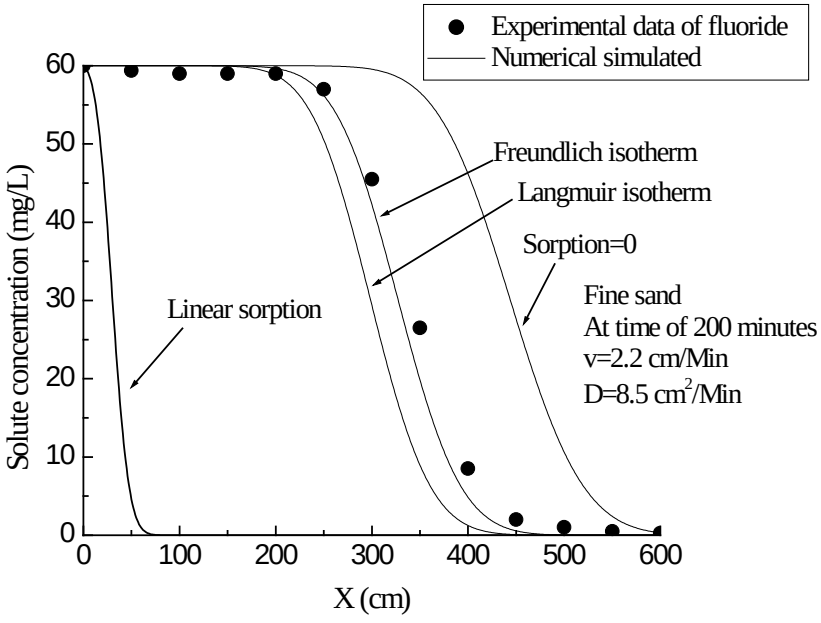

Figure 4.15 Simulation of experimental data of fluoride through fine sand column using linear sorption, Freundlich and Langmuir isotherm, respectively.

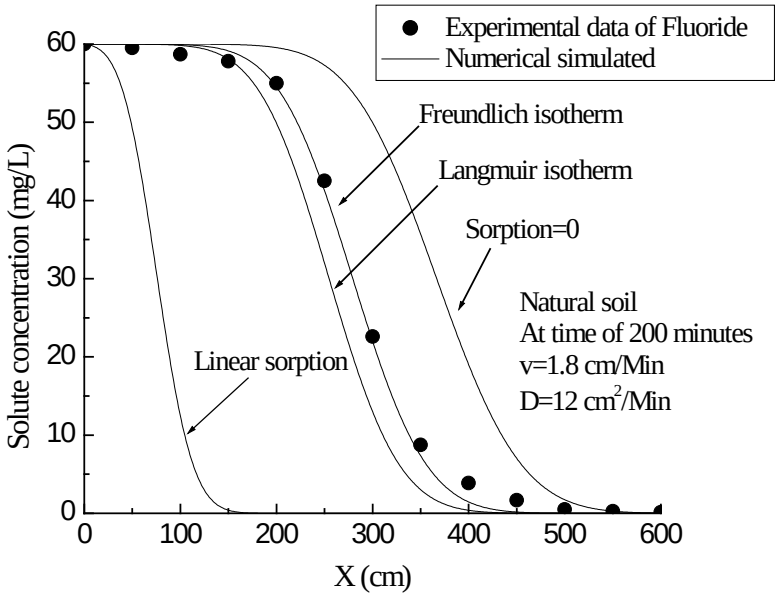

Figure 4.16 Simulation of experimental data of fluoride through natural soil column using linear sorption, Freundlich and Langmuir isotherm, respectively.

4.9 Summary

Present study examined the linear sorption, Freundlich and Langmuir nonlinear isotherm of fluoride through natural soil and fine sand, respectively. Batch sorption parameters were used to simulate fluoride breakthrough curves of experimental observations by using implicit finite difference numerical model of one-dimensional transport equation. On the basis of linearization of Langmuir nonlinear isotherm model, it is shown that the best fit is given by Langmuir -2 linear isotherms in comparison to other Langmuir linear isotherms in case of fine sand. However, in case of natural soil, Langmuir-1 linear isotherm gives the best fit. In case of fine sand, the value of R^2=0.8306 and 0.908 is obtained for Freundlich linear isotherm and Langmuir-2 linear isotherms, respectively. This also indicates that the Langmuir-2 linear isotherms can be preferred in comparison to Freundlich linear isotherm. In case of natural soil, the value of R^2=0.8673 and 0.9272 is obtained for Freundlich linear isotherm and Langmuir-1 linear isotherms, respectively. This also indicates that the Langmuir-1 linear isotherms can be preferred in comparison to Freundlich linear isotherm. Observed experimental data of fluoride has been well simulated using numerical model by using transport parameters, such as pore velocity, v=2.42 cm/min, dispersion coefficient, D=8.5 cm^2/min for fine sand and v=2.2

cm/min and D=12 cm^2/min for natural soil, respectively. It is also shown that the Freundlich sorption model gives best fit of observed spatial concentration along the length of soil column. Finally, this study indicates that Freundlich nonlinear isotherm model incorporated in the transport equation with an implicit finite difference method would provide accurate prediction for reactive transport in the soil column.

Chapter 5

SIMULATION OF BREAKTHROUGH CURVES WITH DISTANCE-DEPENDENT DISPERSION AND VARIABLE MASS TRANSFER COEFICIENTS

5.1 General

In this Chapter, the behavior of breakthrough curves in mixed heterogeneous soil column experiments has been analyzed. Advective dispersive transport equations are used for solute transport through mobile-immobile porous medium. A hybrid finite volume method is used to solve the governing equations for solute concentration in mobile region. In first part of the study, constant dispersion, linear and asymptotic distance dependent dispersion functions are used to describe the scale effect and to simulate experimental breakthrough curves observed in long soil column experiment. Also, a comparative study has been done among distance dependent and constant dispersion models, while simulating the experimental data of solute transport through soil column with constant mass transfer coefficient. In second part of the study, variable mass transfer coefficient as function of pore velocity and travel distance is considered and an empirical relation is derived from observed data from experiments.

5.2 Governing Equations

Mobile-immobile model (MIM) separates the porous medium into mobile and immobile regions. It is assumed that advection-dispersion equation is used for mobile region, and solute exchange between mobile and immobile regions can be described as a first-order process. The porous medium is also partitioned into two fractions of adsorption sites which equilibrate instantaneously with the mobile and immobile liquid regions. The solute adsorption by the solid phase is described with a linear isotherm, and the solute degradation in both the liquid and solid phases is assumed to be a first-order process. Based on the above conceptual model, MIM for reactive transport under steady state flow is given by the following expressions (van Genuchten

and Wagenet, 1989):

$$\left(\theta_m + f\rho K_d\right)\frac{\partial C_m}{\partial t} = \theta_m \frac{\partial}{\partial x}\left(D(x)\frac{\partial C_m}{\partial x}\right) - V_m\theta_m \frac{\partial C_m}{\partial x} - w\left(C_m - C_{im}\right) - \left(\theta_m \mu_{lm} + f\rho K_d \mu_{sm}\right)C_m \qquad (5.1)$$

$$\left(\theta_{im} + (1-f)\rho K_d\right)\frac{\partial C_{im}}{\partial t} = w\left(C_m - C_{im}\right) - \left(\theta_{im}\mu_{\lim} + (1-f)\rho K_d \mu_{sim}\right)C_{im} \qquad (5.2)$$

where, θ_m and θ_{im} are water contents in the mobile and immobile regions, respectively, and $\theta_m + \theta_{im} = \theta$; θ is the total water content of the soil media, C_m and C_{im} are solute concentrations in the mobile and immobile regions (ML^{-3}), respectively; V_m is mobile pore-water velocity (LT^{-1}) and $V_m\,\theta_m$ is equal to flow rate, q (LT^{-1}); w is the first-order mass transfer coefficient (T^{-1}); f and (1− f) represent fractions of adsorption sites that equilibrate instantaneously with the mobile and immobile regions, respectively; ρ is bulk density of the porous medium (ML^{-3}); K_d is distribution coefficient for the linear sorption process ($M^{-1}\ L^3$); μ_{lm} and $\mu_{\lim}$ are the first-order decay coefficients for degradation of solute in the mobile and immobile regions (T^{-1}), respectively; μ_{sm} and μ_{sim} are the first-order decay coefficients for degradation of solute in the mobile and immobile adsorbed solid phases (T^{-1}), respectively; x is spatial coordinate (L); t is time (T); $D(x)$ is the hydrodynamic dispersion coefficient in the mobile region ($L^2\ T^{-1}$).

The dispersivity is generally considered as constant in case of mobile-immobile model (MIM) with constant dispersion, while in case of scale dependent dispersion, the dispersivity is considered as function of distance (Yates, 1990). However, Picken and Grisak (1981b) and Yates (1990) have shown that the dispersivity (α) can be considered as a function of linear and asymptotic function of distance (x). At laboratory scale, distance (x) is the length of soil column experiments. The linear distance-dependent dispersivity increases with distance without bounds, while the asymptotic distance-dependent dispersivity initially increases with distance and ultimately approaches an asymptotic value. The linear distance-dependent dispersion coefficient, as given by Yates (1990) is:

$$D(x) = \alpha(x)V_m = k\,x V_m \qquad (5.3)$$

where $\alpha(x)$ the distance-dependent dispersivity, k is the slope of the dispersivity-distance relationship (dimensionless), x is distance from the source and V_m is mean pore water velocity. The expression of asymptotic dispersivity is given in Chapter 3.

5.3 Numerical Scheme

The governing equations for contaminant transport through mobile-immobile porous media are solved using the split operator approach for advection, dispersion and reaction terms.

5.3.1 Formulation of governing equations

The modified form of Equation 5.1 and 5.2 can be written as:

$$R_m \frac{\partial C_m}{\partial t} = \theta_m \frac{\partial}{\partial x}\left(D(x)\frac{\partial C_m}{\partial x} \right) - q\frac{\partial C_m}{\partial x} + wC_{im} - g_1 C_m \tag{5.4}$$

$$R_{im} \frac{\partial C_{im}}{\partial t} = wC_m - g_2 C_{im} \tag{5.5}$$

where coefficients are defined as:

$$R_m = \theta_m + f\rho K_d \tag{5.6a}$$

$$R_{im} = \theta_{im} + (1-f)\rho K_d \tag{5.6b}$$

$$g_1 = \left(w + \theta_m \mu_{lm} + f\rho K_d \mu_{sm}\right) \tag{5.6c}$$

$$g_2 = \left(w + \theta_{im} \mu_{\lim} + (1-f)\rho K_d \mu_{sim}\right) \tag{5.6d}$$

After applying the operator splitting, the advective term of Equation 5.4 can be written as:

$$\frac{\partial C_m}{\partial t} = -\frac{q}{R_m}\frac{\partial C_m}{\partial x} \tag{5.7}$$

where $q = V_m \theta_m$. Similarly the dispersive transport term can be written as:

$$\frac{\partial C_m}{\partial t} = \frac{\theta_m}{R_a} \frac{\partial}{\partial x}\left(D(x) \frac{\partial C_m}{\partial x} \right) \tag{5.8}$$

And the reactive transport can be written as:

$$R_m \frac{dC_m}{dt} = wC_{im} - g_1 C_m \tag{5.9}$$

$$R_{im} \frac{dC_{im}}{dt} = wC_m - g_2 C_{im} \tag{5.10}$$

Following initial the exit boundary conditions have been used:

$$C_m(x,0) = C_{im}(x,0) = 0 \tag{5.11a}$$

$$\left. \frac{\partial C_m(x,t)}{\partial x} \right|_{x=L} = 0 \tag{5.11b}$$

The constant concentration type boundary condition is

$$C_m(0,t) = C_0 \tag{5.11c}$$

Pulse type boundary condition is:

$$C_m(0,t) = C_0 \qquad \text{for } t \le t_0 \tag{5.11d}$$

$$C_m(0,t) = 0 \qquad \text{for } t > t_0 \tag{5.11e}$$

where C_0 is initial injected solute concentration at inlet of the soil media (M/L^3) and t_0 is the pulse time (T).

5.3.2 Numerical solution

The finite volume method is used for numerically solving the advective transport which is based on monotone upwind schemes for conservation laws (MUSCL) by van Leer (1977a,b).

This method is globally high-order accurate and non-oscillatory. The formulation of this scheme is as follows:

$$\frac{\partial C_m}{\partial t} + \frac{\partial F}{\partial x} = 0 \tag{5.12}$$

where F is advective flux, which can be written as $F = V_m C_m / R_m$

Equation (5.12) can be written in a discrete form by assuming the cell centered concentration as cell averaged concentration as:

$$\frac{\left(C_{mi}^{n+1} - C_{mi}^{n}\right)}{\Delta t} + \frac{\left(\overline{F}_{i+1/2}^{n} - \overline{F}_{i-1/2}^{n}\right)}{\Delta x} = 0 \tag{5.13}$$

where C_{mi} is the cell centered concentration, $\overline{F}_{i+1/2}^{n}$ is time-averaged flux, *n* denotes the time level, Δt represents the time step and Δx represents the space step. Advective flux is computed using a second order upwind method similar to the one adopted by Putti et al. (1990).

Assuming a linear distribution in the cell, the mass concentration value at the cell interface is reconstructed using a MUSCL approach (van Leer 1977a). The gradient of the concentration distribution in the cell *i* for monotonocity, prescribed by the superbee and minimod limiters is (Putti et al. 1990):

$$\left(\delta C_{mi}\right)_{MON} = ave\left(\Delta_{-} C_{mi}, \Delta_{+} C_{mi}\right) \tag{5.14}$$

With

$$\Delta_{-} C_{mi} = C_{mi} - C_{m\,i-1} \tag{5.15a}$$

$$\Delta_{+} C_{mi} = C_{m\,i+1} - C_{mi} \tag{5.15b}$$

where $ave\left(\Delta_{-} C_{mi}, \Delta_{+} C_{mi}\right)$ in Equation (5.14) for minimod and superbee limiters are given by Putti et al. (1990). In this paper, we have adopted least dissipative superbee limiter, which is expressed as:

$$ave\left(\Delta_{-} C_{mi}, \Delta_{+} C_{mi}\right) = \begin{cases} sign(\Delta_{-} C_{mi}) \min(2\left|\Delta_{-} C_{mi}\right|, \max\left(\left|\Delta_{-} C_{mi}\right|, \left|\Delta_{+} C_{mi}\right|, 2\left|\Delta_{+} C_{mi}\right|\right)) & if\ \Delta_{-} C_{mi} \Delta_{+} C_{mi} \rangle 0 \\ 0 & otherwise \end{cases} \tag{5.16}$$

Fluxes at the interface are evaluated as

$$\overline{F}_{i+1/2}^{n} = V_{mi} C_{mi+1/2}^{L} \quad \text{when } V_i > 0 \tag{5.17a}$$

Otherwise

$$\overline{F}^{n}_{i+1/2} = V_{mi+1} C^{R}_{mi+1/2} \qquad (5.17b)$$

where $C^{R}_{mi+1/2} = C_{mi+1} - \frac{1}{2}\delta C_{mi+1}$ and $C^{L}_{mi+1/2} = C_{mi} + \frac{1}{2}\delta C_{mi}$ here δC_{mi} is the gradient of the concentration distribution in the cell *i* while *L* and *R* represent the left and right faces of the cell interface.

Hancock's scheme (van Albada et al. 1982) is usually employed, which is a two step second order accurate explicit scheme. The two half time steps in this method can be represented as predictor and corrector step. The C_{mi} obtained from the predictor step is used for calculation of the fluxes. The same gradient δC_{mi} is used in both predictor and corrector steps. For the above scheme, the time step is limited by the Courant number. For stability of this scheme, the Courant number $C_r = \frac{V_m . \Delta t}{\Delta x}$, should be less than or equal to one.

5.3.3 Dispersive transport equation

The dispersive transport (Equation 5.8) is performed on the concentrations, resulting from the advective transport in each time step. A conventional fully implicit, finite-difference scheme, which is unconditionally stable, is used to obtain the final concentrations at the end of time step. This formulation has the advantage of using an implicit numerical scheme for the dispersive transport, while using an explicit numerical scheme for advection transport there by either advection dominated or dispersion dominated systems can be accurately handled. Remaining equations 5. 9 and 5.10 are solved using explicit numerical method.

5.4 Results and discussion

5.4.1 Concentration profiles with constant, linear and asymptotic dispersion models

Numerical model is used to predict temporal and spatial solute concentration with constant, linear and asymptotic distance dependent dispersivity. Following input parameters i.e., constant dispersivity α =2 m, linear distance coefficient, *k* = 0.1, asymptotic distance dependent parameters, *a* = 2.5 m, *b* =5 m, flow rate, *q*=0.04 m/d, θ_m = 0.3, θ_{im} = 0.1, mass transfer coefficient, *w*=0.01 per day are used during simulation. Figure 5.1 represents the temporal concentration profile predicted at down gradient distance of 5 m and 20 m in the flow direction.

The behavior of temporal concentration profiles is different among constant, linear and asymptotic distance dependent dispersivity. Early arrival of solute concentration has been obtained in case of constant dispersivity as compared to both linear and asymptotic value of dispersivity. Similarly, behavior of spatial solute concentration profiles is different for constant, linear and asymptotic distance dependent dispersivity as shown in Figure 5.2. In case of constant dispersivity (MIMC), the value of solute concentration is smaller at small distance and its value is higher at large travel distance.

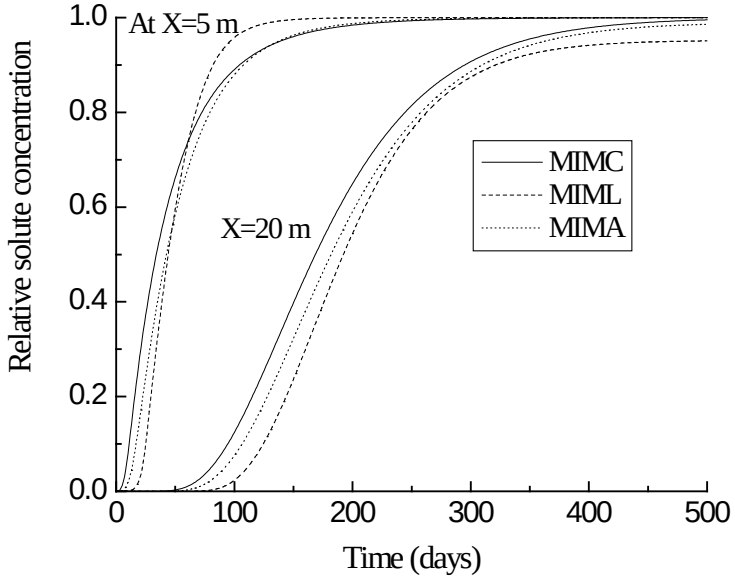

Figure 5.1 Temporal concentration profiles predicted at 5 m and 20 m down gradient distance with constant, linear and asymptotic distance-dependent dispersivity.

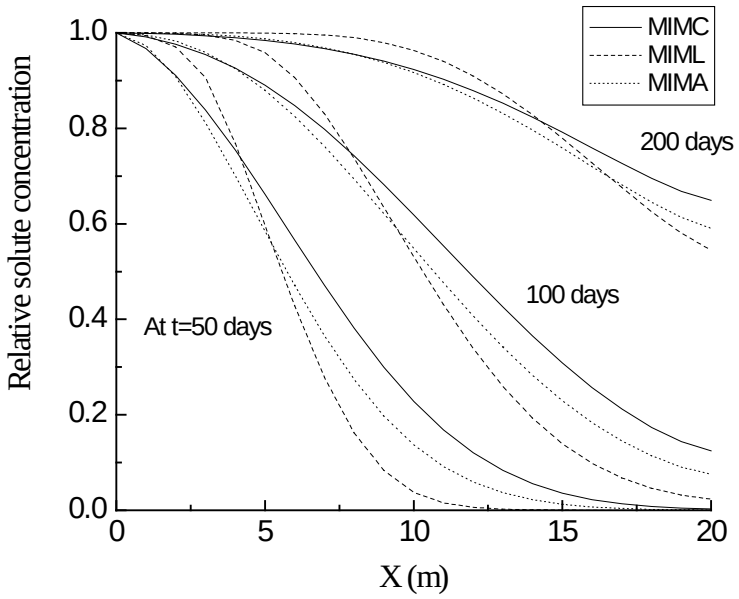

Figure 5.2 Spatial concentration profiles predicted at different transport time with constant, linear and asymptotic distance-dependent dispersivity.

5.4.2 Simulation of breakthrough curves with constant and distance-dependent dispersion models

The numerical model is used to simulate the observed experimental breakthrough curves predicted at different distances of 300 cm, 600 cm, 900 cm, 1200 cm and 1500 cm in the flow direction. Figures 5.3-5.7 show the observed experimental breakthrough curves and numerically simulated results at different distances in the flow direction. Following parameters i.e., flow rate, q = 0.42 cm/min, θ_m = 0.34, θ_{im} = 0.04, mass transfer coefficient, w = 2.42 E-05 per min, dispersivity, α =82.46 cm, linear distance dependent coefficient, k = 0.0824, asymptotic distance dependent coefficients, a = 82.74 cm, b = 148.56 cm are used during simulation. Firstly, we simulated observed experimental data at 1500 cm down gradient distance using mobile immobile with constant, linear and asymptotic distance dependent dispersivity as shown in Figure 5.3. Thus, via best fit simulation of observed breakthrough curve, the value of mass transfer coefficient, constant dispersivity, linear and asymptotic distance dependent parameters have been estimated. Performance of simulations are evaluated by considering root mean square error (RMSE), Nash-Sutcliffe efficiency coefficient (*NSE*) and coefficient of determination (R^2) are used for finding efficiency of simulations as described by

Equations 18(a-c).

$$RMSE = \sqrt{\frac{1}{n}\sum_{i=1}^{n}(C_{iobs} - C_{isim})^2} \tag{5.18a}$$

$$R^2 = \left(\frac{\sum_{i=1}^{n}(C_{iobs} - \overline{C}_{iobs})(C_{isim} - \overline{C}_{isim})}{\sqrt{\sum_{i=1}^{n}(C_{iobs} - \overline{C}_{iobs})^2}\sqrt{\sum_{i=1}^{n}(C_{isim} - \overline{C}_{isim})^2}} \right)^2 \tag{5.18b}$$

$$NSE = 1 - \frac{\sum_{i=1}^{n}(C_{iobs} - C_{isim})^2}{\sum_{i=1}^{n}(C_{iobs} - \overline{C}_{iobs})^2} \tag{5.18c}$$

where C_{iobs} and C_{isim} are ith observed and simulated concentration, respectively, $\overline{C}_{iobs}$ and $\overline{C}_{isim}$ are the mean of observed and simulated concentration, respectively. N is the number representing total observations taken at any particular observational point.

Computed values of root mean square error, coefficient of determination and Nash-Sutcliffe efficiency coefficients are shown in Table 5.1 for mobile immobile model with constant, linear and asymptotic distance dependent dispersivity (i.e., MIMC, MIML and MIMA). The estimated values of R^2= 0.907, *RMSE*=0.035, *NSE* =0.896 in case of MIMC, R^2= 0.984, *RMSE*=0.017, *NSE* =0.976 in case of MIML, R^2= 0.99, *RMSE*=0.011, *NSE* =0.99 in case of MIMA are obtained for simulated breakthrough curve in Figure 5.4. It is seen that the value of R^2 and *NSE* is higher for the case of asymptotic dispersivity model (MIMA) as compared to both constant dispersivity (MIMC) and linear distance dependent (MIML) models. Similarly, to evaluate the performance of simulation of breakthrough curve observed at 1200 cm, 900 cm, 600 cm and 300 cm down gradient distances (Figures 5.4, 5.5, 5.6 and 5.7), the estimated value of R^2, *RMSE*, and *NSE* is shown in Table 5.1. The simulation results of experimental breakthrough curves indicates that the MIMC and MIML models could not give the best fit of observed data and also over estimate the value of dispersivity. The estimated value of dispersivity equal to 82.46 cm, 123.6 cm and 75.28 cm are found for the case of MIMC, MIML and MIMA dispersion models. Thus the value of dispersivity equal to 75.28 cm for the case of MIMA model is lower than other constant and linear dispersion models. Finally, results indicated that the asymptotic (MIMA) model gives best fit of observed data of experimental breakthrough curves in long heterogeneous soil column experiment.

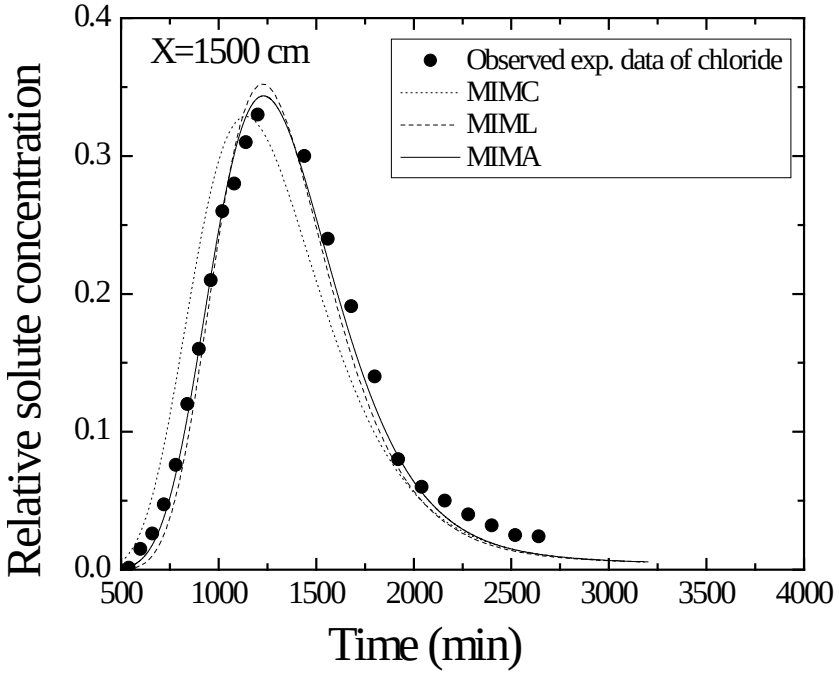

Figure 5.3 Simulated breakthrough curve of experimental data of chloride at 1500 cm down gradient distance in the flow directon.

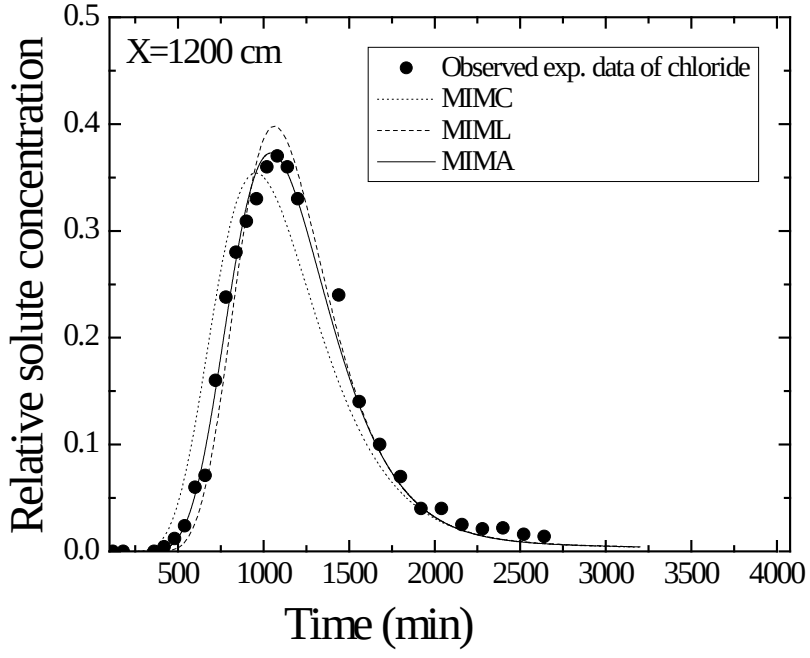

Figure 5.4 Simulated breakthrough curve of experimental data of chloride at 1200 cm down gradient distnace in the flow direction.

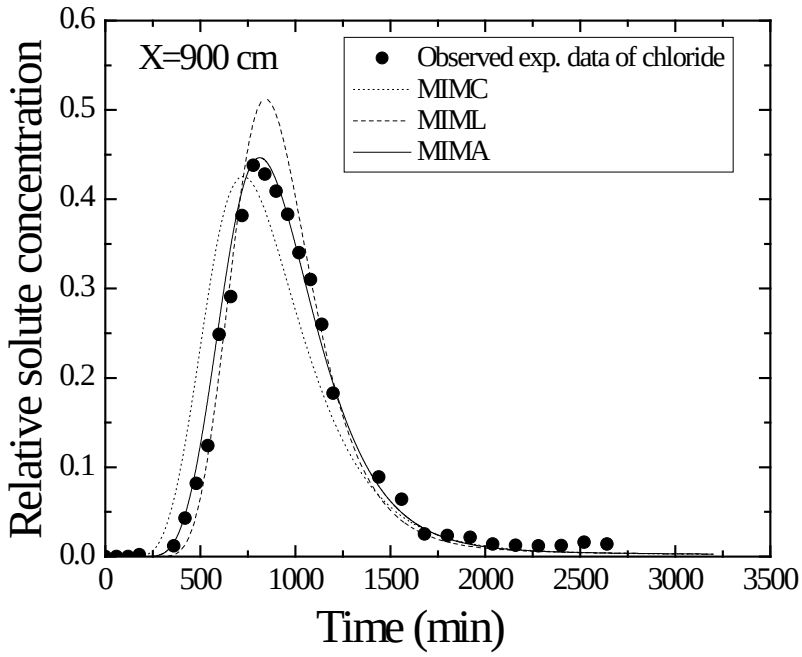

Figure 5.5 Simulated breakthrough curve of experimental data of chloride at 900 cm down gradient distance in the flow direction.

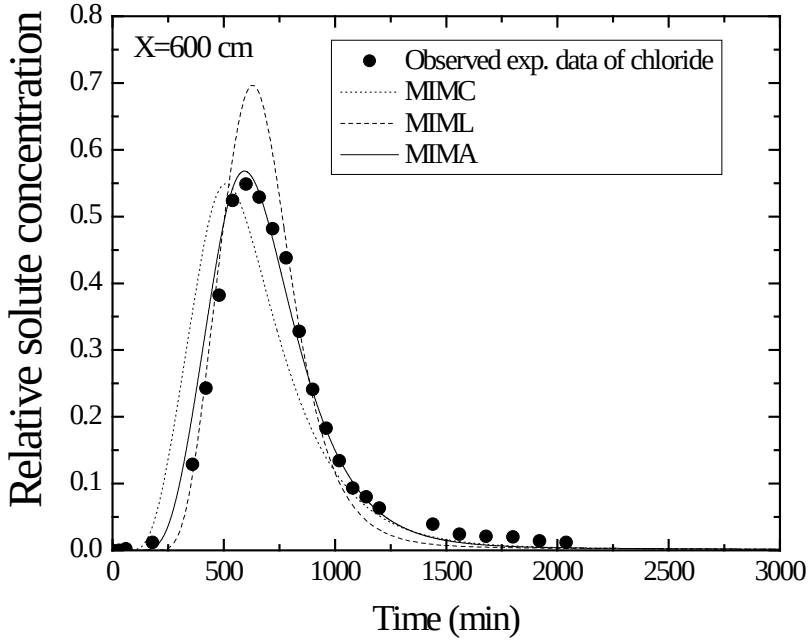

Figure 5.6 Simulated breakthrough curve of experimental data of chloride at 600 cm down gradient distance in the flow direction.

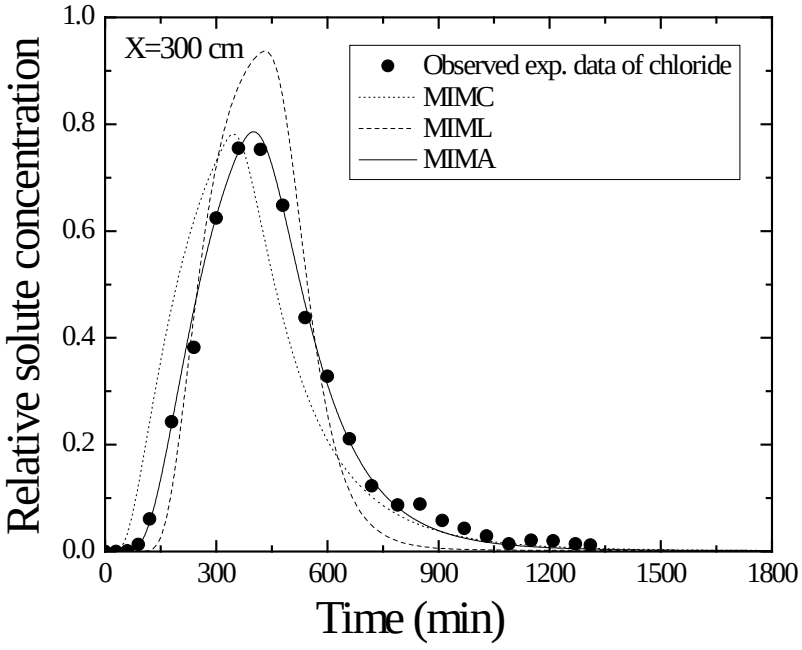

Figure 5.7 Simulated breakthrough curve of experimental data of chloride at 300 cm down gradient distance in the flow direction.

Table 5.1 estimated values of R^2, *RMSE* and Nash Sutcliffe coefficients (*NSE*) for the case of MIMC, MIML and MIMA models

Distance (cm)	MIMC			MIML			MIMA		
	RMSE	R^2	*NSE*	RMSE	R^2	*NSE*	RMSE	R^2	*NSE*
300	0.102	0.84	0.83	0.081	0.97	0.89	0.019	0.995	0.995
600	0.09	0.791	0.778	0.053	0.985	0.923	0.032	0.976	0.972
900	0.061	0.848	0.843	0.031	0.986	0.959	0.018	0.988	0.986
1200	0.039	0.91	0.91	0.022	0.98	0.97	0.013	0.993	0.992
1500	0.035	0.907	0.896	0.017	0.984	0.976	0.011	0.994	0.994

5.4.3 Simulation of breakthrough curves with asymptotic dispersion and variable mass transfer coefficient

Previous study showed that the value of mass transfer coefficient is dependent on system parameters including pore-water velocity, length scale and retardation coefficient (Maraqa

2001). It means that the value of mass transfer coefficient is not constant and it is variable parameter for movement of contaminant through subsurface aquifer. Hence, in this study, it was assumed that the value of mass transfer coefficient is dependent on both pore velocity and travel distance in the flow direction in the experiments. Thus, we estimated the individual value of mass transfer coefficient via simulation of experimental breakthrough curves observed at different down gradient distances i.e., 300cm, 600 cm, 900 cm, 1200 cm and 1500 cm, respectively in the flow direction. Afterwards, a graph between mass transfer coefficient and ratio of pore velocity to the distance is plotted which is shown in Figure 5.8. A power function is used to get the relationship between mass transfer coefficient vs velocity and travel distance. The value of coefficient of determination was found to be equal to R^2=0.991, which shows the best fit curve. From the relationship it was shown that the value of mass transfer coefficient was increasing towards the inlet boundary of the soil column experiment. It means that the value of mass transfer coefficient is changing with the movement of solute transport through porous media in the flow direction. However, the variability of mass transfer coefficient is higher during small transport distance and it variability is smaller at large travel distance.

From above discussion it is found that the accurate prediction of mass transfer coefficient is very significant at laboratory scale and it affects movement of solute transport through porous medium.

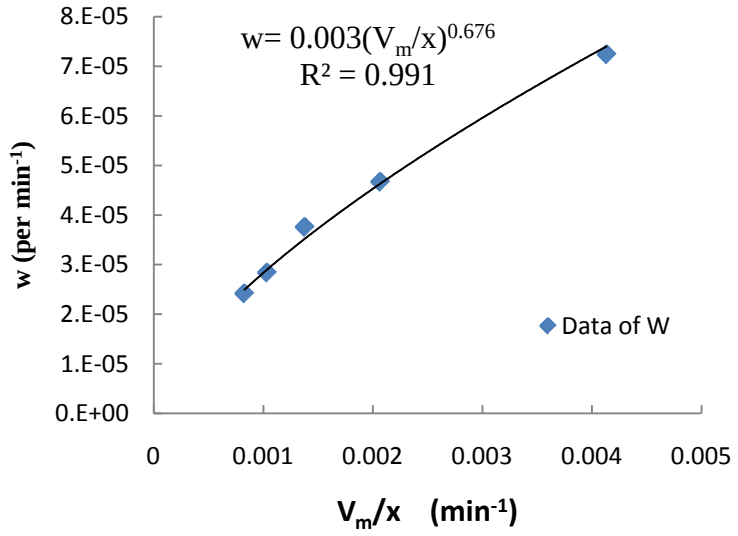

Figure 5.8 Variable mass transfer coefficients vs. ratio of pore velocity to travel distance.

The empirical relationship of mass transfer coefficient with pore velocity and travel distance is used to simulate the observed experimental breakthrough curves. To see the performance of mass transfer coefficient, both constant and variable mass transfer coefficient were used for simulation of breakthrough curves in presence of asymptotic dispersion model (MIMA). Figures 5.9-6.13 show the simulation of breakthrough curves using MIMA model with both constant value of mass transfer coefficient and variable mass transfer coefficients. The estimated value of coefficient of determination, root mean square error and NSE are shown in Table 5.2. It is seen that the accuracy of simulation of observed breakthrough curves were improved for the case of variable mass transfer coefficient as compared to constant value of mass transfer coefficient. However, the behavior of break through curves is similar for both cases of mass transfer coefficient.

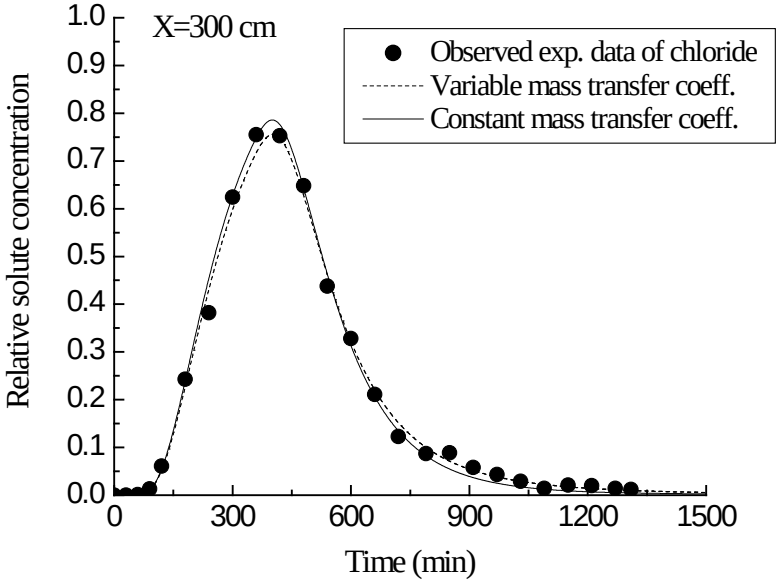

Figure 5.9 Simulation of breakthrough curve of experimental data of chloride at 300 cm down gradient distance using MIMA model with constant mass transfer and variable mass transfer coefficients.

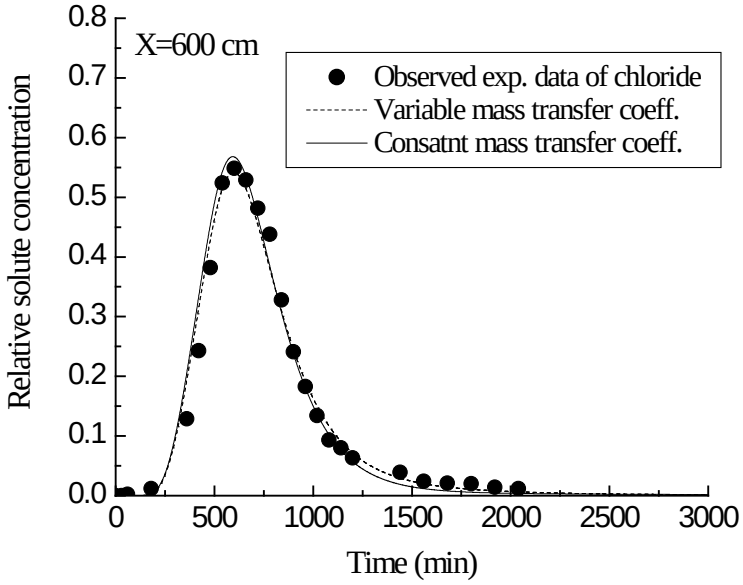

Figure 5.10 Simulation of breakthrough curve of experimental data of chloride at 600 cm down gradient distance using MIMA model with constant mass transfer and variable mass transfer coefficients.

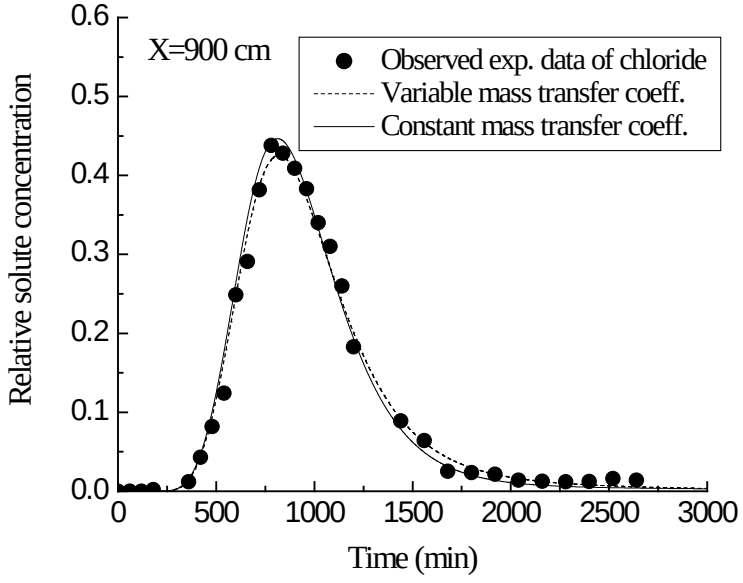

Figure 5.11 Simulation of breakthrough curve of experimental data of chloride at 900 cm down gradient distance using MIMA model with constant mass transfer and variable mass transfer coefficients.

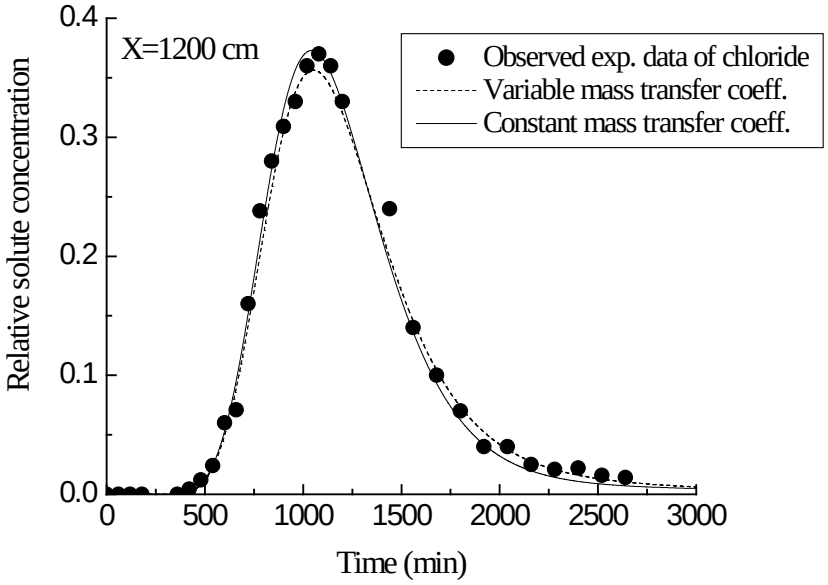

Figure 5.12 Simulation of breakthrough curve of experimental data of chloride at 1200 cm down gradient distance using MIMA model with constant mass transfer and variable mass transfer coefficients.

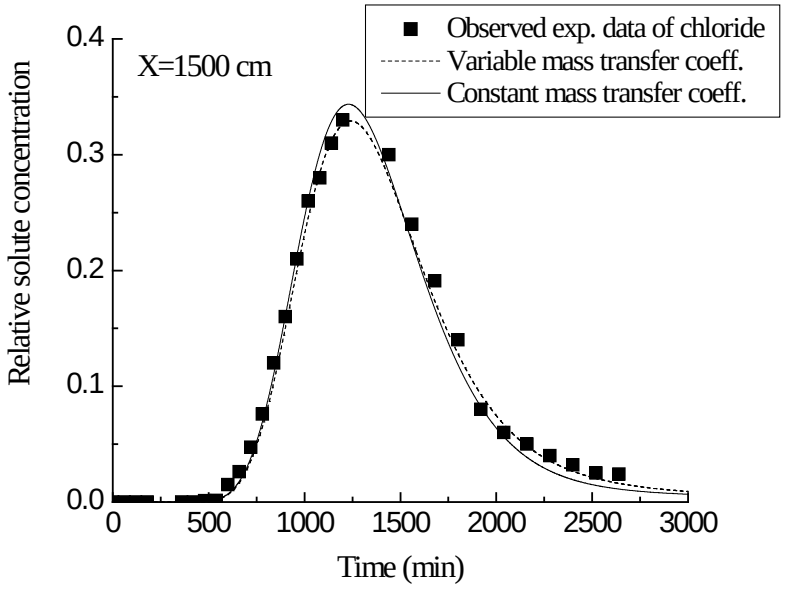

Figure 5.13 Simulation of breakthrough curve of experimental data of chloride at 1500 cm down gradient distance using MIMA model with constant mass transfer and variable mass transfer coefficients.

Table 5.2 Estimated values of R^2, *RMSE* and Nash Sutcliffe coefficients (*NSE*) for constant and variable mass transfer coefficient

Distance (cm)	MIMA					
	variable mass transfer coefficient			constant mass transfer coefficient		
	RMSE	R^2	*NSE*	RMSE	R^2	*NSE*
300	0.013	0.996	0.969	0.019	0.995	0.995
600	0.027	0.981	0.981	0.032	0.976	0.972
900	0.014	0.992	0.992	0.018	0.988	0.986
1200	0.013	0.993	0.989	0.013	0.993	0.992
1500	0.009	0.995	0.993	0.011	0.994	0.994

5.5 Experimental Setup

Figures 5.14a and 5.14b represent the line diagram of soil column experiments in the lab. Different combination of soil materials are filled in the first soil column experiment as shown in Figure 5.14a. It means that soil samples of different material such as gravel, coarse sand, fine sand, silt, natural soil and fine sand are filled in layered in the soil column. In the second part of the soil column experiment as shown in Figure 5.14b, mixed soil of different soil materials are filled in the column. Both set up of layered soil and mixed soil placed in the soil column experiments behave as heterogeneous media.

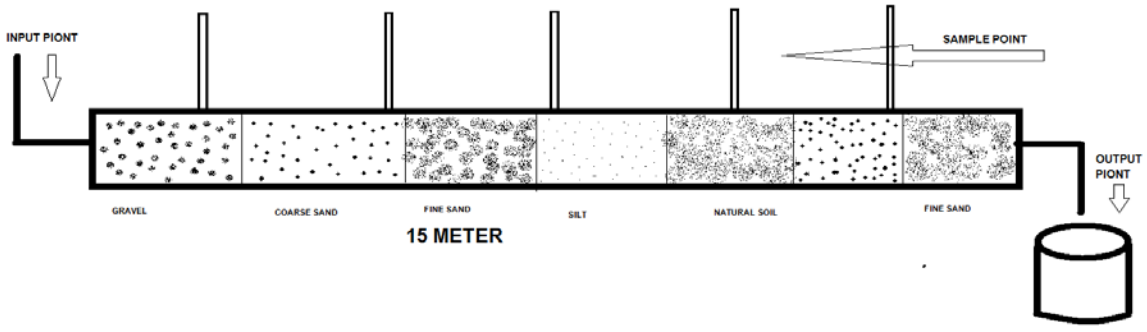

Figure 5.14a Line diagram of experimental set-up for heterogeneous medium for layered soils.

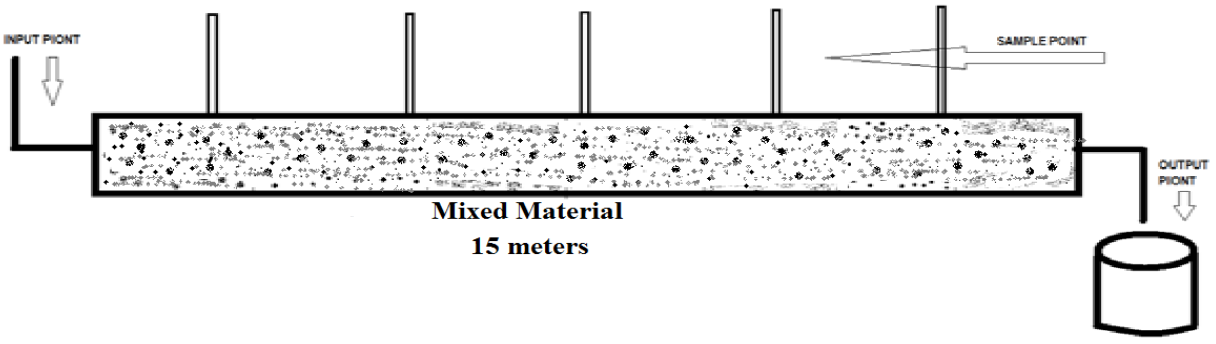

Figure 5.14b Line diagram of experimental set-up for heterogeneous medium for mixed soils.

5.5.1 Experimental Procedure

The length of the column is taken 1500 cm and diameter of the column is 15.24 cm, espectively. The soil column is heterogeneous in nature and is filled with coarse, fine, natural soil, silt and gravels in periodical layers. 300 liter of storage tank in which solution is made was placed near to the column. The experiments are conducted using heterogeneous soil columns, which contained negligible organic content. For sample collection at regular intervals, entire column length was divided in 5 equally distributed distances of 300 cm, afterward the column was saturated slowly by flowing tap water continuously for 72 hrs. To avoid leakage through joints, high quality sealant was applied to joints of the column. The head gradient was introduced by maintaining varying head at input, while keeping output head constant. For a known concentration of solute tracer was introduced in the column from storage tank. Several sets of samples were collected at time of 1 hr interval. Chloride testing was done by silver nitrate titration method. In the titration method 50ml volume of sample is taken and 1ml potassium chromate indicator was mixed, and then titrated with silver nitrate till red brick color appeared. Pulse type boundary condition, was considered in experiment.

5.5.2 Observed Breakthrough Curves In Layered and Mixed Soils

Figures 5.15-17 represent the behavior of observed experimental breakthrough curves through layered and mixed heterogeneous soil media, respectively. The experimental breakthrough curves are predicted at 300 cm, 900cm and 1500 cm down gradient distance in the flow direction during experiment. The observed value of solute concentration for chloride has been compared for both cases of layered soil and mixed soil media. The behaviors of breakthrough curves are similar in both cases of soil media, but the magnitude of solute concentration is not

same for higher transport time. It is also, known that the different types of soil strata affect the value of hydraulic conductivity within the soil media. The physical properties of the soil affect the transport of solute through heterogeneous media. Dispersion is a key process controlling transport of solute in heterogeneous porous medium. Long tailing is also observed in breakthrough curves during large transport time. It indicates that the some magnitude of solute is remained in immobile zone. Velocity also plays an important role in the diffusion process. The steady-state conditions describe the function for the solute behavior. Dispersivity is also defined as the ratio of dispersion coefficient to the effective pore water velocity. Hence, solute transport in soil and groundwater is generally affected by a large number of physical, chemical and microbial processes and medium properties.

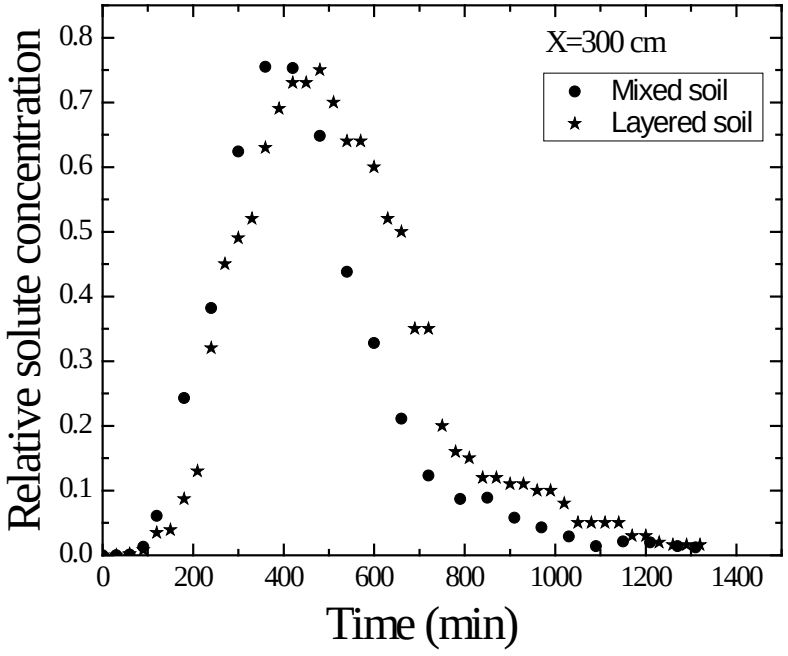

Figure 5.15 Break through curves of experimental data for chloride at 300cm distance in heterogeneous soil.

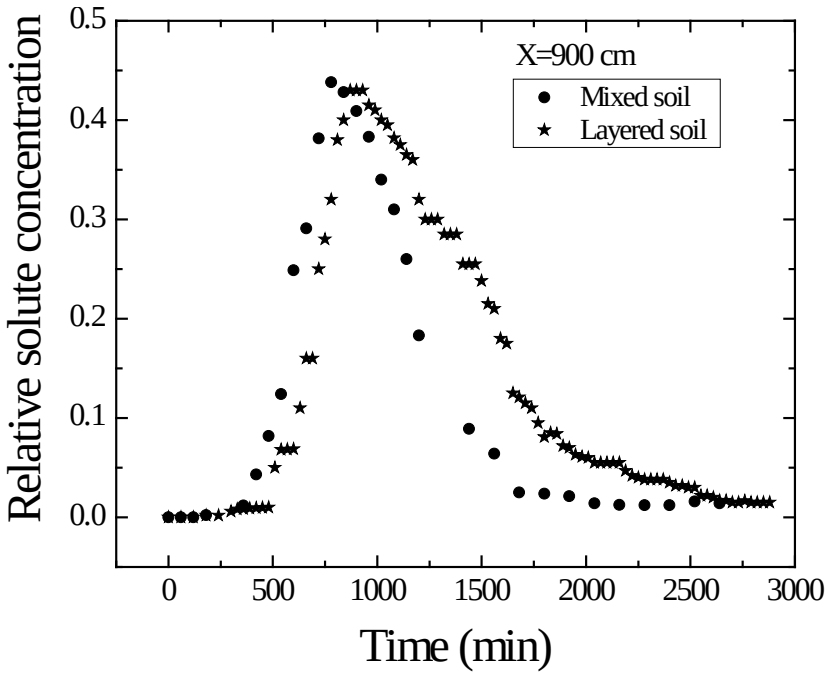

Figure 5.16 Break through curves of experimental data for chloride at 900cm distance in heterogeneous soil.

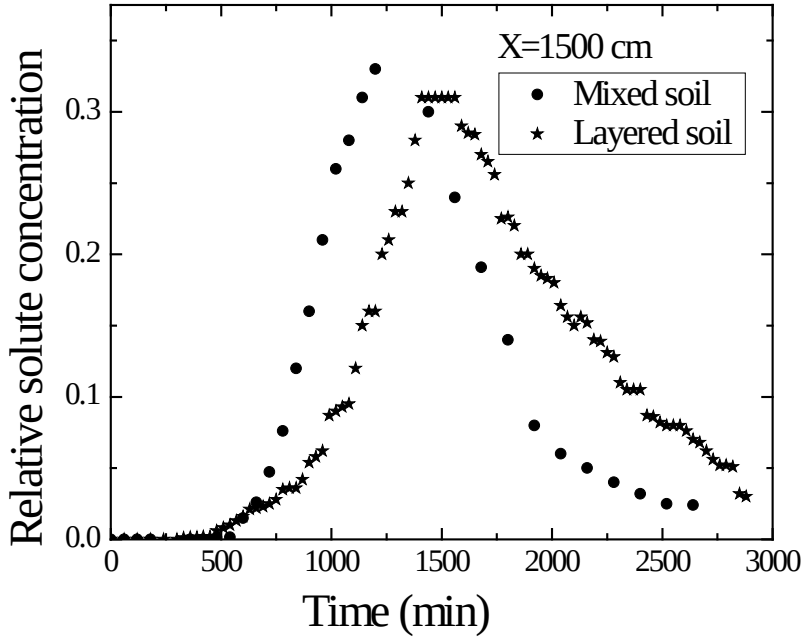

Figure 5.17 Break through curves of experimental data for chloride at 1500cm distance in heterogeneous soil.

5.6 Summary

Breakthrough curve for non-reactive solute shows early appearance due to strong dispersion in layered soil as compared to mixed. Long tailing is also observed due to presence of solute in porous space. It is also seen that the stratification i.e., layered and mixed soil media affect the behavior of predicted breakthrough curves in long heterogeneous soil column experiments. The behaviors of breakthrough curves are very irregular and exhibited extensive tailing. It means that the variation of pore velocity in heterogeneous porous media is much larger as compared to homogeneous porous media. It means that the large variation of hydraulic conductivity increase the dispersion of solute in heterogeneous porous media.

In this study, observed experimental break through curves have been simulated using mobile-immobile constantant, linear and asymptotic distance-dependent dispersivity. The results show that the variation of pore velocity in heterogeneous porous media is much larger as compared to homogeneous porous media. It is shown that early arival of solute concentration has been obtained in case of constant dispersivity as compared to both linear and assymptotic value of dispersivity.

Finally, it is also shown that the MIMA model gives the best fit curve of experimental breakthrough curve in long heterogeneous soil column experiment as compared to both MIMC and MIML models. Estimated value of dispersivity is smaller in case of MIMA model as compared to both MIMC and MIML models. Thus MIMA model is efficient to capture the evolution distance dependent dispersion behavior. Accurate prediction of mass transfer coefficient is also essential and significant for transport of contaminant through porous media. Hence asymptotic dispersivity including variable mass transfer coefficient can be useful for describing solute transport in long heterogeneous porous media.

Chapter 6

Reactive solute transport through triple-permeability porous medium

6.1 General

This chapter describes the reactive solute transport through porous media such as the fractured rock masses or soils consisting of triple pore regions. Triple advective-dispersive transport equations considering equilibrium sorption and first-order degradation rate coefficients are used. Both the finite-volume method (FVM) and the implicit finite-difference method (FDM) have been used to develop the numerical model for reactive solute transport through triple-permeability medium. The performance of FVM and FDM methods has been analysed in terms of concentration profiles for smaller and higher values of Peclet numbers. In addition to this, the behavior of spatial moments is also analyzed.

6.2 Mathematical model

One-dimensional advection-dispersion transport equation is presented for solute transport through triple-permeability medium. Figure 6.1 describes the solute transport through triple-permeability porous medium consisting of three regions 1, 2 and 3.

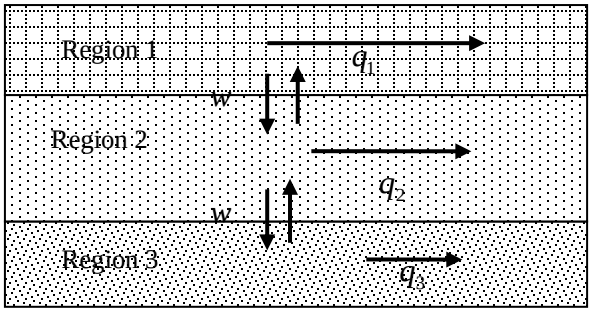

Figure 6.1 Schematic diagrams of triple-permeability media with advection-dispersion transport model.

A first order mass transfer coefficient is used to describe the solute exchange between regions of 1 or 2 and 2 or 3. The governing eqution for solute transport in an arbitrary region *i*, which equals 1 or 2 and 2 or 3, is affected by the transport in the other region *j*, which equals 2 or 1 and 3 or 2, as is given in Equation (6.1). The advective-dispersive transport equation including the equilibrium sorption and the first-order degradation rate constant is given below (Lapidus and Amundson 1952 and Leij et al. 2012):

$$\theta_i R_i \frac{\partial C_i}{\partial t} + \theta_i v_i \frac{\partial C_i}{\partial x} = \theta_i D_i \frac{\partial^2 C_i}{\partial x^2} - w\left(C_i - C_j\right) - \theta_i \mu_i \tag{6.1}$$

where t is the time (T); x is the distance (L); C_i and C_j are the aqueous phase solute concentrations for three regions, expressed as mass of solute per aqueous volume in regions i and j, respectively (M/L^3); w is the first-order mass transfer coefficient (T^{-1}); D_i is the hydrodynamic dispersion coefficient for region i (L^2/T); v_i is the pore water velocity for region i (L/T); R_i is the retardation factor to account for sorption of the solute by solid phase; μ_i is the first-order degradation rate coefficient (T^{-1}); and θ_i is the volumetric water content given as volume of water in region i per total bulk volume (L^3/L^3). The total volumetric water content for the entire porous medium is $\theta(=\theta_1+\theta_2+\theta_3)$. The Darcy flux $q_i = v_i\,\theta_i$ and dispersivity $\alpha_i = D_i / v_i$ are related to pore-water velocity and dispersion coefficient. The retardation factor is defined as $R_i = 1 + \rho K_{di} / \theta_i$, where ρ is the bulk density (M/L^3); and K_{di} is a distribution coefficient for equilibrium partitioning between the solid and aqueous phases, which is expressed as the volume of aqueous phase in region i per mass of solid phase (L^3/M). A solute will travel at a different speed through the pore regions because of a difference in permeability.

6.2.1 Boundary conditions

The following initial conditions are given as:

$$C_i(x,0) = 0 \tag{6.2a}$$

$$\frac{\partial C_i}{\partial x}(\infty, t) = 0 \tag{6.2b}$$

Constant boundary condition is given as:

$$C_i(x,t) = C_0 \tag{6.2c}$$

Pulse type boundary condition is given as:

$$C_i(x,t) = C_0 \quad \text{for } t \le t_0 \tag{6.2d}$$

$$C_i(x,t) = 0 \qquad \text{for } t > t_0 \tag{6.2e}$$

where C_0 is the injected solute concentration and t_0 is the pulse time.

The total amount of solute present in the porous medium,that is, in the aqueous and sorbed phases of three regions, is expressed with the total concentration defined by the weighted sum of volume averaged concentrations as:

$$C_t = \left(\theta_1 R_1 C_1 + \theta_2 R_2 C_2 + \theta_3 R_3 C_3\right)/\theta \tag{6.3a}$$

For the analysis of breakthrough curves, for example, determined from effluent samples collected during the solute transport in soil column, the solute concentration can be defined as the ratio of advective solute and water flux.

$$C_e = \left(q_1 C_1 + q_2 C_2 + q_3 C_3\right)/q \tag{6.3b}$$

where $q = q_1 + q_2 + q_3$.

6.3 Numerical Methods

An implict finite difference numerical method has been used to get the solution of one-dimensional advective dispersive transport Eq. (6.1) for solute transport through triple medium. The numerical model first determines the solute concentration in the first region of the current

time step, using solute concentration in the second region at previous time step. Similarly, the solute concentration is determined in the second region, using the solute concentration in the first region at previous time step. Then the solute concentration is determined in the third region at the current time step. Once the concentration is determined for third region, the solution proceeds to the next time step witout iteration. A tridiagonal coefficient matrix was obtained, which solved the equation more efficiently. The finite volume method was also used to the solution of governing equations, which is described below.

6.3.1 Formulation of governing equations for triple-permeability medium

The governing transport equations for three regions can be written as:

$$\theta_1 R_1 \frac{\partial C_1}{\partial t} + \theta_1 v_1 \frac{\partial C_1}{\partial x} = \theta_1 D_1 \frac{\partial^2 C_1}{\partial x^2} - w(C_1 - C_2) - \theta_1 \mu_1 \tag{6.4}$$

$$\theta_2 R_2 \frac{\partial C_2}{\partial t} + \theta_2 v_2 \frac{\partial C_2}{\partial x} = \theta_2 D_2 \frac{\partial^2 C_2}{\partial x^2} - w(C_2 - C_1) - \theta_2 \mu_2 \tag{6.5}$$

$$\theta_3 R_3 \frac{\partial C_3}{\partial t} + \theta_3 v_3 \frac{\partial C_3}{\partial x} = \theta_3 D_3 \frac{\partial^2 C_3}{\partial x^2} - w(C_3 - C_2) - \theta_3 \mu_3 \tag{6.6}$$

The advective terms of Eqs. (4), (5) and (6) can be written as:

$$\frac{\partial C_1}{\partial t} = -\frac{v_1}{R_1} \frac{\partial C_1}{\partial x} \tag{6.7}$$

$$\frac{\partial C_2}{\partial t} = -\frac{v_2}{R_2} \frac{\partial C_2}{\partial x} \tag{6.8}$$

$$\frac{\partial C_3}{\partial t} = -\frac{v_3}{R_3} \frac{\partial C_3}{\partial x} \tag{6.9}$$

Similarly, the dispersive transport terms can be expressed as:

$$\frac{\partial C_1}{\partial t} = \frac{D_1}{R_1} \frac{\partial^2 C_1}{\partial x^2} \tag{6.10}$$

$$\frac{\partial C_2}{\partial t} = \frac{D_2}{R_2}\frac{\partial^2 C_2}{\partial x^2} \tag{6.11}$$

$$\frac{\partial C_3}{\partial t} = \frac{D_3}{R_3}\frac{\partial^2 C_3}{\partial x^2} \tag{6.12}$$

And remaining equations can be written as:

$$\theta_1 R_1 \frac{\partial C_1}{\partial t} = -w(C_1 - C_2) - \theta_1 \mu_1 C_1 \tag{6.13}$$

$$\theta_2 R_2 \frac{\partial C_2}{\partial t} = -w(C_2 - C_1) - \theta_2 \mu_2 C_2 \tag{6.14}$$

$$\theta_3 R_3 \frac{\partial C_3}{\partial t} = -w(C_3 - C_2) - \theta_3 \mu_3 C_3 \tag{6.15}$$

6.3.2 Procedure of numerical solution

The finite volume numerical method is used for solving the advective transport which is based on monotone upwind schemes for conservation laws (MUSCL) by van Leer (1977a,b). This method is globally high-order accurate and non-oscillatory. The formulation of this scheme is extended for solute transport as:

$$\frac{\partial C}{\partial t} + \frac{\partial F}{\partial x} = 0 \tag{6.16}$$

where C can be replaced by C_1, C_2 and C_3; F is the advecrive flux, which can be written as $F = \frac{v}{R}C$. Equation (6.16) can be written in a discrete form by assuming the cell centered concentration C_i as cell averaged concentration:

$$\frac{\left(C_i^{n+1} - C_i^n\right)}{\Delta t} + \frac{\left(\overline{F}_{i+1/2}^n - \overline{F}_{i-1/2}^n\right)}{\Delta x} = 0 \tag{6.17}$$

where C_i is the cell centered concentration, $\overline{F}^{n}_{i+1/2}$ is the time average flux, n denotes the time stage, Δt represents the time step and Δx represents the space step. Advective flux is computed using a second order upwind method similar to the one adopted by Putti et al. (1990). Assuming a linear distribution in the cell, the mass concentration value at the cell interface is reconstructed using a MUSCL approach (van Leer 1977a). Other procedure has been explained in Chapter 5.

6.3.3 Dispersive transport equation

The dispersive transport simulations from Equations (6.10), (6.11) and (6.12) are performed on the concentrations, resulting from the advective transport in each time step. A conventional fully implicit, finite-difference scheme, which is unconditionally stable, is used to obtain the final concentrations at the end of time step. This formulation has the advantage of using an implicit numerical scheme for the dispersive transport, while using an explicit numerical scheme for advection transport there by either advection dominated or dispersion dominated systems can be accurately handled. Remaining Equations (6.13-6.15) are solved using explicit numerical method and formulations are expressed below.

$$\theta_1 R_1 \frac{C_{1i}^{n+1} - C_{1i}^{n}}{\Delta t} = -w\left(C_{1i}^{n} - C_{2i}^{n}\right) - \theta_1 \mu_1 C_{1i}^{n} \tag{6.18}$$

$$\theta_2 R_2 \frac{C_{2i}^{n+1} - C_{2i}^{n}}{\Delta t} = -w\left(C_{2i}^{n} - C_{1i}^{n}\right) - \theta_2 \mu_2 C_{2i}^{n} \tag{6.19}$$

$$\theta_3 R_3 \frac{C_{3i}^{n+1} - C_{3i}^{n}}{\Delta t} = -w\left(C_{3i}^{n} - C_{2i}^{n}\right) - \theta_3 \mu_3 C_{3i}^{n} \tag{6.20}$$

6.3.4 Verification of numerical model

Both finite volume and finite difference numerical methods were verified with analytical solution of Sciortino et al. (2015) for solute transport through dual-permeability medium. Figure 6.2 represents the temporal concentration profiles predicted at 25 cm down gradient distance in the flow direction using input parameters as pulse time, t_0 = 0.5 day; flow rate q_1 = 10 cm/day; q_2 = 5 cm/day; volumetric water content θ_1 = 0.1; θ_2 = 0.4; dispersivity α_1 =0.5 cm and α_2 =2.5 cm. The excellent agreement of the numerical results with the analytical solution

verified the model with Courant number Cr equal to 0.5 and Peclet number ($\mathrm{Pe} = \frac{v.\Delta x}{D}$) equal to 0.5.

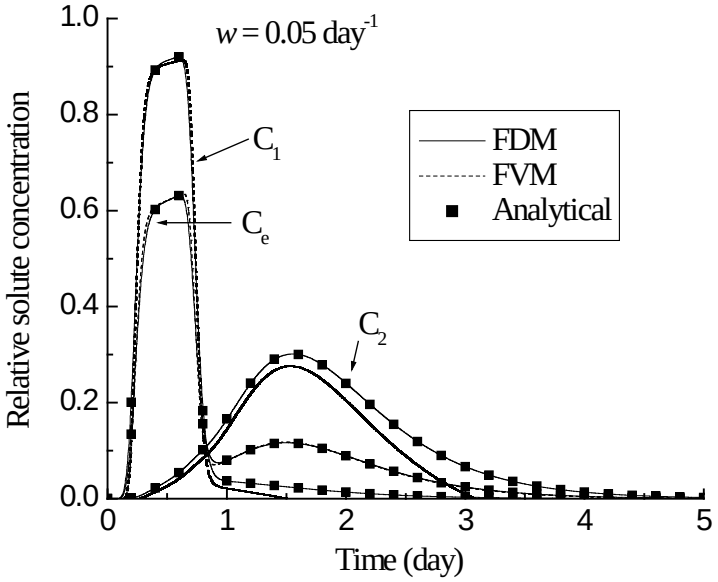

Figure 6.2 Comparison of breakthrough curves obtained from FDM, FVM and analytical solutions for solute C_1 C_2 and C_e at x = 25 cm and pulse input t_0 = 0.5 day.

6.4 Application of model

6.4.1 Concentration profiles

The results of concentration profiles have been compared between FVM and FDM for small and higher values of Peclet number (Pe=0.5 and 200). Values of input parameters such as q_1 = 10 cm/day; θ_1 = 0.1; q_2 = 7.5 cm/day; θ_2 = 0.25; q_3 = 4 cm/day; θ_3 = 0.4; dispersivity $\alpha_1 = \alpha_2 = \alpha_3$ =0.05 cm and pulse time t_0 = 0.2 day are used during simulation. Spatial solute concentration profiles for solute concentration C_1, C_2 and C_3 for small value of mass transfer coefficient (w = 0.01 day^{-1}) and higher value (w = 5 day^{-1}) are shown in Figures 6.3a and 6.3b, respectively. The value of Peclet number, Pe=0.5 has been used. It is observed that the magnitude of solute concentration remained the same for both cases of FVM and FDM. However, only very small deviation is found in solute concentration C_1 in the presence of small value of mass transfer coefficient. The solute concentrations C_1, C_2 and C_3 travel small distance

due to higher value of mass transfer coefficient, w = 5 day^{-1}. It means that a higher value of mass transfer coefficient retards the solute plume in the porous medium.

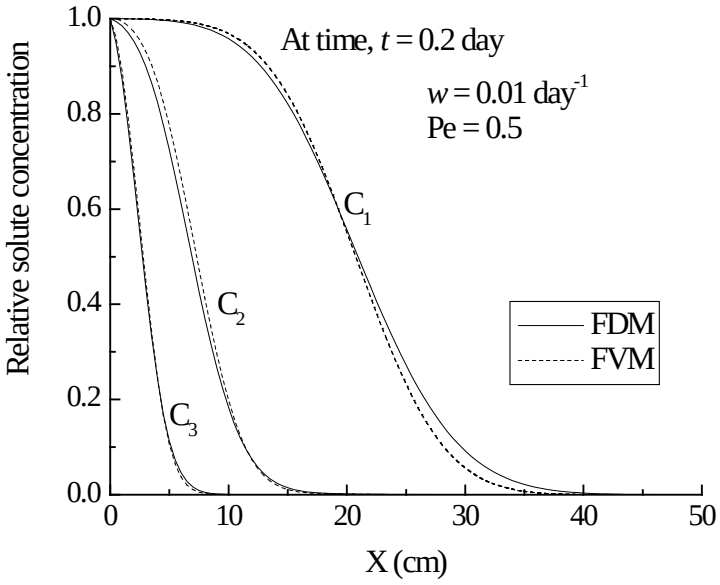

Figure 6.3a Spatial concentration profiles for solutes C_1, C_2 and C_3 for Peclet number Pe = 0.5 and small value of mass transfer coefficient w = 0.01 day^{1} using FDM and FVM.

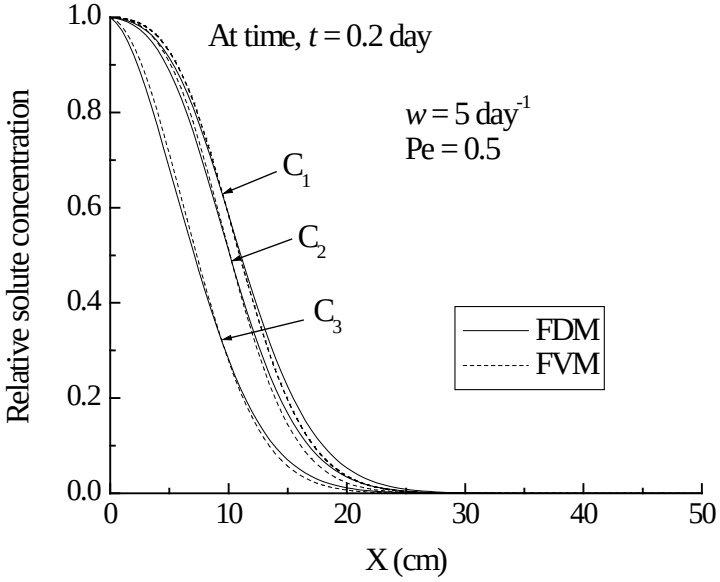

Figure 6.3b Spatial concentration profiles for solutes C_1, C_2 and C_3 for Peclet number Pe = 0.5 and higher value of mass transfer coefficient w = 5 day^{-1} using FDM and FVM.

Figure 6.4a shows the spatial concentration profile for small value of mass transfer coefficient (w = 0.01 day^{-1}) and Peclet number equal to 2. It is found that the deviation occurs in the results of concentration profiles as predicted from both FVM and FDM. However, the deviation in the results of concentration profile for C_1 is large as compared to C_2 and C_3. Figure 6.4b shows the concnetration profiles for C_1, C_2 and C_3 for a higher value of mass transfer coefficient (w = 5 day^{-1}). It is seen that the results of concentration prfiles remain the same in both numerical FVM and FDM methods. Hence, it can be concluded that both FVM and FDM models give the same results for Peclet number (Pe=2) in the presence of a higher value of mass transfer coeffiicient.

Figures 6.5a and 6.5b show the results of concentration profiles for C_1, C_2 and C_3 for Peclet number equal to 200 and for values of mass transfer coefficient equal to 0.01 and 5 day^{-1}. The numerical oscilation is observed in case of FDM method, while oscillation free results is seen in case of FVM method. It means that the implict finite difference method cannot be used in case of a higher value of peclet number, while the finite volume method gives the accurate results for solute concentration for small and higher values of peclet number. Hence, the FVM method can be used for simulation of concentration profiles for solute through porous media for any value of Peclet number.

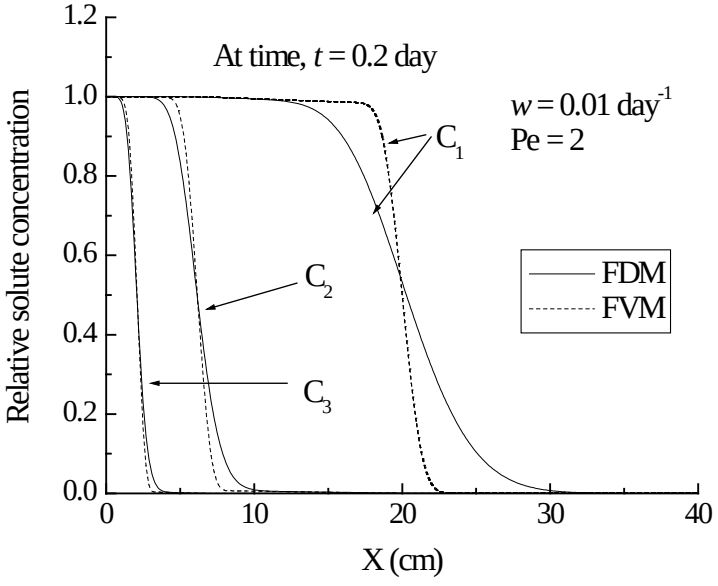

Figure 6.4a Spatial concentration profiles for solutes C_1, C_2 and C_3 for Peclet number Pe = 2 and smaller value of mass transfer coefficient w = 0.01day^{-1} using FDM and FVM.

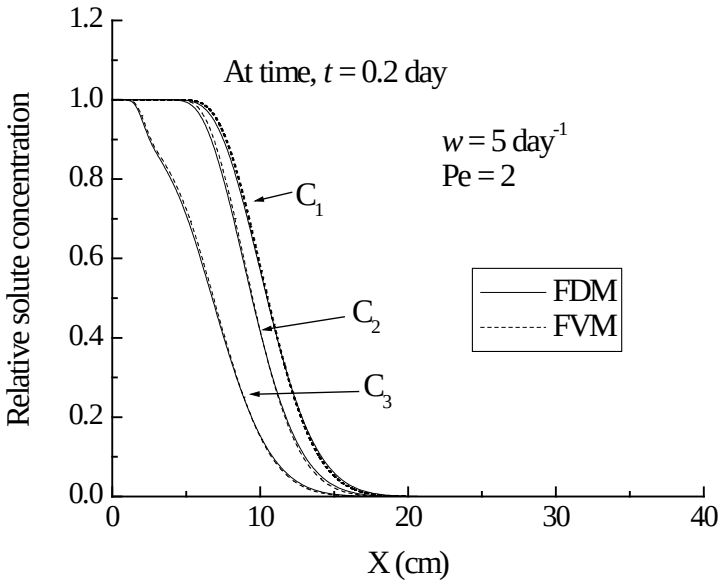

Figure 6.4b Spatial concentration profiles for solutes C_1, C_2 and C_3 for Peclet number Pe = 2 and higher value of mass transfer coefficient w = 5 day^{-1} using FDM and FVM.

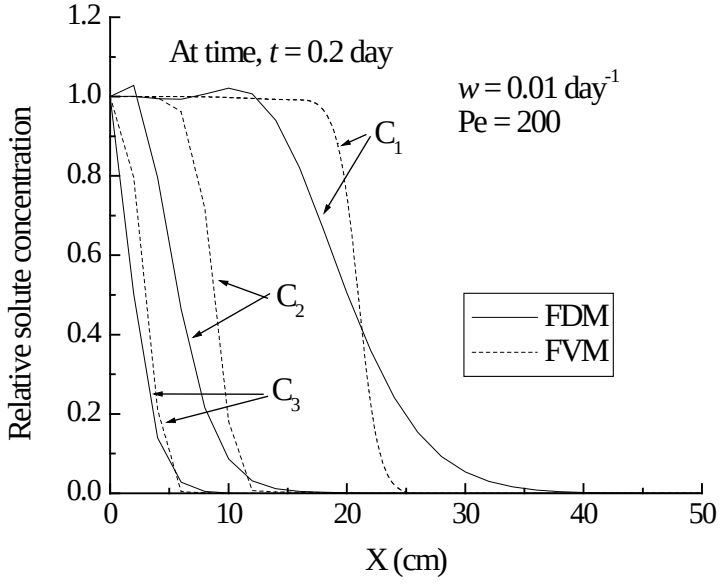

Figure 6.5a Spatial concentration profiles for solutes C_1, C_2 and C_3 for Peclet number Pe = 200 and smaller value of mass transfer coefficient w = 0.01day^{-1} using FDM and FVM.

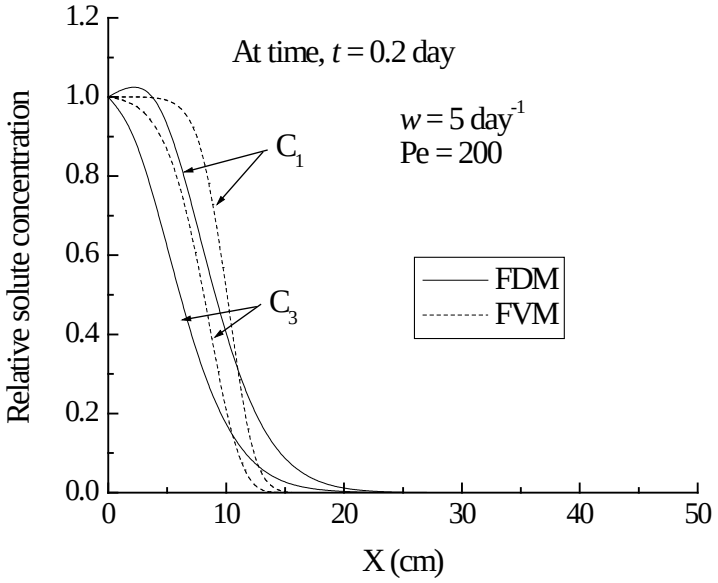

Figure 6.5b Spatial concentration profiles for solutes C_1, C_2 and C_3 for Peclet number Pe = 200 and higher value of mass transfer coefficient w = 5 day^{-1} using FDM and FVM.

Figures 6.6a and 6.6b show the results of concentration profiles for two values of mass transfer coefficient (0.01 and 1 day^{-1}) and predicted at time of t = 0.025 day and 0.1day, respectively. During a small transport time (t = 0.025 day), the diference is lower in solute concentration for both values of mas transfer coefficient. However, at higher transport time (t = 0.1 day), the difference in solute concentration increases for both values of mass transfer coefficient. It means that the transport time affects the solute concentartion in three regions with mass transfer coefficient.

Figures 6.7a and 6.7b show the results of concentration profiles for two values of first-order degradation rate coefficient (0.01 and 1 day^{-1}) and predicted at time of t = 0.1 day and 0.2 day, respectively. During the small transport time (t = 0.1 day), the diiference is lower in solute concentration for both values of degradtion rate coefficient. However, at higher transport time (t = 0.2 day), the difference in solute concentration increases for both values of degradation rate coefficient. It means that the magnitude of solute concentration remains almost the same for a small transport time. However, the behavior and magnitude of concentration profiless are different for solutes C_1, C_2 and C_3 at higher transport times.

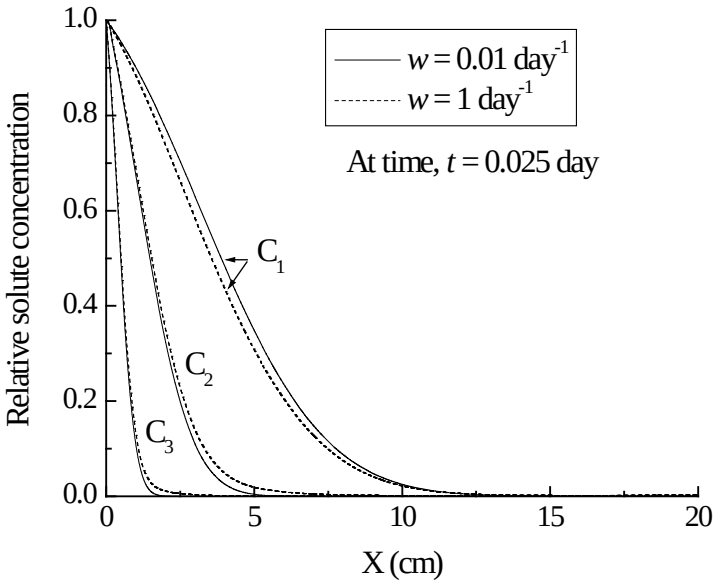

Figure 6.6a Spatial concentration profiles for solutes C_1, C_2 and C_3 for two values of mass transfer coefficient predicted at time t = 0.025 day.

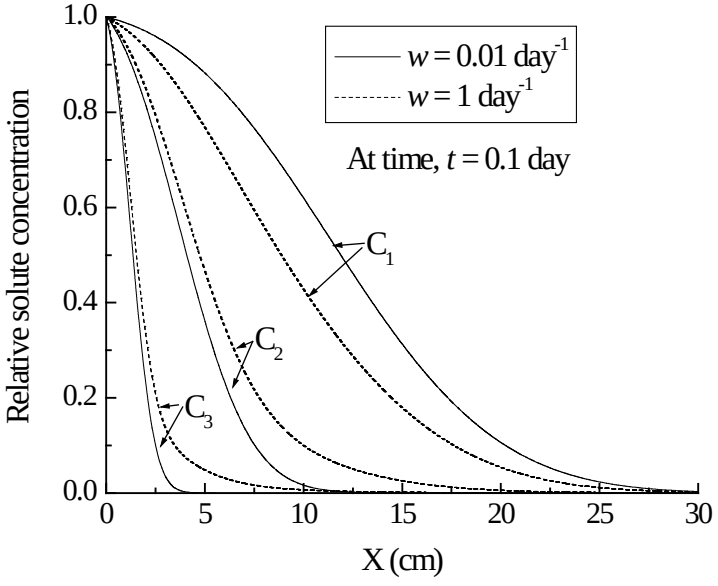

Figure 6.6b Spatial concentration profiles for solutes C_1, C_2 and C_3 for two values of mass transfer coefficient predicted at time t = 0.1 day.

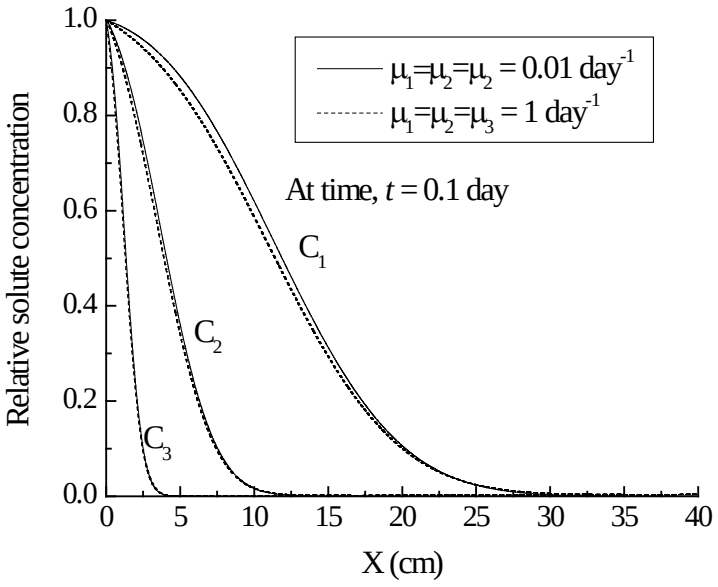

Figure 6.7a Spatial concentration profiles for C_1, C_2 and C_3 for two values of first-order degradation rate coefficients predicted at time t = 0.1 day.

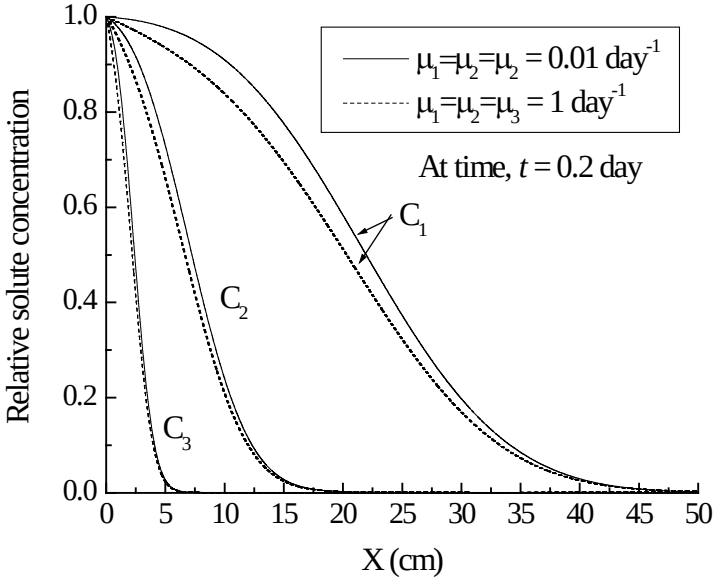

Figure 6.7b Spatial concentration profiles for solutes C_1, C_2 and C_3 for two values of first-order degradation coefficient predicted at time t = 0.2 day.

The result of spatial concentration profiles for C_1, C_2 and C_3 for two values of retardation factor is shown in Figure 6.8. As expected, the magnitude of solute concentration is reduced due to

the higher value of retaradtion factor. The behavior of concentration profiles are non-linear with travel distance. The value of equilibrium sortpion,that is, the retardation factor is the same and the values of pore velocity are different in three regions of porous medium. Hence the retardation rate of solute plume is different in three regions.

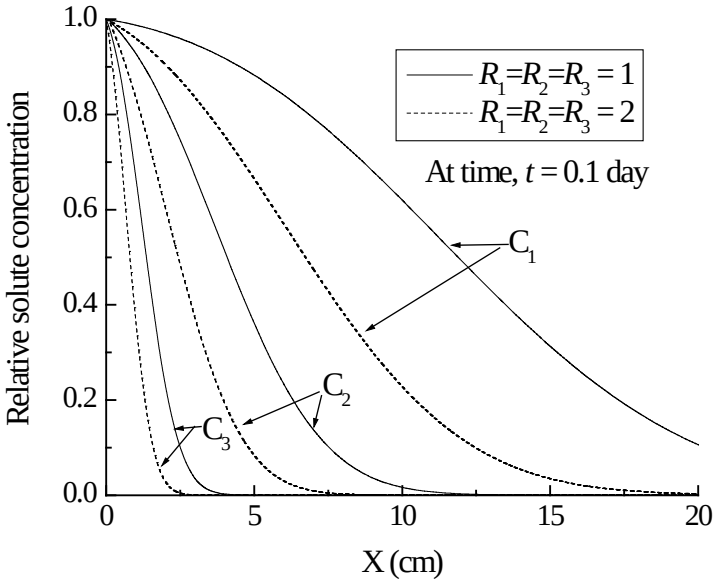

Figure 6.8 Spatial concentration profiles for solutes C_1, C_2 and C_3 for two values of retardation coefficient predicted at time t = 0.1 day.

6.4.2 Spatial moments

Spatial moments describe the location and shape of the solute plume, that is, the position of the centroid and the spreading around the centroid, and these moments are useful in describing the transport process of solute through porous media. The spatial moments can be obtained for the solute concentration distribution using a similar approach given by Guven et al. (1984). The first and second spatial moments for solute in the porous medium are given, respectively, by:

$$X_1 = (1/M)\int_0^\infty xC dx \tag{6.21a}$$

$$X_2 = (1/M)\int_0^\infty x^2 C dx - X_1^2 \tag{6.21b}$$

with

$$M = \int_0^{\infty} C dx \tag{6.21c}$$

where M is the mass of solute in porous medium, X_1 is the first spatial moment (mean travel distance), and X_2 is the second spatial moment (variance) in x coordinate direction. The expressions of spatial moments are valid for a concentration pulse source. Since a constant continuous source is applied as a boundary condition at the inlet of fracture, a first spatial derivative of concentration in the porous medium is used to obtain an equivalent pulse.

The results of spatial moments for solutes C_1, C_2, C_3 C_t and C_e are discussed in the presence of mass tansfer, first-order degradation coefficeints and retardation factor. Figures 6.9a, 6.9b and 6.9c show the results of mean travel distance for values of mass transfer coefficient w = 0.05, 0.5 and 5 day^{-1}, respectively. During samll transport time, the behavior of mean travel distance is non-linear for small value of mass transfer coefficient. The magnitude of mean travel distance is higher for solute C_1 as compared to other solutes, because the value of pore water velocity is large in the first region as compared to other two regions. However, in the presence of large value of mass transfer coefficient w = 5 day^{-1}, the magnitue of mean travel distance remains the same for all the solutes in the regions of medium.

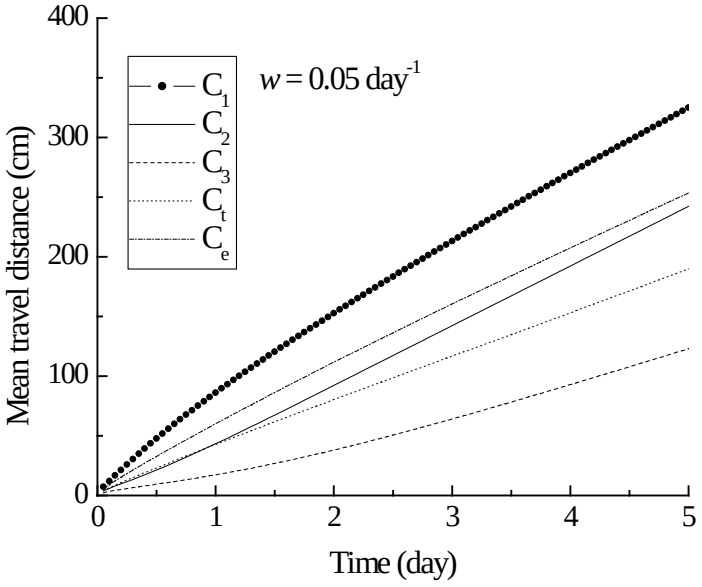

Figure 6.9a Mean travel distance for solute concentration in triple-permeability media for value of mass transfer coefficient w = 0.05 day^{-1}.

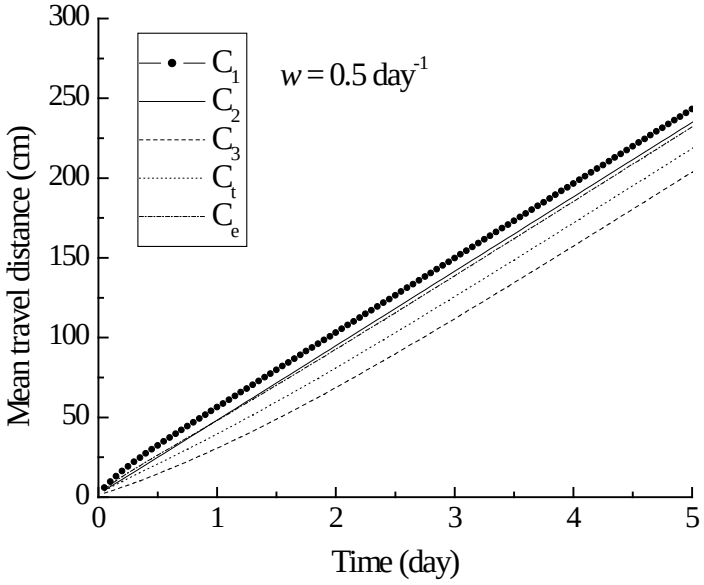

Figure 6.9b Mean travel distance for solute concentration in triple-permeability media for value of mass transfer coefficient $w = 0.5$ day^{-1}.

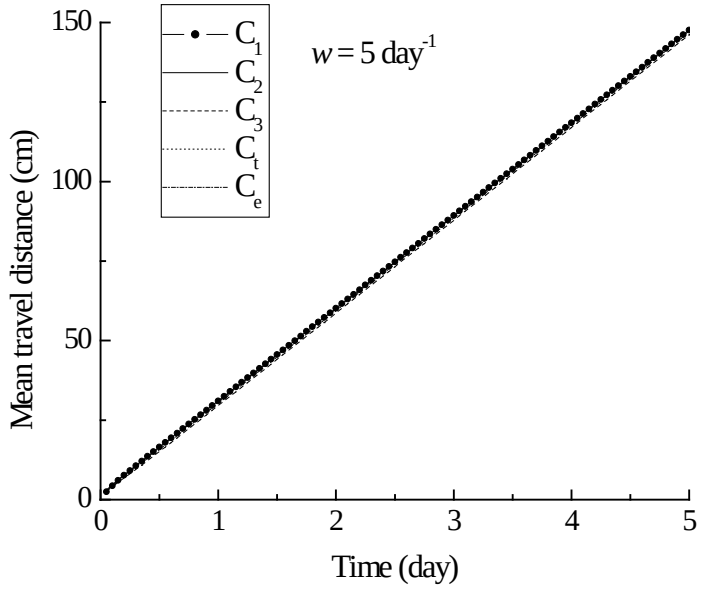

Figure 6.9c Mean travel distance for solute concentration in triple-permeability media for value of mass transfer coefficient $w = 5$ day^{-1}.

Figures 6.10a, 6.10b, 6.10c show the results of variance for solutes C_1, C_2, C_3 C_t and C_e with different values of mass transfer coefficient. In case of mass transfer w = 0.01 day^{-1}, the magnitude of spreading or variance of solutes increases with an increase in the transport time. But in the case of large value of mass tranfer coefficeint w = 5 day^{-1}, the magnitude of variance remains the same for all the solutes and linearly increases with an increase in transport time.

Figures 6.11a and 6.11b represent the results of mean travel distance and spreading beavior of effluent solute (C_e) for different values of retardation factor. A higher value of retardation factor (equal to 2 or 5) leads to reduce the magnitude of both mean travel distance and variance along with transport time. Similarly, the higher value of decay rate coefficient reduces the mean travel distance and variance for large transport time, but the magnitude remains the same during the small transport time as shown in Figures 6.12a and 6.12b. It is also seen that the behavior of spreading of effluent solute is non-uniform during the intermediate transport time.

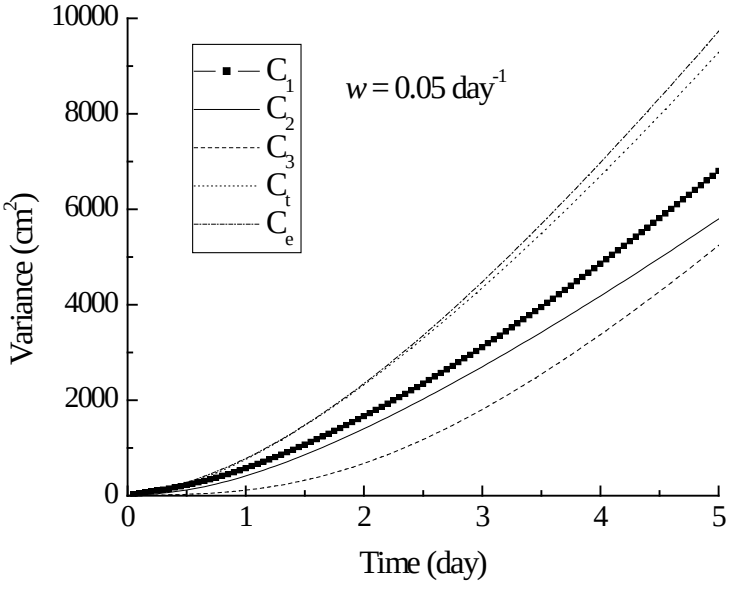

Figure 6.10a Variance for solute concentration in triple-permeability media for value of mass transfer coefficient w = 0.05 day^{-1}.

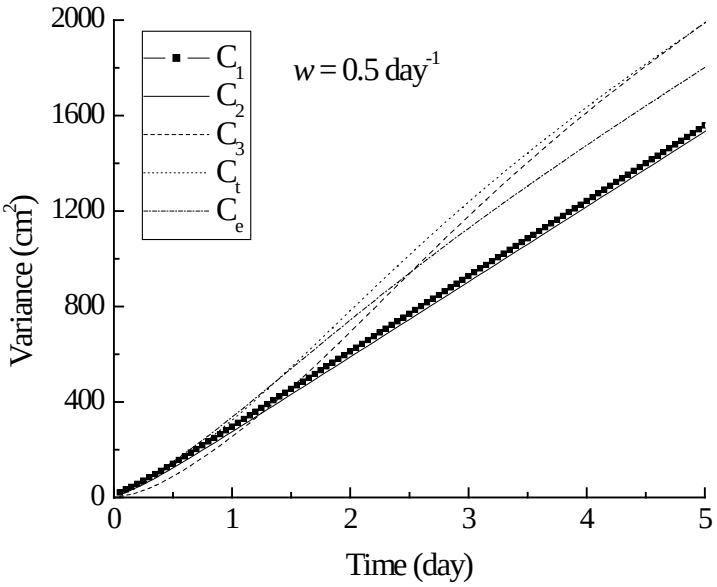

Figure 6.10b Variance for solute concentration in triple-permeability media for value of mass transfer coefficient $w = 0.5$ day^{-1}.

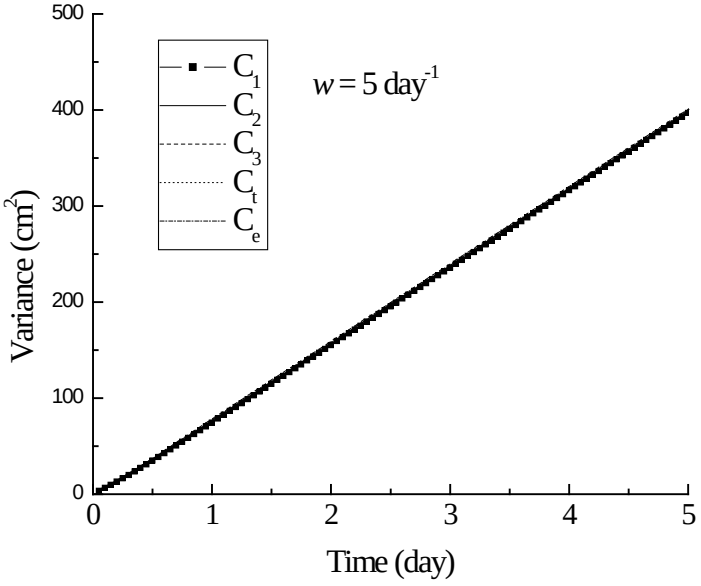

Figure 6.10c Variance for solute concentration in triple-permeability media for value of mass transfer coefficient $w = 5$ day^{-1}.

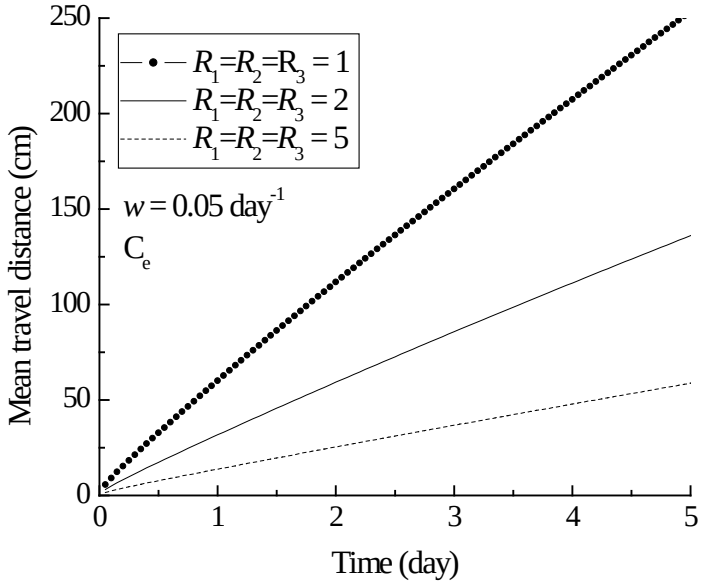

Figure 6.11a Mean travel distance for solute concentration C_e in triple-permeability media for different values of retardation factor.

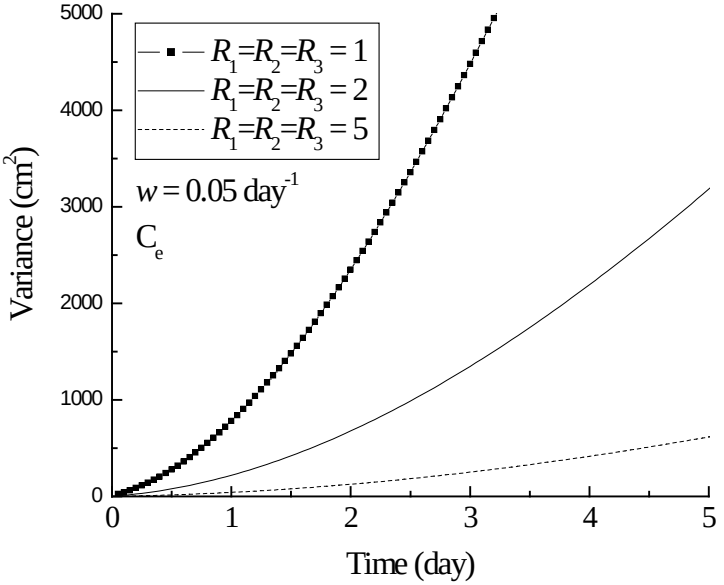

Figure 6.11bVariance for solute concentration C_e in triple-permeability media for different values of retardation factor.

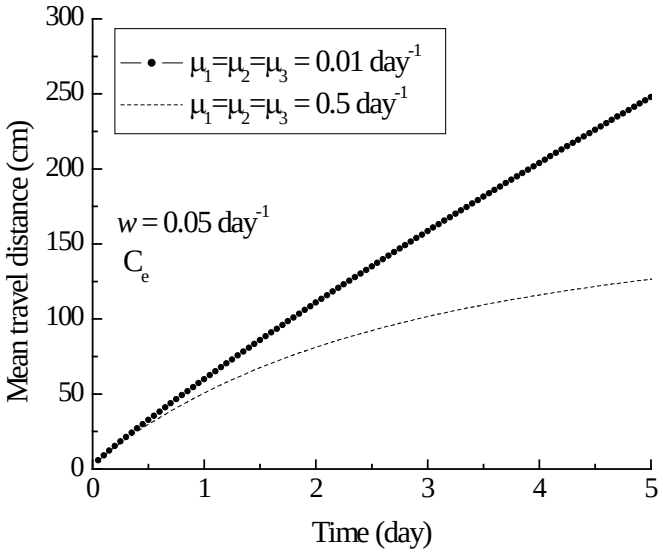

Figure 6.12a Mean travel distance for solute concentration C_e in triple-permeability media for different values of first-order degradation rate coefficient.

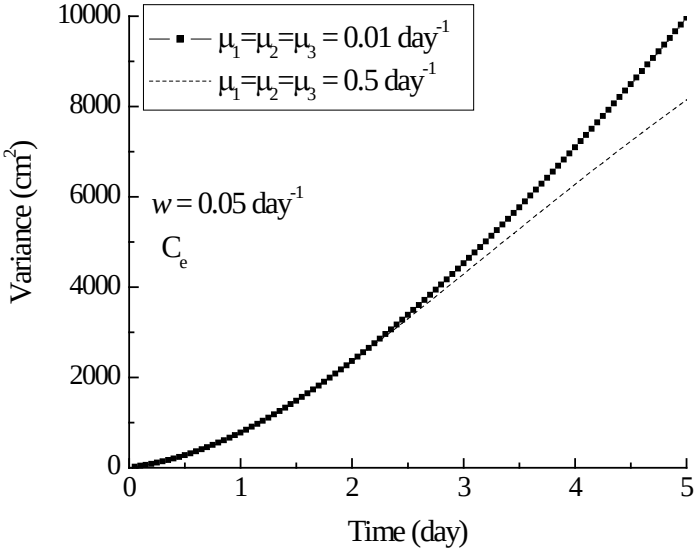

Figure 6.12b Variance for solute concentration C_e in triple-permeability media for different values of first-order degradation rate coefficient.

6.5 Summary

In this chapter, a numerical model has been developed for the governing equation of reactive solute transport through triple-permeability porous medium using the finite-volume method (FVM) and the implicit finite-difference method (FDM). The concentration profiles indicate that the performance of both FDM and FVM are the same for the Peclet number equal to 0.5 in the presence of small and higher values of mass transfer rate coefficient. In the case of Peclet number equal to 2, the concentration profiles remain the same by FDM and FVM in the presence of higher value of mass transfer rate coefficient. However, a significant difference in the results is obtained for both methods in the case of small value of mass transfer coefficient.

In the case of Peclet number equal to 200, the numerical oscillation has been obtained by FDM, while oscillation-free result is seen by FVM in the presence of both small and higher values of mass transfer coefficient. Hence, the FVM can be used for the simulation of solute transport through porous media for any value of Peclet number. The results of mean travel distance and spreading behaviour of solutes remain the same in the case of higher values of mass transfer coefficient. Higher value of mass transfer, first-order degradation rate and retardation factor lead to reduce the magnitude of mean travel distance and spreading of solute in the porous medium. During the small transport time, the behaviour of spreading of solute is non-uniform and it becomes linear for higher transport times. This study can be useful for remediation of contaminant transport through triple permeability medium.

Chapter 7

7 SUMMARY AND CONCLUSIONS

7.1 Summary

In this study, an advection-dispersion-reaction equation is used, which accounts for both physical non-equilibrium (PNE) and sorption non-equilibrium (SNE) for reactive solute transport through porous media. PNE is accounted by a diffusive mass transfer between the advective and the non-advective regions. SNE is accounted by using a two-site conceptualization for both advective and non-advective regions, where at the first site, the sorption is assumed to be governed by an instantaneous equilibrium adsorption isotherm and at the second site, the sorption is described by a first order rate-limited process.

Semi-analytical solution for multiprocess non-equilibrium transport model with asymptotic distance-dependent dispersion has been developed for reactive transport through heterogeneous porous media. Analytical solution was developed using the Laplace transform technique, which was then numerically inverted to time domain, to obtain solute concentration in the advective region. The present semi-analytical solutions were compared with the existing analytical solutions developed for heterogeneous porous medium (Gao et al., 2012) and a very good agreement between the present model and the available analytical solutions were obtained.

The applicability of asymptotic distance-dependent dispersion model was evaluated by simulating the experimental data of 1500 cm long heterogeneous soil column. Batch sorption experiment has been done to estimate linear and nonlinear sorption coefficients for natural soil and fine sand, respectively. These sorption coefficients were used to simulate observed breakthrough curves for fluoride transport through soil column experiments. Also, variable mass transfer coefficient is used to simulate observed breakthrough curves in the presence of

asymptotic dispersion model. Finally, the performance for advection and dispersion dominant cases for reactive transport through triple-permeaility porous media was studied.

7.2 Conclusions

Following conclusions are made from the study:

1. Semi-analytical solution of multiprocess non-equilibrium transport equations with asymptotic distance-dependent dispersivity functions are derived for reactive solute transport through heterogeneous porous media. This model includes both physical and chemical non-equilibrium simultaneously. Therefore, this model is more general and it can be more applicable for reactive transport through porous media.

2. It was also observed that asymptotic distance-dependent dispersivity model gives a good fit to the observed breakthrough curves as compared to constant dispersion model. The simulated results of observed data demonstrated that multiprocess non-equilibrium with constant dispersion model could not adequately describe solute transport in large heterogeneous soil column and it overestimated solute transport dispersion at foregoing distances away from 1500 cm long soil column experiments.

3. On the basis of linearization of Langmuir nonlinear isotherm model, it is shown that the best fit is given by Langmuir -2 linear isotherms in comparison to other Langmuir linear isotherms in case of fine sand. However, in case of natural soil, Langmuir-1 linear isotherm gives the best fit. In case of fine sand, the value of coefficient of determination, R^2=0.8306 and 0.908 is obtained for Freundlich linear isotherm and Langmuir-2 linear isotherms, respectively. This also indicates that the Langmuir-2 linear isotherms can be preferred in comparison to Freundlich linear isotherm.

4. In case of natural soil, the value of R^2=0.8673 and 0.9272 is obtained for Freundlich linear isotherm and Langmuir-1 linear isotherms, respectively. This also indicates that the Langmuir-1 linear isotherms can be preferred in comparison to Freundlich linear isotherm.

5. Observed experimental breakthrough curves were simulated using linear and nonlinear sorption models. It is shown that the Freundlich sorption model gives best fit of observed spatial concentration profile along the length of soil column. This study also indicates that Freundlich nonlinear isotherm model incorporated in the transport equation with an implicit finite difference method would provide accurate prediction for reactive transport in the soil column. Also, estimated linear and nonlinear sorption and transport parameters for fluoride can be useful for safe disposal of solid-wastes and planning of future landfill sites.

6. Various experiments were conducted in the laboratory to understand the behavior of solute transport through horizontal heterogeneous long soil column filled with mixed soil media. The results show that the variation of pore velocity in heterogeneous porous media is much larger as compared to homogeneous porous media. It means that the large variation of hydraulic conductivity increases the dispersion of solute in heterogeneous porous media.

7. It is also shown that the MIMA model gives the best fit curve of experimental breakthrough curves through long heterogeneous soil column experiment as compared to both MIMC and MIML models. Estimated value of dispersivity is smaller in case of MIMA model as compared to both MIMC and MIML models. Thus, MIMA model is efficient to capture the evolution distance dependent dispersion behavior.

8. An empirical relationship of mass transfer coefficient with pore velocity and travel distance was developed. The variable mass transfer coefficient enhanced the simulation of experimental breakthrough curves as compared to constant value of mass transfer coefficient. Hence, accurate prediction of mass transfer coefficient is also essential and significant for transport of contaminant through porous media. Hence, asymptotic dispersivity including variable mass transfer coefficient can be useful for describing solute transport in long heterogeneous porous media.

9. The results of concentration profiles are compared in the presence of small and higher

values of Peclet number using both FDM and FVM methods for movement of solute through triple-permeability media. In the presence of small value of mass transfer coefficient (w=0.01 day^{-1}) and Peclet number equal to 0.5 and 2, it is shown that deviation occurs in the results of concentration profiles as predicted by both FVM and FDM methods. However, the results are remaining same in the presence of higher value of mass transfer coefficient (w=5 day^{-1}).

10. In the case of Peclet number equal to 200, the numerical oscillation has been obtained by FDM, while oscillation-free result is seen by FVM in the presence of both small and higher values of mass transfer coefficient. Hence, the FVM can be used for the simulation of solute transport through porous media for any value of Peclet number.

11. The behavior of spatial concentration profiles is predicted in three regions of triple-permeability media, respectively. The results show that the behavior of concentration profiles is not symmetrical for movement of solute in three regions, respectively. It is also shown that the higher value of mass transfer coefficient, first-order degradation and sorption coefficients are lead to reduce the magnitude of solute concentration along the travel distance.

12. The results of mean travel distance and spreading behaviour of solutes remain the same in the case of higher values of mass transfer coefficient. Higher value of mass transfer, first-order degradation rate and retardation factor lead to reduce the magnitude of mean travel distance and spreading of solute in the porous medium. During the small transport time, the behaviour of spreading of solute is non-uniform and it becomes linear for higher transport times. This study can be useful for remediation of contaminant transport through triple permeability medium.

7.3 Research Contribution

Overall following major research contribution can be made out of the study:

1. This study presents a general semi-analytical solution of multiprocess non-equilibrium with asymptotic distance dependent dispersivity function, which is more useful for simulating reactive transport through porous media at filed scale. Further, mass transfer

coefficient is considered as a constant and variable parameter during simulation of experimental data.

2. This study also shows the estimation of linear and nonlinear sorption parameters for fluoride transport through porous media. It shown that the Freundlich nonlinear sorption gave best fit of spatial concentration profile for reactive transport through porous media as compared to linear and Langmuir sorption model.

3. Both FDM and FVM numerical methods have been used to study the behavior of concentration profiles in the presence of small and higher value of Peclet number and mass transfer coefficients.

7.4 Scope of future works

The present work is focused on the development of semi-analytical solution of MPNE transport equations with asymptotic distance-dependent dispersivity functions, and this model has been used to simulate the experimental breakthrough curves through heterogeneous long soil column experiments in the lab. However, it is required to further explore the future investigations as mentioned below:

1. Field experiments can be carried out to get the experimental data through heterogeneous porous media for understanding the effect of physical and chemical non-equilibrium and scale effects.
2. In the present study, only asymptotic distance-dependent dispersivity has been considered, further study can be extended incorporating time dependent dispersivity.
3. Only one type of reactive solute, i.e. Fluoride, has been considered in the present work. Options to include many other reactive solutes should be considered in future work.
4. Stochastic approach can also be used to investigate the effect of heterogeneity of porous media.

BIBLIOGRAPHY

1. Abulaban, A., and Nieber, J.L., (2000). “Modeling the effects of nonlinear equilibrium sorption on the transport of solute plumes in saturated heterogeneous porous media.” Adv. Water Resour., vol. 23(8), 893-905.
2. Al-Tabbaa, A., Ayotamuno, J. M., and Martin, R. J., (2000). “One-dimensional solute transport in stratified sands at short travel distances.” J. Hazard. Mat.,73(1), 1-15.
3. Apha, A. WPCF (1995). “Standard methods for the examination of water and wastewater.” American Public Health Association, Washington, DC..
4. Aral, M., and Liao, B., (1996). “Analytical Solutions for Two-Dimensional Transport Equation with Time-Dependent Dispersion Coefficients.” J. Hydrol. Eng., 1(1), 20–32.
5. Avila, M. A. S., and Breiter, R., (2009). “Modelling the Competitive Sorption Process of Multiple Solutes during their Transport in Porous Media.” Env.Mod. Asses., 14(5), 615-629.
6. Barry, D. A., and Sposito, G., (1989). “Analytical solution of a convection-dispersion model with time-dependent transport coefficients.” Water Resour. Res., 25 (12), 2407–2416.
7. Bear, J., (1972). “Dynamics of Fluids in Porous Media.” 764 pp., Elsevier, New York.
8. Bear, J., (1979). “Hydraulics of Groundwater.” McGraw-Hill, New York.
9. Berkowitz, B., Emmanuel, S., and Scher, H., (2008). “Non-Fickian transport and multiple-rate mass transfer in porous media.” Water Resour. Res., 44, W03402, doi:10.1029/2007WR005906.
10. Bethge, E. and Mohrlok, U., (2008). “Uncertainty assessment for contaminant leaching from flood water retention areas, in: Calibration and Reliability in Groundwater Modelling, redibility of Modelling.” IAHS Publication, 320, IAHS Press, Oxfordshire, Great Britain, 27–33.
11. Bhallamudi, S. M., Panday, S., & Huyakorn, P. S. (2003). “Sub-timing in fluid flow and transport simulations.” Advances in water resources, *26*(5), 477-489.
12. Bond, W. J., and Wierenga, P. J., (1990). “Immobile water during solute transport in unsaturated sand columns.” Water Resour. Res., 26(10), 2475-2481.

13. Boving, T. B., and Grathwohl, P., (2001). “Tracer diffusion coefficients in sedimentary rocks: correlation to porosity and hydraulic conductivity.” J. Cont. Hydrol., 53 (1), 85-100.
14. Boving, T.B., (2014). “Forensic Analysis of MTBE Contamination Using Basic Hydrogeologic Concepts.” J Forensic Sci, July 2014, Vol. 59, No. 4, DOI: 10.1111/1556-4029.12510
15. Brindha, K., and Elango, L., (2011). “Fluoride in Groundwater: Causes, Implications and Mitigation Measures.” In: Monroy S.D. (Ed.). Fluoride Properties Applications and Environmental Management, 111-136.
16. Brusseau, M.L., Jessup, R.E., and Rao, P.S.C., (1989). “Modeling the transport of solutes influenced by multiprocess non-equilibrium.” Water Resour. Res., 25(9), 1971-1988.
17. Brusseau, M. L., (1991). “Application of a Multiprocess non-equilibrium sorption model to solute transport in a stratified porous medium.” Water Resour. Res., 27 (4). 589-595.
18. Brusseau, M.L., (1992). “Transport of rate limited sorbing solute in heterogeneous porous media: Application of a one dimensional multifactor nonideality model to field data.” Water Resour. Res., 28 (9), 2485-2497.
19. Brusseau, M. L., Jessup, R. E., and Rao, P. S. C. (1992). “Modeling solute transport influenced by multiprocess non-equilibrium and transformation reactions.” Water Resour. Res., 28(1), 175-182.
20. Brusseau, M. L., (1994). “Transport of reactive contaminants in heterogeneous porous media.” Reviews of Geophysics, 32(3), 285-313.
21. Brusseau, M. L., Hu, Q., and Srivastava, R., (1997). “Using flow interruption to identify factors causing nonideal contaminant transport.” J. Cont. Hydrol., 24(3), 205-219.
22. Burr, D.T., Sudicky, E.A, and Naff, R.L., (1994). “Nonreactive and reactive solute transport in three-dimensional heterogeneous porous media: Mean displacement, plume spreading, and uncertainty.” Water Resour. Res., 30 (3), 791-815.
23. Chapra, S.C., and Canale, R.P. (2000). “Numerical methods for engineers with programming and software.” Third edition,Tata McGraw-Hill, New Delhi.

24. Chastanet, J., and Wood, B. D., (2008). “Mass transfer process in a two-region medium.” Water Resour. Res., 44(5).
25. Chaudhuri, A. and Sekhar, M. (2007). “Stochastic finite element method for analysis of transport of nonlinearly sorbing solutes in three-dimensional heterogeneous porous media”. Water Resour. Res., (43), W07442, doi:10.1029/2006WR004892.
26. Chen, J.S., Liu, C.W., Liao, C.M., (2002). A novel analytical power series solution for solute transport in a radially convergent flow field. J. Hydrol. 266, 120-138.
27. Chen, J. S., Liu, C. W., Hsu, H. T., and Liao, C. M., (2003). “A Laplace transform power series solution for solute transport in a convergent flow field with scale-dependent dispersion.” Water Resour. Res., 39(8).
28. Chen, J.S., Ni, C.F., Liang, C.P., Chiang, C.C., 2008a. Analytical power series solution for contaminant transport with hyperbolic asymptotic distance-dependent dispersivity. J. Hydrol. 362, 142–149.
29. Chen, J. S., Ni, C. F., and Liang, C. P., (2008). “Analytical power series solutions to the two-dimensional advection–dispersion equation with distance-dependent dispersivities.” Hydrol. Proc., 22(24), 4670-4678.
30. Chiou, C.T., Peters, L.J, and Freed, V.H., (1979). “A physical concept of soil-water equilibria for non-ionic organic compounds.” Science, 206(16), 831-832.
31. Dagan, G., (1982). “Stochastic modelling of groundwater flow by unconditional and conditional probabilities. 2. The solute transport.” Water Resour. Res., 18 (4), 835-848.
32. Dagan, G. (1984). “Solute transport in heterogeneous porous formations.” J. Fluid Mech., 145, 151-177.
33. Deng, F.-W., Cushman, J. H., and Delleur, J. W. (1993). “A Fast Fourier Transform Stochastic analysis of the contaminant transport problem.” Water Resour. Res., 29(9), 3241-3247
34. Delay F, Porel G, Banton O., (1998). “An approach to transport in heterogeneous porous media using the truncated temporal moment equations: theory and numerical validation.” Transp. Porous Med., 32 (2). 199–232.
35. Dentz, M., Gouze, P., Carrera, J., (2011). “Effective non-local reaction kinetics for transport in physically and chemically heterogeneous media.” J. Cont. Hydrol., 222-236.

36. de Hoog, F.R., Knight, J.H., Stokes, A.N., (1982). "An improved method for numerical inversion of Laplace transforms." SIAM J. Sc. Stat. Computing, 3(3), 357-366.
37. De Smedt, F., and Wierenga, P. J., (1984). "Solute transfer through columns of glass beads." Water Resour. Res., 20(2). 225-232.
38. Duijn Van, C. J., and, van derZee, S. E. A. T. M., (1986). "Solute transport parallel to an interface separating two different porous materials." Water Resour. Res., 22 (13). 1779–1789.
39. Dykhuizen, R.C., (1991). "Asymptotic solutions for solute transport in dual velocity media." Mathematical Geology, vol., 23 (3). 383-401.
40. Eaton, A.D.,C lesceri, L.S., Greenberg, A.E., Franson, M.A.H., 1995. Standard methods for the examination of water and waste water. American Public Health Association.
41. Eldho, T. I., and Vasudeva Rao, B., (1997). "Simulation of two-dimensional contaminant transport with dual reciprocity boundary elements." Engineering analysis with boundary elements, 20(3), 213-228.
42. Elzein, A. H., and Booker, J. R., (1999). "Ground water pollution by organic compounds: A two- dimensional analysis of contaminant transport in stratified porous media with multiple sources of non-equilibrium partitioning." Int. J. Numer. Anal. Meth. Geomech., 23(14), 1717-1732.
43. Fetter, C.W. (1999). Contaminant hydrogeology, vol. 500, Prentice Hall, NJ.
44. Fitts, C. R., (2002). "Groundwater Science." Academic, San Diego, Calif.
45. Freeze, R. A., and Cherry, J. A., (1979). "Groundwater, Prentice-Hall, Englewood Cliffs, N. J.
46. Freundlich, H., (1906). "Uber die adsorption in iosungen." Zeitschrift fur physikalische Chemie, vol. 57, 385-470.
47. Furman, A., and Neumann, S.P., (2003). "Laplace-Transform Analytic Element Solution of Transient Flow in Porous Media." Adv. Water Resour., 26(12), 1229-1237.
48. Gao, G., Feng, S., Zhan, H., Huang, G., and Ma, X., (2009). "Evaluation of anomalous solute transport in a large heterogeneous soil column with mobile-immobile model." J. Hydrol. Eng., 14(9). 966-974.

49. Gao, G., H. Zhan, S. Feng, B. Fu, Y. Ma, and Huang, G., (2010). “A new mobile-immobile model for reactive solute transport with scale-dependent dispersion”. Water Resour. Res., 46(8), W08533.
50. Gao, G., Zhan, H., Feng, S., Fu, B., Huang, G. (2012) “A mobile–immobile model with an asymptotic scale-dependent dispersion function.” Journal of Hydrology 424–425 (2012) 172–183
51. Gelhar, L.W., Welty, W., Rehfeldt, K.R., (1992). A critical review of data on field-scale dispersion in aquifers. Water Resour. Res. 28(7), 1955-1974.
52. Gelhar, L. W., (1993). “Stochastic Subsurface Hydrology.” Prentice-Hall, Englewood Cliffs, NJ.
53. Gerke, Horst H., and, Van Genutcheten, M. Th., (1996). “Macroscopic representation of structural geometry for simulating water and solute movement in dual-porosity media.” Adv. Water Resour., 19(6), 343-357.
54. Goltz, M. N., and Roberts, P. V., (1986). “Three-dimensional solutions for solute transport in an infinite medium with mobile and immobile zones.” Water Resour. Res., 22 (7), 1139-1148.
55. Goltz, M. N., and Oxley, M. E., (1991). “Analytical modeling of aquifer decontamination by pumping when transport is affected by rate-limited sorption.” Water Resour. Res., 27(4), 547-556.
56. Gupta, M. K., Singh A. K., and Srivastava, R. K., (2009). “Kinetic Sorption Studies of Heavy Metal Contamination on Indian Expansive Soil.” E-J. Chem., 6(4), 1125-1132.
57. Guven, O., Molz, F.J., and Melville, J.G. (1984). “An analysis of dispersion in a stratified aquifer.” Water Resour. Res., 20(10),1337–1354
58. Huang, K., M. T. van Genuchten, and R. Zhang (1996). Exact solutions for One dimensional transport with asymptotic scale dependent dispersion. Appl. Math. Model. 20, 298–308.
59. Huang, H., Huang, Q., and Zhan, H., (2006). “Evidence of one dimensional scale-dependent fractional advection-dispersion.” J. Cont. Hydrol., 85(1), 53-71.
60. Hunt, B., (1998). “Contaminant source solutions with scale-dependent dispersivities.” J. Hydrol. Eng., 3(4), 268-275.
61. Hunt, B., (2002). “Scale-dependent dispersion from pit.” J. Hydrol. Eng., 7 (2), 168-174.

62. Jarvis, N. J., Jansson, P. E., Dik, P. E., and Messing, I., (1991). “Modelling water and solute transport in macroporous soil. I. Model description and sensitivity analysis.” J. Soil Sc., 42(1), 59-70.
63. Jury, W. A., and Utermann, J., (1992). “Solute transport through layered soil profiles: Zero and perfect travel time correlation models.” Transp. Porous Med., 8(3), 277-297
64. Kartha, S. A., and Srivastava, R., (2008a). “Effect of immobile water content on contaminant transport in unsaturated zone.” J. Hydro-Env. Res., 1(3), 206-215.
65. Kartha, S. A., and Srivastava, R., (2008b). “Effect of slow and fast moving liquid zones on solute transport in porous media.” Transp. Porous Med., 75(2), 227-247.
66. Kartha, S. A, and Srivastava, R., (2012). “Slow and fast transport in heap leaching of precious metals.” Transp. in Porous Med., 94(3), 707-727.
67. Kreyszig, E., (1999). Advanced Engineering Mathematics. Eighth ed. John Wiley, New York.
68. Kumar, G. S., and Sekhar, M., (2005). “Spatial moment analysis for transport of non-reactive solutes in a fracture-matrix system.” J. Hydrol. Eng., 10 (3), 192-199.
69. Kumar, G. S., Sekhar, M., and Misra, D., (2006). “Time dependent dispersivity behavior of non-reactive solutes in a system of parallel fractures.” Hydrol. Earth Sys. Sc. Disc., 3(3), 895-923.
70. Kuranchie, A., Shukla, S., Habibi, D., (2015). “Electrical resistivity of iron ore mine tailings produced in Western Australia.” International Journal of Mining, Reclamation and Environment, 29(3), 191-200, DOI: 10.1080/17480930.2014.941551
71. Lapidus, L., and Amundson, N.R., (1952). Mathematics of adsorption in beds. VI. The effect of longitudinal diffusion in ion exchange and chromatographic columns. J. of Physical Chemistry, 56, 984-988.
72. Langmuir, I., (1916). The constitution and fundamental properties of solids and liquids, Part I Solids. J. of the American Chemical Society, vol 38, 2221-2295.
73. Leij, F. J., and Bradford, S. A., (2009). “Combined physical and chemical non-equilibrium transport model: analytical solution, moments, and application to colloids.” J. Cont. Hydrol., 110(3), 87–99.
74. Leij, F. J., Toride, N., Field, M. S., and Sciortino, A., (2012). “Solute transport in dual-permeability porous media.” Water Resour. Res., 48(4).

75. Mackay, D. M., Freyberg, D. L., Roberts, P. V., and, Cherry, J. A., (1986). “A natural gradient experiment on solute transport in a sand aquifer: 1. Approach and overview of plume movement.” Water Resour. Res., 22(13), 2017–2029.

76. Maraqa, M. A. (2001). “Prediction of mass-transfer coefficient for solute transport in porous media.” Journal of contaminant hydrology, 50(1), 1-19.

77. Matheron, G., and de Marsily, G., (1980). “Is Transport in Porous Media Always Diffusive? A Counterexample.” Water Resour. Res., 16(5), 901-917.

78. Meenal, M., and Eldho, T. I., (2012). “Two-dimensional contaminant transport modeling using meshfree point collocation method (PCM).” Eng. Ana. with Bound. Elem., 36(4), 551-561.

79. Meenal, M., and Eldho T.I., (2013). “Aquifer Decontamination Studies Using a Meshfree Point Collocation Method (PCM).” Journal of Ground Water Research, AGGS, 2(1), 163-172, ISSN: 2321-4783.

80. Moench, M., (1991). “Social Issues in Western U.S. Groundwater Management: An Overview.” Oakland, Pacific Institute.

81. Mohrlok, U., Kienle, J., and Teutsch, G., (1997). “Parameter identification in double-continuum models applied to karst aquifers.” In Proceedings of the 12th International Congress of Speleology,10-17 August 1997, La Chaux-de-Fonds, Switzerland, Vol. 2, 163-166.

82. Mohrlok, U., Samuel Kirubaharan, C., and Eldho, T. I., (2010). “Transport Characteristics in 3D Groundwater Circulation Flow Field by Experimental and Numerical Investigations.” Practice Periodical of Hazardous, Toxic, and Radioactive Waste Management, 14(3), 185-194.

83. Molz, F. J., Guven, O., and Melville, J. G., (1983). “An examination of scale – dependent dispersion coefficient.” Ground Water, 21(6). 715-725.

84. Morales, I. Atoyan, J.A., Amador, J.A., Boving, T.B., (2014). “Transport of Pathogen Surrogates in Soil Treatment Units: Numerical Modeling.” Water. 6, 818-838; DOI: 10.3390/w6040818.

85. Nandi, B.K., Goswami, A., Purkait, M.K., 2009. Adsorption characteristics of brilliant green dye on kaolin. J. Hazardous Materials, Vol 161, 387-395.

86. Neville, C. J., Ibaraki, M., and Sudicky, E. A., (2000). “Solute transport with multiprocess non-equilibrium: A semi-analytical solution approach.” J. Cont. Hydrol., 44(2), 141–159.
87. Ogata, A., and Banks, R. B., (1961). “A solution of the differential equation of longitudinal dispersion in porous media.” U. S. Geol. Surv. Prof. Pap. 411-A.
88. Ogata, A., (1970). “Theory of dispersion in a granular medium.” U.S. Geol. Surv. Prof., Paper 411-I.
89. Pang, L., and Hunt, B., (2001). “Solutions and verification of scale-dependent dispersion model.” J. Cont. Hydrol., 53(1), 21-39.
90. Parimal, S., Prasad, M. and Bhaskar, U., 2010. Prediction of Equilibrium Sorption Isotherm: Comparison of Linear and Nonlinear Methods. Ind. Eng. Chem. 49, 2882-2888.
91. Park, E. and Zhan, H., (2003). “Hydraulics of horizontal wells in fractured shallow aquifer systems.” J. Hydrol., 281(1), 147–158.
92. Pickens, J. F., Jackson, R. E., Inch, K. J., and Merritt, W. F. (1981a). “Measurement of distribution coefficients using a radial injection dual-tracer test.” Water Resour. Res., 17(3), 529-544.
93. Pickens, J. F., and Grisak, G. E., (1981b). “Modeling of scale dependent dispersion in hydrogeologic systems.” Water Resour. Res., 17(6), 1701-1711.
94. Putti, M., Yeh, W., and Mulder W.A., (1990). A Triangular Finite Volume Approach with High Resolution Upwind Terms for the Solution of Groundwater Transport Equations. Water Resour. Res., 26(12), 2865-2880.
95. Rao, S. V. N., Sreenivasulu, V., Bhallamudi, S. M., Thandaveswara, B. S., & Sudheer, K. P. (2004). Planning groundwater development in coastal aquifers/Planification du développement de la ressource en eau souterraine des aquifères côtiers. *Hydrological Sciences Journal*, *49*(1), 155-170.
96. Remson, I., Hornberger, I. G. M., and Molz, F. J., (1971). “Numerical Methods in Subsurface Hydrology.” Wiley-Intersience New York.
97. Roberts, P. V., Goltz, M. N., and, Mackay, D. M., (1986). “A natural gradient experiment on solute transport in a sand aquifer: 3. Retardation estimates and mass balances for organic solutes.” Water Resour. Res., 22(13), 2047–2058.

98. Robinson, N. I., Sharp Jr, J. M., and Kreisel, I., (1998). “Contaminant transport in sets of parallel finite fractures with fracture skins.” J. Cont. Hydrol., 31(1), 83-109.

99. Sciortino, A., Leij, F. J., Caputo, M. C., & Toride, N. (2015). “Modeling transport in dual-permeability media with unequal dispersivity and velocity.” J. of Hydrol. Eng., 04014075.

100. Sekhar, M., Suresh Kumar, G., and Misra, D., (2006). “Numerical modeling and analysis of solute velocity and macrodispersion for linearly and nonlinearly sorbing solutes in a single fracture with matrix diffusion.” J. Hydrol. Eng., 11(4), 319-328.

101. Selim, H. M., and Mansell, R. S., (1976). “Analytical solution of the equation of reactive solutes through soils.” Water Resour. Res., 12(3), 528-532.

102. Selim, H. M., Ma, L., and Zhu, H., (1999). “Predicting Solute Transport in Soils Second-Order Two-Site Models.” S. Sc. Soc. America J., 63(4), 768-777.

103. Serrano,S. E., (2001). Solute transport under non-linear sorption and decay. Water Res. Vol. 35, (6), p. 1525-1533.

104. Sharma, P. K. And Srivastava, R. (2012). “Concentration profiles and spatial moments for reactive transport through porous media.” ASCE Journal of Hazardous, Toxic, and Radioactive Waste, Vol. 16 (2), P-125-133.

105. Sharma, P. K., Savant, V.A., Shukla, S. K., and Khan, Z. (2014) “Experimental and numerical simulation of contaminant transport through layered soil”. International Journal of Geotechnical Engineering. Vol. 8(4), 345-351, DOI 10.1179/1939787913Y.0000000014.

106. Sharma, P. K., Shukla, S. K., Choudhary, R., & Swami, D. (2016). “Modeling for solute transport in mobile–immobile soil column experiment.” *ISH Journal of Hydraulic Engineering*, *22*(2), 204-211.

107. Shashidhar, T., Bhallamudi, S. M., and Philip, L. (2007). “Development and validation of a model of bio-barriers for remediation of Cr (VI) contaminated aquifers using laboratory column experiments.” J. of hazardous materials, 145(3), 437-452.

108. Singh, M. K., Ahamad, S. and Singh, V. P., (2011). “Analytical Solution for One-Dimensional Solute Dispersion with Time-Dependent Source Concentration along Uniform Groundwater Flow in a Homogeneous Porous Formation.” J. Eng. Mech. Vol., pp., in press.

109. Singh, M. K., Singh, V. P., Kumari, P. and Das, P., (2012). “Analytical and Numerical Approaches to Horizontal Non-Reactive Solute Dispersion in a Semi-Infinite Aquifer.” J. Ground Water Res., 1(1), 42-51.

110. Singh, M. K., Singh, Premlata, and Singh, V. P., (2010). “Analytical Solution for Solute Transport along and against Time Dependent Source Concentration in Homogeneous Finite Aquifers.” Adv. Theor. and Appl. Mech., 3(3), 99-110.

111. Srivastava, R., and Brusseau, M. L., (1996). “Nonideal transport of reactive solutes in heterogeneous porous media: 1. Numerical model development and moments analysis.” J. Cont. Hydrol., 24 (2), 117-143.

112. Srivastava, R., Sharma, P.K., and Brusseau, M. L., (2002). “Spatial moments for reactive transport in heterogeneous porous media.” J. Hydrol. Engg., ASCE 7 (4), 336-341.

113. Starr, R. C., Gillham, R. W., and Sudicky, E. A., (1985). “Experimental investigation of solute transport in stratified porous media, 2. The reactive case.” Water Resources. Res., 21(7), 1043-1050.

114. Sternberg, S. P., and Greenkorn, R. A., (1994). “An experimental investigation of dispersion in layered porous media.” Transp. Porous Med., 15(1). 15-30.

115. Sudicky, E. A., Gillham, R.W., and Frind, E. O., (1985). “Experimental investigation of solute transport in stratified porous media, 1. The nonreactive case.” Water Resour. Res., 21(7), 1035-1041.

116. Tang, D. H., Frind, E. O., and Sudicky, E. A., (1981). “Contaminant transport in fractured porous media: Analytical solution for a single fracture.” Water Resour. Res. 17(3), 555-564.

117. Tang, Y., and Aral, M. M., (1992). “Contaminant transport in layered porous media: 1. General solution.” Water Resour. Res., 28(5), 1389-1397.

118. Taylor, G., (1953). “Dispersion of soluble matter in solvent flowing slowly through a tube.” Proceedings of the Royal Society of London. Series A. Mathematical and Physical Sciences, 219(1137), 186-203.

119. Toride, N., Inoue, M., and Leij, F. J., (2003). “Hydrodynamic dispersion in an unsaturated dune sand.” S. Sc. Soc. America J., 67(3), 703-712.

120. van Albada, G.D., van Leer, B., and Robers Jr., W.W., (1982) A Comparative Study of Computational Methods in Cosmic Gas Dynamics. Astronomy and Astrophysics. 108: 76-86.

121. van Leer, B., (1977a). Towards the Ultimate Conservative Difference Scheme III: Upstream Centred Finite Difference Schemes for Ideal Compressible Flow. J. Comput. Phys., 23: 263-275.

122. van Leer, B., (1977b). Towards the Ultimate Conservative Difference Scheme IV: A New Approach to Numerical Convection. J. Comput. Phys., 23: 276-299.

123. van Genuchten, M, Th., and Alves, W. J. (1982). Analytical solutions of the one-dimensional convective-dispersive solute transport equation. US Dept. Agriculture Tech. Bull. No.1661 151p.

124. Valocchi, A. J., (1985). "Validity of the local equilibrium assumption for modeling sorbing solute transport through homogeneous soils." Water Resour. Res., 21(6), 808-820.

125. Valocchi, A. J., (1988). "Theoretical analysis of deviations from local equilibrium during sorbing solute transport through idealized stratified aquifers." J. Cont. Hydrol., *2*(3), 191-207.

126. Van Genutcheten, M.Th., and Alves, W.J., 1982. Analytical solution of one dimensional convective-dispersion solute transport equation. Tech. Bull. Regist Med. Technol., 1-51.

127. Valocchi, A. J., (1989). "Spatial moment analysis of the transport of kinetically adsorbing solutes through stratified aquifers." Water Resour. Res. 25(2), 273-279.

128. van Genuchten, M. Th., Davidson, J. M., and Wierenga, P. J., (1974). "An evaluation of kinetic and equilibrium equations for the prediction of pesticide movement through porous media." S. Sci. America. Proc., 38(1), 29-35.

129. van Genuchten, M. Th., and Wierenga, P. J., (1976). "Mass transfer studies in sorbing porous media: Analytical solutions." Soil Sci. Soc. America. J., 40(3), 473-479.

130. van Genuchten, M. Th., and Wierenga, P. J., (1977). "Mass transfer studies in sorbing porous media: II. Experimental evaluation with tritium (3H2O)." S. Sc. Soc. America J., 41(2), 272-278.

131. van Genuchten, M. Th., and Wagenet, R. J., (1989). "Two-site/two-region models for pesticide transport and degradation: Theoretical development and analytical solutions." Soil Sci. Am. J., 53(5), 1303-1310.

132. Vanderborght, J., Vereecken, H., (2007). Review of dispersivities for transport modelling in soil. J. Vadose Zone, (6), 29-52.

133. Weng, C.H., Sharma, Y.C. Chu, S.H., 2008. Adsorption of Cr (VI) from aqueous solution by spent activated clay. J. of Hazardous Materials, vol. 155, 65-75.

134. Xu, L., and Brusseau, M. L., (1996). “Semi-analytical Solution for Solute Transport in Porous Media with Multiple Spatially Variable Reaction Processes.” Water Resour. Res., 32(7), 1985-1991.

135. Yates, S. R., (1990). “An analytical solution for one-dimensional transport in heterogeneous porous media.” Water Resour. Res., 28(8), 2149-2154.

136. Yates, S. R., (1992). “An analytical solution for one-dimensional transport in heterogeneous porous media with an exponential dispersion function.” Water Resour. Res., 26(10), 2331-2338.

137. Zhan, H., (1998). “Transport of waste leakage in stratified formations.” Adv. Water Resour., 22(2), 159-168.

138. Zhou, L., and Selim, H. M., (2003). “Scale dependent dispersion in soil: an overview.” Adv. Agron., 80, 223-263.

LIST OF PUBLICATIONS

1. Abgaze, T. A., and Sharma, P. K. (2015). Solute transport through porous media with scale-dependent dispersion and variable mass transfer coefficient. ISH Journal of Hydraulic Engineering, 21(3), 298-311.

2. Sharma, P. K., & Abgaze, T. A. (2015). Solute transport through porous media using asymptotic dispersivity. Sadhana Journal, Indian Academy of Sciences, (Springer publisher), 40(5), 1595-1609.

3. Sharma, P. K., Ojha, C. S. P., Abegaze, T. A., Swami, D., and Yadav, A. (2015). Simulation of Fluoride Transport through Fine Sand Column Experiments. Journal of Hydrogeology & Hydrologic Engineering, 4:2.

4. Abgaze, T. A., Sharma, P. K. and Swami Deepak. (2014) Modeling solute transport through porous media with scale dependent dispersion. HYDRO 2014 INTERNTIONAL Conference, December 18-20, 2014, at M.A.N.I.T. Bhopal, India.